12-2019

AN EXAMINATION OF METHODS TO DETERMINE THE FLAMMABILITY CHARACTERISTICS OF ELECTRICAL CABLES EXPOSED TO EXTENDED PERIODS OF RADIATION IN NUCLEAR FACILITIES

Justin Thomas Beeler
University of Tennessee, jbeele12@vols.utk.edu

To the Graduate Council:

I am submitting herewith a dissertation written by Justin Thomas Beeler entitled "AN EXAMINATION OF METHODS TO DETERMINE THE FLAMMABILITY CHARACTERISTICS OF ELECTRICAL CABLES EXPOSED TO EXTENDED PERIODS OF RADIATION IN NUCLEAR FACILITIES." I have examined the final electronic copy of this dissertation for form and content and recommend that it be accepted in partial fulfillment of the requirements for the degree of Doctor of Philosophy, with a major in Electrical Engineering.

David Icove, Major Professor

We have read this dissertation and recommend its acceptance:

Benjamin J. Blalock, James E. Lyne, Aly Fathy

Accepted for the Council:

Dixie L. Thompson

Vice Provost and Dean of the Graduate School

(Original signatures are on file with official student records.)

AN EXAMINATION OF METHODS TO DETERMINE THE FLAMMABILITY CHARACTERISTICS OF ELECTRICAL CABLES EXPOSED TO EXTENDED PERIODS OF RADIATION IN NUCLEAR FACILITIES

A Dissertation Presented for the

Doctor of Philosophy

Degree

The University of Tennessee, Knoxville

Justin T. Beeler

December 2019

Dedication

To

My Mother

Who has loved and supported me every step of the way.

Acknowledgments

I would like to thank Dr. David Icove for his unwavering support and guidance while pursuing my degree. His vast knowledge of the field and devotion in overseeing my work has allowed me to perform at my best. I also want to thank Drs. Evans Lyne, Benjamin Blalock, and Aly Fathy for serving on my committee and for their support along the way.

Additionally, I want to thank Mark Henry Salley and Gabriel Taylor from the U.S.NRC who helped direct me in finding contacts for beginning my research. Their help provided a foundation for the entire research project.

I am very grateful for the outside support that I received. Dr. Robert Duckworth at ORNL helped tremendously by supplying me with samples used for experimentation and guidance on testing procedures. Dr. H.M. Hashemian and everyone at Analysis and Measurement Services Corporation (AMS) also gave me support and testing materials that were instrumental to the success of this project.

Dr. Elizabeth C. Buc and Paul Runde at the Fire and Materials Research Laboratory were extremely generous in allowing me to perform the testing at their facility. The facility was equipped with all of the equipment that I needed for the research. Dr. Buc provided excellent guidance and support for testing the samples at her facility; while, Paul Runde was

knowledgeable and supportive in showing me how to use the equipment. Their help on the project was invaluable to me, and I am very thankful.

Abstract

It is well known that prolonged low-level radiation compromises the flame spread ratings of insulated electrical cables, particularly those used in nuclear power plants, fuel production, and research facilities. This dissertation addresses the effects that thermal aging and irradiation have on the flammability characteristics of cable jackets (insulation around the conductor). It also seeks to develop a passive method to predict flame spread ratings for these aging cables.

Changes in the inductive and capacitive reactance can alter the resonant frequency of the cable. These changes in reactance can be quantified as the cable is irradiated or thermally aged. Various testing methods are used to quantify the flammability characteristics of the cables. These tests are used to develop a complete understanding of how the irradiation or thermal aging impact the jacket and conductor of the cable.

Table of Contents

List of Tables

List of Figures

Chapter 1

Introduction

1.1 Overview

Electrical cable has been used for over a hundred years to provide a means of transferring electrical energy from one source to another. Wire jacket insulation was developed to insulate the wire from conductivity to other sources, from EMF (electromagnetic field), from EMI (electromagnetic induction), and to protect the conductor from physical damage. The cable jacket is necessary for normal operation, but it presents a problem as it is a fuel source for a potential fire. The cable jackets used in practice are designed to have a specific fire rating that prolongs the ignition point of the jacket and burns slowly to help reduce the overall impact.

Maintaining the flammability characteristics of these types of cables is important to prevent an untimely disaster. Electrical cable is used to control everything from light switches to control of nuclear reactors' cooling systems. If a cable fire gets too large, it can cause complete shutdowns of nuclear plants or even compromising the reactor itself (Sawyer &

Elsner, 1976). Thus, maintaining the original characteristics of cable used in the industry is a meaningful endeavor.

Aging cable can cause various forms of degradation that can alter or even compromise the cable's jacket. Typically, cable is rated for use up to 60 to 80 years under normal operating conditions. Additional exposures in the form of irradiation or thermal aging can impact this rating. These exposures can accelerate the aging process of the cable. Figure 1.1 is a visual representation of the types of aging that can impact the characteristics of the cable.

Thermal aging and irradiation are two very different forms of accelerated aging (in the form of heating), that cable can be exposed to in daily operations. It is essential to consider the extent of the aging caused by these two forms. Altered performance, compromised jacket, and reduced safety ratings are some of the possible considerations as a result of prolonged exposure.

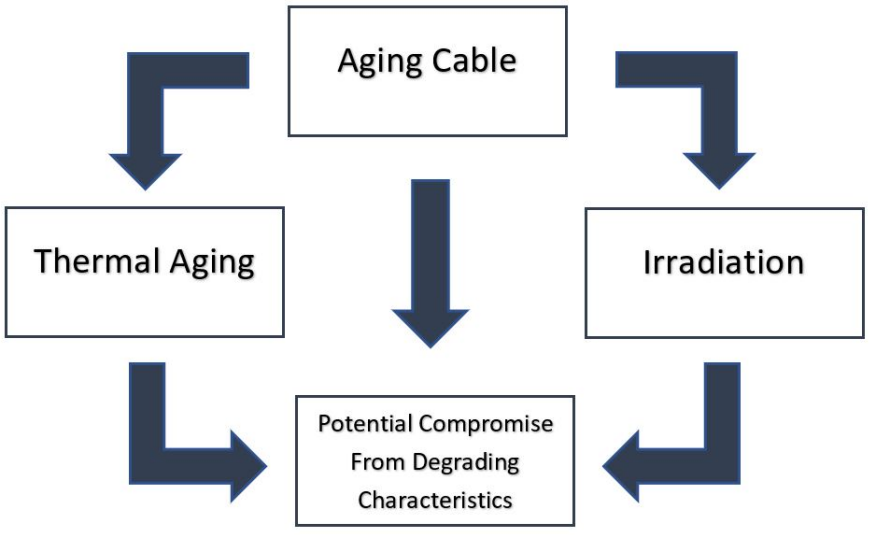

Figure 1.1: Direct and indirect aging of cable used in industry.

1.2 Problem Statement

The flammability rating of cable used in practice is important to the safety of personnel and equipment. In practice, the cable is tested to determine how many years it can continue to be used. If the cable is compromised in any way, then it is removed from service. There is little understanding of the effects that thermal aging and irradiation have on the flammability characteristics of the cable jacket. A change in the flammability characteristics could require the cable to be removed from service either earlier or later than it usually would be. This research is to contribute to the development of an understanding of how irradiation and thermal aging of the cable jacket affects the respective flammability characteristics. The research also seeks to develop an approach for passively measuring the changes in the flammability characteristics of cable used in practice.

1.3 Research Motivation

Nuclear power plants have strict guidelines to follow for the utilization of wire. The cable must be sized correctly, insulated from radiation, and be flame retardant to a certain point. Cable fires in nuclear power plants can be catastrophic due to the importance of system control in a plant. Previous work has been done to determine the flammability risks associated with cable racks and how the flame can quickly propagate to all the cables on the racks(Plastics, 2001). Studies have also been done to determine the degradation of the effectiveness of cables that have been radiated for a period(Seguchi et al., 2010)(He & Brazis Jr., 2012). It has been noted that irradiation exposure likely affects the flammability characteristics of the cable sheathing, but it has not been quantified by testing. It is essential

to understand how long a cable can be used before the sheathing or cable is compromised due to radiation. Currently, determining if a cable has been compromised by irradiation can only be done by physical testing of the jacket. Some methods do not require the cable to be removed but are limited to a specific area of the cable and do not evaluate the entire length (unless the cable has exposed conductors and is completely compromised) (Simmons et al., 2012) (Glass et al., 2017) (Campbell et al., 2012).

The resonant frequency of a cable is an important parameter to consider as it is a function of the physical and material properties. Typically, the resonant frequency changes as a function of the inductive and capacitive reactance of the cable. An increase or decrease in the reactance can cause the resonant frequency to shift in one direction or the other and can be quantified. The concern is whether the resonant frequency changes due to irradiation/thermal aging. It is possible that the irradiation may change the relative capacitance that the cable and sheathing represent. It is essential to be able to passively measure the frequency resonance of the cable and determine what it is.

1.4 Research Goals

The following are the specific goals of this research.

- *Characterize the physical changes of cable exposed to thermal aging or irradiation.*

  This research will evaluate the physical changes of cable that are exposed to various amounts of thermal aging or irradiation. This will be accomplished by evaluating the samples using the following tests: Elasticity Testing, Scanning Electron Microscope (SEM), and Fourier-Transform Infrared Spectroscopy (FTIR).

- *Characterize the changes in flammability characteristics of exposed cable.*

  The flammability characteristics of each sample will be evaluated to determine the impact that aging has across the typical lifespan of these cables. Assessing the flammability characteristics is done by conducting the following tests: Differential Scanning Calorimeter (DSC), Thermo-Gravimetric Analysis (TGA), Cone Calorimeter, and UL 94 Vertical Flame Spread Test. These tests provide an understanding of the specific changes in characteristics and also determines if the continued use of these cables compromises the safety rating introduced by industry standards.

- *Evaluate a passive method of measuring the changing reactance of an in situ cable as it is exposed to various forms of aging.*

  This research also presents a method of measuring the changes in reactance of a cable with various amounts of aging exposure. This testing is performed by treating the multi-conductor cable as a transmission line and recording the reactance as a function of frequency.

- *Analysis of the numerical results to correlate the flammability characteristics to the changes in reactance.*

  The changes in reactance are correlated to the progressive exposure of thermal aging or irradiation. Equating the reactance to the amount of aging also allows the variation in flammability characteristics to be approximated. This is done by taking all of the numerical data presented in the research and evaluating it.

1.5 Thesis Outline

The sequence of this research is demonstrated as follows. First, the aged cable's characteristics will be broken down and evaluated from physical testing. This will provide an understanding of the measured changes in flammability characteristics for the same cables. Then the contributing aspects of the shifting reactance will be considered to determine the reasons behind it. These three components will be compared to evaluate the impact that the aging has on the flammability characteristics, provide an understanding of what physical alterations contribute to the changes, and instantiate a method for measuring these changes.

This document is organized as follows: Chapter 2 will present a comprehensive literature review on the concepts related to this research including, cable composition, jacket material/aging, cable fires, physical causes of fire, electrical causes of fire, physical irradiation, and in situ testing methods. Chapter 3 presents the methodology for the research, which conclusively evaluates the impact that aging has on cable. This chapter also discusses how the cable samples were procured and artificially aged. The chapter wraps up by evaluating each of the testing methods that were used to characterize the samples. Chapter 4 focuses on presenting the data that was recorded from each of the tests. This data details the implications for the physical, flammability, and reactance characteristics of the aged cable jackets. Chapter 5 discusses the data and forms ideas around the results that were collected. This section also begins to correlate all of the data to form the final conclusion of the research. Chapter 6 is used to summarize the research by discussing the contributions, limitations, and future research.

Chapter 2

State of the Art

2.1 Electrical Cable Composition

Electrical cables are vital components that support a wide variety of residential and industrial applications. Miles and miles of cables are embedded within the infrastructure of a majority of facilities. These cables are responsible for the power distribution, power transmission, communication, and instrumentation, providing support to safety systems during disastrous events (Tewarson & Khan, 1989). For instance, electric cables are essential to nuclear power plant systems because they provide power, communications, system control, and support during severe situations, such as loss of coolant accident (LOCA), core melt accident, or hydrogen burning (Konecna, 2017). The most common types of cables used in industry, especially nuclear power plants are power, control, instrument, thermocouple, and specialty cables.

Electrical cables are composed of a conductor shield, conductor, insulation shield, insulation, concentric neutral, and jacket as shown in Figure 2.1. The core of the electrical

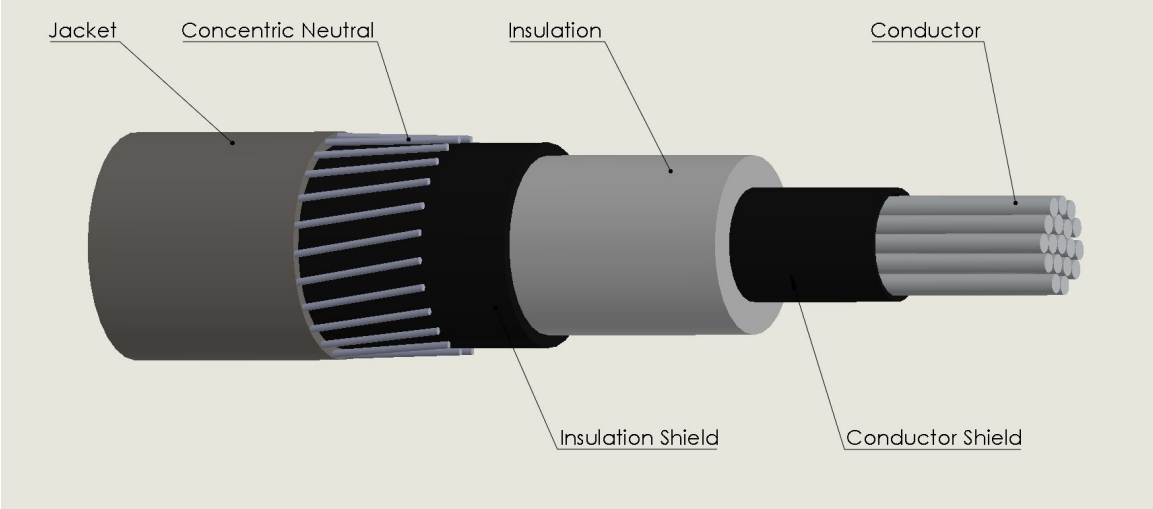

Figure 2.1: The components of an electrical wire. Adapted from (Short, 2004).

cable, the conductor, is made from either aluminum or copper phase. Copper conductors are regularly used in a variety of industrial applications due to its low resistivity and higher ampacity for a particular size. Aluminum conductors are less expensive and are lighter than their counterparts. The conductors are extruded into strands in order to increase the flexibility of the cable. According to ASTM standards (ASTM, 2017), Class B cables are the standard for power cables, but for a more flexible wire, Class C is used, by adding more strands. Each strand is wound in the opposite direction. The cable shield is a copper tape barrier that provides a path for return currents and for fault currents while also providing protection against lightning strikes and other fault sources. The shield is also known as sheath (Short, 2004).

The metallic conductor is encased within an insulation hallow cylindrical core made of a type of synthetic polymeric material. The insulation is housed in the jacket for protection against external sources. The configuration of the conductor may be composed of either a single, multi or triplex conductor.

Researcher's attention has been focused on cable longevity through monitoring of cable conditions and gaining a better understanding of the flammability and degradation behavior under extreme heat conditions (U.S. Congress, 1993) (Salley, 2000) (Milter & Steckler, 1995) (NRC, 2013).

2.2 Insulation Materials

The insulation within the electrical cables is designed to hold back electrons, provide support for a conductor at a specific voltage, resist high temperatures during short circuits

and heavy loading, and must be flexible to work (Short, 2004).

In the last 40 years, there has been an increase in polymer-insulated cables with polyethylene-based insulation. There is a large variety of synthetic polymers used in cables varying in chemical structure, thickness, and additives such as flame-retardants. The types of cables used in a nuclear power plant are as follow instrumentation cables, power cables, and control cables (Berg et al., 2012).

Materials typically used for the insulating jacket are either thermoplastics or thermosetting (thermoset) polymers. These polymers are known for displaying different material behavior when exposed to a fire environment. When thermoplastic is exposed to a heat source, the soft material becomes malleable and fluid and more prolonged exposure can result in melting. The opposite behavior is observed in thermoset. Thermoset becomes more rigid and char begins to develop when exposed to heat. Thermosetting polymers used for the cable jacket include the following materials: silicon rubber, ethylene-propylene rubber (EPR), and cross-linked polyethylene (XLPE). Thermoplastic cables include the following material: Teflon (PTFE), polyethylene (PE), polypropylene (PP) and polyvinylchloride (PVC) (Murphy, 2004).

The most common polymeric materials used in nuclear power plants that conform to ICEA/NEMA specifications are XLPE, EPR, and silicon rubber per ICEA S-66-524, S-68-516, and S-19-81, respectively. Cables classified as flame retardant typically consist of either low-voltage XLPE or EPR insulation. The majority of XLPEs materials are manufactured with flame-retardants. EPR can be processed without flame-retardant. This type of material is usually paired with a CPSE jacket to provide flame-retardant characteristics.

XLPE is a synthetic thermosetting polymer that consists of cross-linked agents, such as dicumyl peroxide, embedded within the LDPE polymer chains. The cross-linking bonds within this material interconnect with the polymer chains, which gives the XLPE a semi-crystalline structure and increases the mechanical properties such as stiffness. The vulcanization process also produces electrical characteristics similar to thermoplastic PE. XLPE is a stronger performing material at high temperatures when compared to PE (Hampton et al., 2007). The insulation strength of XLPE is similar to PE but is more rigid. Another type of XLPE is the Tree-Retardant Cross-Linked Polyethylene (TR-XLPE). Tree-retardant is added to XLPE to slow down water tree growth within the cable under voltage. Water tree growth has been known to cause electrical stress that increases over a period of months or years. After the initiation of water tree growth occurs, electrical trees continue to rapidly spread until the insulation protection failed and developed an electrical fault at the water tree location.

EPR is a thermoset polymer made from chemical combining of ethylene and propylene. This thermoset is processed using a high-temperature steam curing process in order to set the crosslinking agents. Combined with clay fillers, the stiffness of this material is suitable for cable applications. When compared to the other insulating material, EPR is very rubbery and flexible and the insulation strength, when compared to XLPE, is only half. The unique characteristic of this polymer is that as it ages, the insulation strength does not depreciate as much as XLPE. The advantage of using EPR is that this material has a high resistance to water trees, lower dielectric loss, good high-temperature performance, maintain a significant amount of stiffness and insulation strength at high temperatures.

2.3 Jacketing Material

The primary purpose of the jacket is to separate the conducting material to prevent short-circuiting. Other benefits of the jacket are to provide mechanical protection from water, cutting sources, weathers, etc. Several materials used for jacket materials are PVC, linear LDPE (LLDPE) (U.S. Congress, 1993). LLPDE is a more advantageous material to use for cable jackets than PVC. LLPDE possesses better mechanical properties, higher working temperature limits, strong moisture barrier protection, and lower coefficient of friction (COF). Some jacket materials have semiconducting properties, which can provide mechanical and moisture barrier protection, and performs as an excellent grounding conductor.

2.4 Electrical Cables and Fires

A major cable fire incident occurred at the Browns Ferry Nuclear Plant in Decatur, AL on March 22, 1975. Browns Ferry is a three boiling water reactors (BWRs) plant with the electrical capability of 1.097 GW (Sawyer & Elsner, 1976). A candle was used to check the efficiency of the blockage of the flame-retarded coated polyurethane (PU) foam between the reactor building and the cable room. At 12:20 pm, the pressure differential directed the candle flame into the penetration seal, igniting the plastic foam sheeting in the cable spreading room and the fire continued to spread to the cable tray system located 20 feet above the floor in the reactor building. Between 5:30 pm and 6:00 pm, a shift engineer got approval to use water to extinguish the fire. Around 7:30pm, after the cables had been burning for several hours, the fire was extinguished (Sawyer & Elsner, 1976).

The costly outcome of the cable fire resulted in about $10 million in direct damages and around $200 million in fuel replacement. The cable system in the cable spreading room suffered severe cable damage of about 3ft starting from the penetration seals. In the reactor building, cable damages were found about 20 feet horizontally and 40 feet vertically in parallel with the wall. In total, the fire destroyed about 1600 cables in 26 cable trays. The fire melted the aluminum conduits and cracked steel conduits. There was a strong presence of smoke and soot possessing dangerous corrosive products from the burning cable jackets. Fire incidents due to cable failure not only affect nuclear power plants (Chaudhary et al., 2015) but also ships, aircrafts (of the Navy., 1969), residential homes, and shops (He & Brazis Jr., 2012). Table 2.1 and 2.2 summarizes occurrence of a few cable fire incidents.

The frequency of fire cable incidents prompted the Nuclear Regulatory Commission (NRC) and Underwriters Laboratories (UL) to reevaluate the fire potential of all cables used in U.S. nuclear power plants and other industrial/residential areas. Cable fires not only occur at nuclear power plants but also on ships, on construction sites, in infrastructures and in homes. Due to the damages caused by electrical fires, much research has been focused on investigating the fragility and flammability of electrical cables when exposed to fire.

2.5 Physical Sources of Cable Insulation Damages

Electrical cables are responsible for distributing power through the entire area of the nuclear power plant and other facilities into other electricity-dependent systems. The power cables are embedded within the infrastructure of the facilities in risers, ducts, ceiling voids, cable trays, cable channels, and conduits or even in open-support structure (Botha, 2017).

Table 2.1: Electrical Fire Incident in Nuclear Power Plants.

Name	Year	Causes	Damages
Nuclear			
San Onofre (USA)	1968	Varying Cable Layout Caused Spontaneous Cable Fire	0 personnel settlement - $400 million
Browns Ferry (USA)	1975	Fire in Cable Room	$10 million in direct loss and $300-500 million in indirect loss
Greifswald (Germany)	1975	Considerable Cable Fire	N/A

Note. Information for cable fires from (Chaudhary et al., 2015).

Table 2.2: Electrical Fires in Transportation.

Name	Year	Causes	Damages
Transportation			
US Forrestal (USA)	1969	Electrical connection between Triple Ejector Rack and rocket harness (TER) before launch	134 personnel died 161 injuries
Trans World Airlines Flight 808, Boeing 747-141	1996	A short-circuit outside of the center wing fuel tank, caused a high voltage ignition	230 personnel died

Note. Cable fire information derived from (of the Navy., 1969) and (Board, 1996).

Table 2.3 summarizes the ignition source and exposure risk that can lead to an electrical fire.

Several physical mechanisms linked with the ignition of electrical fires that have been identified in the literature are: overloaded circuits, poor cable connections, large amounts of thermal insulation, the breakdown of dielectric in insulators, tracking arcs, displacement of hot particles, and other phenomena (Babrauska, 2008).

2.5.1 Poor Connections

As illustrated in Table 2.2 the US Forrestal fire, poor connections can establish an unwanted electrical connection that could lead to a failure in either the cable or the connecting device leading to fire ignition or in the mentioned incident, a malfunction of the device leading to other catastrophic severe events. What makes this type of mechanism such a severe issue is due to a problematic detection level.

2.5.2 Arcing Tracking

Several types of faults have been (Taylor, 2012) identified that could lead to a fire incident. The typical failure mode of electrical cables is an open circuit, short-to-ground, hot short, and insulation resistance degradation. Open circuit failure mode occurs due to the conductor failure, such as fracture strand of the conductor. Short-to-ground circuit occurs when a grounded medium, comes into contact with a conductor as shown in Figure 2.2.

Table 2.3: Failure Mechanism in Electrical Cables

Failure Mechanism	Type of Fire Risk	Cause
Arcing	Ignition/Combustion	Carbonization of insulation, externally induced ionization of air,short circuits
Exessive Ohmic Heating (No Arching)	Ignition/Combustion	Gross overloads, excessive thermal insulation, stray currents and ground faults, over voltage, poor connections
External Heating	Ignition/Combustion	Ejection of hot particles

Note. Ignition/combustion characteristics derived from (Botha, 2017).

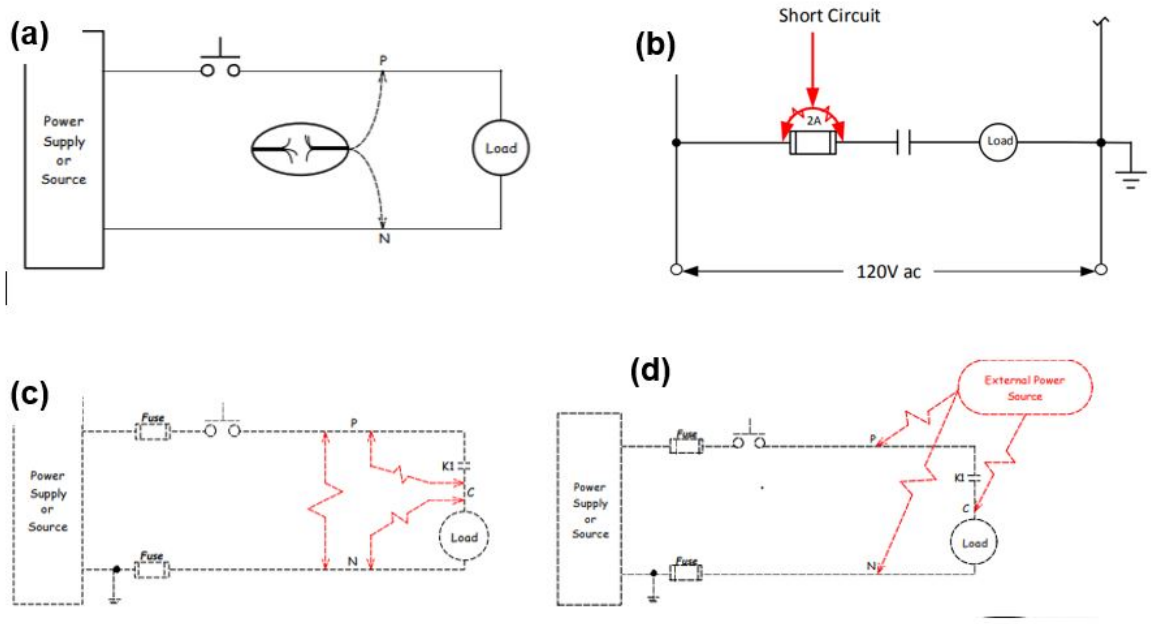

Figure 2.2: Schematic of (a) open circuit, (b) short circuit, Hot-short (c) internal and (d) external cable failures. Adapted from (Taylor, 2012) (Laboratory, 2016) (NRC, 2013)

There are two types of arcing that may trigger an electrical fire, arcing across a carbonized path (AACP) and arcing in the air (AIA). In the case of arcing, the path is created by external factors such as heat exposure from another heat source or carbonization of the electrical insulation due to burning. AACP mechanism may occur under wet and dry conditions, also known as wet and dry tracking. Wet tracking occurs when a wet polluted path can form across the insulator, extending from conductors to conductors at a different potential. Dry tracking occurs in the absence of moisture.

Fire ignition may occur under AIA. This arc tracking mechanism can occur when an open circuit is present within the cable, such as when two shorted conductors are in contact if there is a poor connection between the cables with the connecting device, or during AACP.

2.6 Electrical Fire Mechanism

When a cable jacket is exposed to a heat source, whether its from an external or internal source, the vapor that is generated is known as the pyrolysis process. Pyrolysis is a decomposition process of solid fuel. The resulting vapors are mixed into the air to create a flammable mixture comprised of carbon and oxygen. This dangerous mixture continues to oxidize and becomes susceptible to self-igniting or igniting from other heat sources. This phase is known as ignition.

Self-ignition occurs when the insulating material undergoes a chemical reaction producing heat that could either be internally stored within the material or released into the system through the boundaries. Once the amount of heat has exceeded the cable system heat transferring capacity, a thermal explosion can occur which can lead to self-ignition. To determine the self-ignition temperatures,the NT FIRE 045 method - Solid Materials: Spontaneous Ignition Temperature By Continuous Heating (Method, 1992), is typically used by placing the sample into an oven where the temperature is continuously and linearly raised until spontaneous ignition occurs. Another type of fire ignition mechanism that cables may experience is known as short-circuit ignition. During short-circuiting, an arc is created between nearby wires. An arc elevates the temperature of the cables, producing a small volume of intense heat. This can lead to degradation of the conductor (Turtola, 1999).

Due to the exposure of the heat flux, a pyrolysis front is formed and spreads across the surface of the jacket, known as fire propagation and rate at which the fire spread is also known as fire propagation rate. For fire propagation to reach a steady rate, convective heat release rates must have a certain amount of heat flux to exceed lower flammability

limit and maintain pyrolysis (Tewarson, 1994). The pyrolysis reaction rate increases rapidly with increasing temperatures. The final phase is known as combustion. Combustion occurs when the pyrolysis byproducts mix with air, oxidize, and generate heat and byproducts. Combustion is always resultant of vapors in a gas phase and solid material (the jacket) for the solid phase. This is because the carbon material just gets displaced in one of those two ways and the carbon is the fuel source for all fires.

Quantified by the National Institute of Standard and Technology (NIST) and the Factory Mutual Research Corporation (FMRC), the behavior of fire propagation can be divided into three categories: non-accelerating behavior, decelerating/non-propagating behavior, and accelerating behavior (Tewarson, 1994). Decelerating/Non-propagating behavior being when the propagation of the fire decreases over time. When the fire propagates past the source at a slow rate, it is known as non-accelerating behavior. Accelerating behavior describes the flame propagation going beyond the source at a rapid pace.

2.7 Electrical Field Effect on Cable Fires

Various testing procedures and simulations have been created in order to characterize the fire performance of the electrical wires. M.K. Kim et al. investigated the propagation rate of a flame over PE insulated electrical wire by applying AC fields. It was shown that by applying a low frequency of AC voltage to the flame, the flame would extinguish itself while high frequencies increased the propagation rate (M. Kim & Chung, 2011).

S. J. Lin et al. researched the impact that electrical fields have on flame propagation along an insulated wire with varying frequencies. Results showed that the propagation of the flame

along the wire increased because of nearby electric flux present at one end of the wire, which displayed three characteristics based on the applied voltage. Within each characteristic and dependent on the applied AC frequency sub-regime were created and displaying different flame shape and behaviors as the AC voltage and frequency increase the deposition of soot particles. More prolonged exposure to high frequency and voltage resulted in the dripping of the molten PE, which in turn reduced the propagation rate, and extinguishing the flame(Lin et al., 2007).

2.8 Radiation Effect on the Cable Behavior

Electrical power cables insulation and jacket may be subjected to several different types of environmental stressors, including radiation, temperature, moisture, humidity, vibration, chemical exposure, and mechanical stresses. Continuous exposure to these stressors can lead to degrading insulation and jacket materials and failure in cable function.

Electric cables exposed to a range of temperature and humidity conditions may result in insulation material degradation over time. Depending on the composition of the insulation material, the dielectric breakdown voltage varies. For example, if the insulation breakdown voltage falls below 7kV, the increased frequency of the voltage will continue to flow at a lower magnitude, leading to a higher carbonization rate of the insulation material and higher probability of becoming an ignition source from arcing.

H. Yang et al. used a Pyrolysis Combustion Flow Calorimeter to find the decomposition from thermal exposure for varying cable samples and their flammability characteristics. Yang reported that the highest flammability risk is from the PVC cables when compared to other

cable jackets due to having a decomposition temperature range between 200°C -300 °C. PE jacket remained chemically stable until 350 °C (Yang, 2013).

Radiation techniques, such as aging or irritation of the insulating jacket involves a physical and chemical process with their rate dependent on the surrounding applied temperature. An investigation conducted by Sandia National Laboratories investigated the thermal aging effects on the damage capability of fire produced by the electric cables. Qualified nuclear cable material was characterized. The cables material characterized in this report were XLPE and EPR insulations and neoprene and Hypalon jacket materials (Nowlen, 1991). The material behavior was compared under both aged and unaged conditions when exposed to a constant temperature until the conductors shorted out. Results showed that aged cables (Neoprene/XLPE) have a higher thermal damage threshold (325-330 °C) that is 25-35 °C higher than unaged cables (350-365 °C). In case of the Hypalon jacket/EPR Insulation cable, the aged cables (345-350 °C) displayed high vulnerability to thermal damage than compared to the unaged cables (365-370 °C). This study concluded that the thermal aging effect on electric power cables is dependent more on the insulation material composition than the jacket material. Evaluating the thermal damage threshold alone is not enough to adequately evaluate the flammability characteristics of the electrical wires.

The aging behavior of ethylene-propylene rubber (EPR) and chlorinated polyethylene (CPE) jacket material at an exposure temperature of 140 °C showed that a tensile behavior, elongation-at-break was about 50% after 50 days and Fourier Transform Infrared Spectroscopy (FTIR) revealed a change in chemical bonds. With the use of a carbonyl index (CI), it was discovered that as the EPR experiences thermal exposure in the air, oxygen atoms are deposited into the polymer backbone, which increased the carbonyl bonding. During the

aging process, the carbon bonds were disrupted, and the methylene bonds decreased. The author suggested that FTIR would be a useful tool to monitor the in situ conditions of the cables (Fifield & Shin, 2017).

An investigation carried out in the Savannah River Nuclear Reactor characterized cable degradation using a series of tests such as tensile testing, infrared spectroscopy, mandrel bend tests, chemiluminescence measurements, radiation aging, and thermal aging (Mecheri et al., 2013). A 60 m cable was removed from the plant C-reactor and characterized the degradation behavior. The cable is composed of a seven (7) copper conductor encapsulated in different color medium density PE insulation material surrounded by a thin nylon sleeve and shielded by a PVC jacket with about 12 years of radiation exposure. Visual results showed that the external surface of the PVC jacket had no signed of embrittlement. Under the jacket, the PE insulation material was brittle and varied in flexibility along the length of the cable. Tensile test results showed a significant reduction in the elongation behavior of the PE insulation while the PVC jacket material behavior remained the same as unaged cable. Accelerated aging results showed that both separately; the degradation was significant with similar rates. Cables that were aged in this experiment showed various degradation characteristics similar to those deteriorated cables in the nuclear reactors (Gillen et al., 1982).

As mentioned, irreparable damage to the material while in service can be caused by thermal aging. Thermally aged XLPE has significantly lower mechanical and electrical properties and changes in crystallinity when compared to unaged XLPE. Thermally aged XLPE showed significant material degradation after being aged under 135 °C and 150 °C. The thermal degradation mechanism identified included decomposition reactions, polymer chains break, and oxidation.

Cables subjected to irradiation damage affect both mechanical and electrical properties. Studies show that for some type of PE materials (such as PEs, PVCs, and EPRs) as the radiation dose increases the degradation of the mechanical properties increases (Maier & Stolarz, 1983). Irradiation can lead to a radiation-induced degradation process, producing gases that evolved with respect to the amount of oxygen and the polymers molecular structure. Past studies have shown that heavily irradiated cables material can cause the gases to be entrapped within the polymer structure that produces an increase in the internal pressure, resulting in a strain within the structure (Bowler & Liu, 2015). This can cause deterioration in both electrical and mechanical properties. The polymer material under irradiation conditions results in molecular changes such as de-polymerization, chain cross-linking, chain scission, and oxidation. If the polymer is dominated by the chain scission molecular behavior under irradiation, the material significantly deteriorates.

2.9 In Situ Testing Methods

The variety of tests available are only able to provide a particular aspect of the mechanical and electrical performance under specific configurations and conditions (Glass et al., 2017). Destructive testing methods do not provide adequate in-service performance information, repeatability of the tests is limited, and the cables under evaluation do not experience the same environmental stressors equally. In order to accurately characterize the aging behavior of cables, more in situ methods (also known as cable monitoring) have been developed to monitor and assess the cable degradation with respect to operating time (Simmons et al.,

2012). The following sections will cover frequency-domain reflectometry, reverse time-domain reflectometry, impedance tests, and time-domain reflectometry.

2.9.1 Time-Domain Reflectometry

Time-domain reflectometry (TDR) is a radar detection technique used to measure the reflections of a step or impulse signal along a single conductor to detect and locate any changes in the conductor impedance (Glass et al., 2017) (Jones et al., 2002). A sensing waveguide is connected to a coaxial cable and an electromagnetic (EM) pulse is transmitted into it. A cable comprised of a uniform impedance network, subjected to an EM pulse, will have no reflections and the signal will be entirely absorbed by the receiving termination (Lin et al., 2007). A cable with a compromised impedance network, such as open or short circuits, or a combination of mechanical or physical damages that affect the functionality of the cable, will display reflections while simultaneously redirecting the signal back to the source. To determine the location of the defect within the impedance network of the cable under investigation is to determine the distance traveled by the reflected signal. The distance traveled by the reflected signal can be quantified by the product of the signal velocity and signal propagation time. TDR can determine the magnitude of the impedance change within the cables by analyzing the reflected signal amplitude and inherent cable attenuation characteristics. TDR testing units are available to perform in situ evaluation of nuclear power plant cables. This low-voltage test can be conducted with no risk to the cables, assessing the condition of the conductor for any anomalies. Little information can be obtained on the subtle changes in the cables insulation.

The advantages of using TDR is that the testing method is easy to employ, uses inexpensive equipment, has low test voltage. Additionally, its period testing can provide historical data of aging cables and can locate the area of cable systems through impedance detection method. The disadvantages of using TDR for cable degradation assessment are the high level of skills required to conduct testing and analysis, interference from electrical noise, locating impedance discontinuity is dependent on the correct velocity of propagation (Hernandez-Mejia, 2016).

2.9.2 Reverse Time-Domain Reflectometry

Reverse time-domain reflectometry (RTDR) is a method used to test the shielding quality around the conductor multi-axial cable. In order to evaluate the quality of the shielding, a high-frequency pulse is transmitted through the shielding material, and a return signal is monitored. The coupling point can be determined by the time delay recorded. RTDR coupled with TDR can find the location of the connections, splices, fault, and the end of the device (Campbell et al., 2012).

2.9.3 Impedance Test

Impedance tests are useful in characterizing breaks, splices, and faulty connections. LCR is often coupled with TDR to further identify any faults within the circuit due to moisture intrusion, short circuit, open circuit, etc. (Campbell et al., 2012). Measurements are taken by using an LCR specific instrument that implements an AC signal at certain frequencies

to validate the characteristic of the cable. Cable degradation behavior is determined by the mismatches, imbalances, or unexpected impedances that are recorded (Agency, 2012).

2.9.4 Frequency-Domain Reflectometry

One method for inspecting the characteristics of cables is the Frequency-domain reflectometry method known as (FDR), (Glass et al., 2017) (Adl-Zarrabi & Kakavand, 2015) FDR is used to detect and localize faults in a single conductor of a cable. This process is conducted by sending a frequency down the lines and measuring the resultant response. The non-destructive nature of this inspection techniques comes from the low-voltage signal, of > 5 voltage, applied along the length of the cable, which does not oppose any risks to the cable or operators. The physical location of signal reflections can be determined by converting the frequency-domain data into a time-domain format. The sensitivity to cable degradation is higher in FDR than in TDR. TDR is limited to finding out if the conductor is open circuit or short circuit. Cable degradation can be characterized further by FDR, specifically in insulation degradation. Cable degradation associated with thermal degradation using FDA in XLPE and EPR cables is a limited and ongoing research area.

The benefit of using FDR is that this method is capable of locating faults and cable aging-related degradation, differentiating between mechanical and thermal damage, locating and monitoring thermal hot spots, monitoring cable aging in thermally stressed environments, inaccessible areas, and in conduits, and determining the characteristics of the entire length of the cable from one spot (Corporation, 2015).

2.10 Summary of State of the Art

In summary, the majority of the studies carried out on qualified nuclear cable have focused on the material degradation properties, with respect to insulation material properties and various environmental conditions. Research in this area concentrated on the characterization of the mechanism that leads to cable fires. Several mathematical models have been developed to analyze and predict the flammability characteristic of power cables. There is still a lack of literature available to evaluate the irradiation or thermal aging effects on the flammability characteristic of the cable jacket material.

Chapter 3

Experimental Procedure

3.1 Overview

This chapter represents the experimental methodology for determining the changes in the aging cable. The acquisition and conditioning of the cable samples are discussed in detail, followed by the methodology behind the physical characteristics, and flammability characteristics. Also, the testing methodology for in situ testing of the cable (to determine its' relative changes in flammability characteristics) is evaluated. All of these points are used to consider the impact that aging has on the cable's overall qualification to continue operations. The conceptual model for this research is shown in Figure 3.1 below.

3.2 Methodology

The experimental work can be divided into a few main groups of research stages that are interlinked into one another:

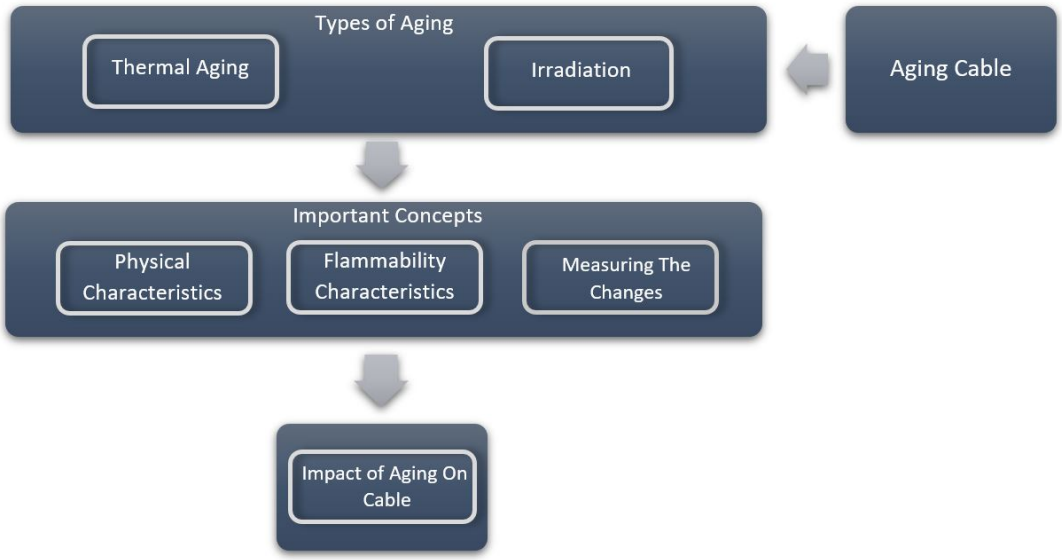

Figure 3.1: Conceptual model that describes the prevailing logic behind the research.

1) The cable jacket's physical characteristics. This was done to investigate the physical changes that occur with thermal aging and irradiation. The physical changes are determined by using the following tests: Elasticity Testing, Fourier-Transform Infrared Spectroscopy (FTIR), and Scanning Electron Microscope (SEM).

2) The cable's flammability characteristics. The effects that thermal aging and irradiation have on the cable's flammability characteristics are dependent on the physical changes of the cable's jacket. The flammability characteristics are determined by using the following tests: Differential Scanning Calorimeter, Thermo-Gravimetric Analysis, Cone Calorimeter, and UL 94 Flame Spread Test.

3) The resultant change in the cable's reactance. The change in the cable's reactance can be quantified and correlated to the flammability characteristics of the cable. This testing is

done by treating the cable as a transmission line and recording the reactance as a function of input frequency. To the knowledge of the author, this is the first time that the effects of thermal aging and irradiation have been correlated to the flammability characteristics (of cable used in industry) and a method for determining these changes has been studied.

3.3 Conditioning of Cable

3.3.1 Cable Samples

The cable samples obtained for testing were allocated based on the availability of resources and what is commonly used in practice. The three types of cable that were used are Rockbestos Firewall III XLPE insulated 3 conductor cable, General Cable's ULTROL 60+ Power (3 conductors with a ground) Cable, and Boston Insulated Wire (BIW) cable. Table 3.1 is an illustration of the number of nuclear power plants that use these cables in daily operation.

Rockbestos Firewall III XLPE insulated cable is a class 1E flame retardant/radiation resistant power cable for use in nuclear applications.

Table 3.1: Cable Manufacturer and Usage in Nuclear Power Plants.

Rank	Manufacturer	Insulation	# Plants
1	Rockbestos Firewall III	XLPE	61
2	ULTROL 60+	XLPE	30
9	BIW	EPR	19

Note. Plant statistics derived from (Fifield & Duckworth, 2016).

The cable is thermoset (meaning that the polymer chains are cross-linked with other molecules, hence Cross-Linked Polyethylene-XLPE) resulting in a more robust cable jacket that will not melt but rather burn until it decomposes. This cable has a minimum thermal life expectancy of 40 years at 90°C in nuclear applications (Marmon, 2016). The cable consists of 3 conductors insulated individually with a jacket around all of the conductors. Figure 3.2 is a cross-section image of the unaged Firewall III cable (the cable that is considered stock and not influenced by thermal aging or irradiation) taken with a microscope.

General Cable's ULTROL 60+ XLPE insulated Cable is a class 1E flame retardant/radiation resistant power cable for use in nuclear applications. The cable is rated for 600 V, and consists of 3 conductors, and a ground that is also a shielding. This cable is thermoset and is qualified for 60 years of service life in nuclear applications (Cable, 2013). Figure 3.3 is a cross-sectional image of the unaged ULTROL 60+ cable.

Boston Insulated Wire (BIW) EPR insulated cable is flame and radiation resistant. This cable is rated for 600 V and is intended for instrumentation. The cable consists of two conductors and ground with shielding. The two conductors are #16 AWG, and the drain/ground is #18 AWG. This cable is thermoset. Figure 3.4 is a cross-sectional image of the unaged BIW cable.

The cable is either thermally aged or irradiated. It was necessary to have a complete understanding of how much the sample was thermally aged or irradiated. The Firewall III cable samples consist of 7 different types. The first sample is unaged cable; this cable is an unused stock that has not been subjected to thermal aging or irradiation. The second sample is irradiated for 120 days at 140 Gy/hr (Gray/hr) using a Cobalt 60 source. The third sample is thermally aged for 15 days at 120°C using a furnace.

Figure 3.2: Cross sectional microscope image of Unaged Rockbestos Firewall III XLPE insulated cable.

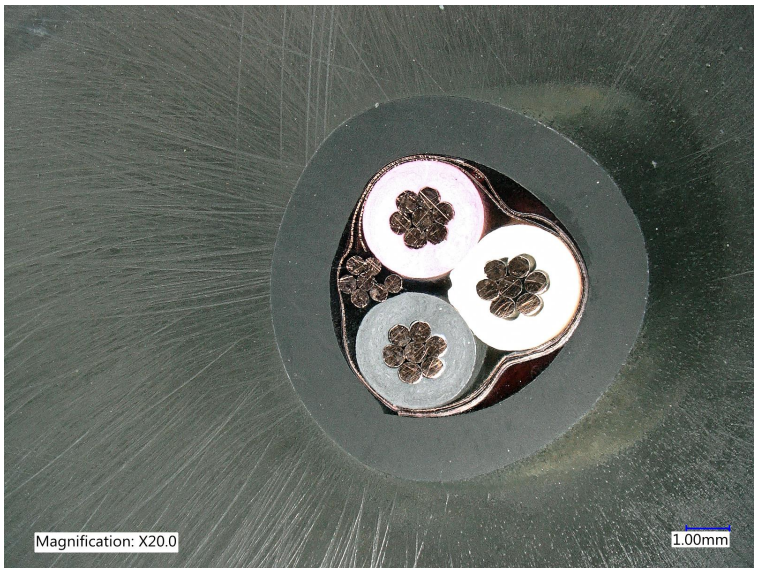

Figure 3.3: Cross sectional microscope image of Unaged ULTROL 60+ XLPE insulated cable.

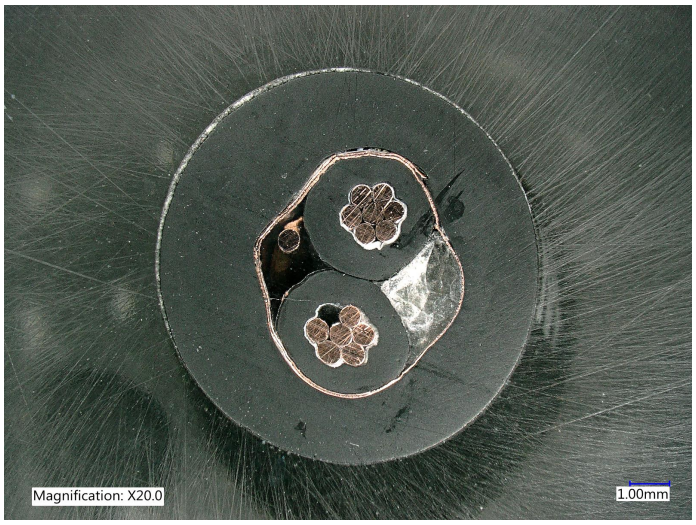

Figure 3.4: Cross sectional microscope image of Unaged Boston Insulated Wire (BIW) EPR insulated cable.

The fourth and fifth samples are thermally aged for 30 days and 45 days respectively at 120°C. The sixth and seventh samples are irradiated for 30 days and 60 days respectively at 140 Gy/hr. Table 3.2 is a summation of all of the samples used for testing.

The ULTROL 60+ cable has 2 different samples. The first sample is unaged and is used as a control. The second sample is thermally aged for 7 days at 150°C. The Boston Insulated Wire has 2 samples as well where one is unaged, and the other is thermally aged for 7 days at 150°C. These samples provide a progressive foundation of the changes that thermal aging and irradiation have on the cable. Figure 3.5 is an image of a holder containing a small piece of each of the 11 samples used for testing.

3.3.2 Thermally Aged

For the cable samples to be used for testing it was necessary to have a full and accurate understanding of the aging characteristics of the cable.

Table 3.2: Thermally Aged and Irradiated Cable Samples.

Sample	Cable Type	Aging Characteristic
1	Rockbestos Firewall III	Unaged
2	Rockbestos Firewall III	Irradiated for 120 days at 140 Gy/hr
3	Rockbestos Firewall III	Thermally Aged for 15 days at 120°C
4	Rockbestos Firewall III	Thermally Aged for 30 days at 120°C
5	Rockbestos Firewall III	Thermally Aged for 45 days at 120°C
6	Rockbestos Firewall III	Irradiated for 30 days at 140 Gy/hr
7	Rockbestos Firewall III	Irradiated for 60 days at 140 Gy/hr
8	ULTROL 60+	Unaged
9	ULTROL 60+	Thermally Aged for 7 days at 150°C
10	Boston Insulated Wire	Unaged
11	Boston Insulated Wire	Thermally Aged for 7 days at 150°C

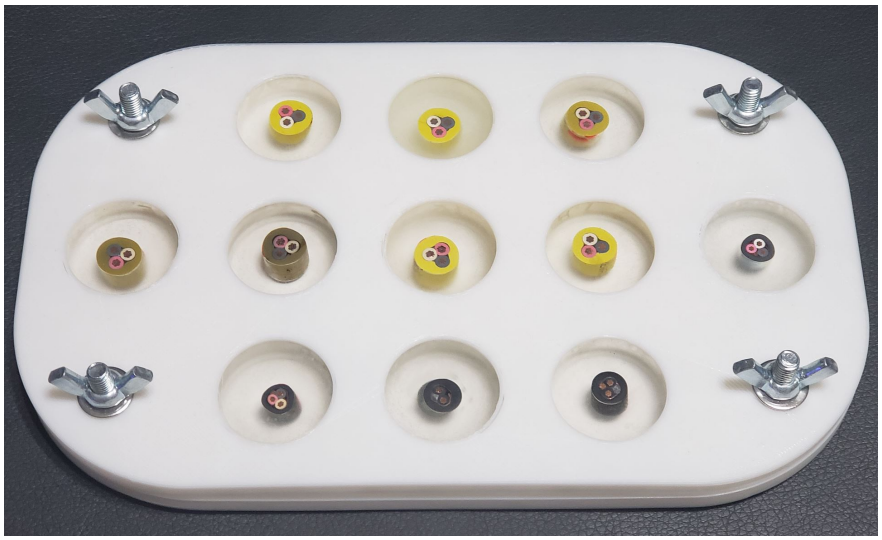

Figure 3.5: Sample holder containing a small piece of each sample. From top left to bottom right: Sample 1 - Firewall III unaged, Sample 2 - Firewall III irradiated (120 days at 140 Gy/hr), Sample 3 - Firewall III thermally aged (15 days at 120°C), Sample 4 - Firewall III thermally aged (30 days at 120°C), Sample 5 - Firewall III thermally aged (45 days at 120°C), Sample 6 - Firewall III irradiated (30 days at 140 Gy/hr), Sample 7 - Firewall III irradiated (60 days at 140 Gy/hr), Sample 8 - ULTROL 60+ unaged, Sample 9 - ULTROL 60+ thermally aged for 7 days at 150°C, Sample 10 - Boston Insulated Cable Unaged, Sample 11 - Boston Insulated Cable thermally aged for 7 days at 150°C.

The cable samples were placed into a furnace to age them to a predetermined amount. This allows for not only the control of total exposure but also the control over exposure rate that the cable undergoes. This process was used to get accurate amounts of thermally aged samples. Part A of Figure 3.6 shows a furnace that is used to thermally age cable and part B of the figure shows how the samples are arranged inside of the furnace. The samples are hung by a small wire and spaced out to allow a more uniform amount of heat to be taken into the samples. The samples obtained were thermally aged at 120°C and 150°C. The 120°C thermal aging is standard practice as it can be done for a longer period of time without any adverse effects that arise from heating the samples to quickly (such as burning the samples). The 150°C thermal aging is acceptable as the samples were only subjected to that temperature for 7 days and thus no adverse effects were observed.

3.3.3 Irradiated

The Rockbestos Firewall III cable was the only cable that was irradiated for testing. This cable was sectioned out and irradiated at different levels to obtain an understanding of how the progression of irradiation impacts the tests. Controlled irradiation of cable is difficult as obtaining a method of irradiation is not well established. Oak Ridge National Laboratory (ORNL) provided this project with a means of irradiating cable to the desired levels. ORNL has a spent Cobalt 60 fuel source that is ideal for gamma irradiation of this nature. The pressure vessel/irradiation chamber is shown in Figure 3.7.

The irradiation chamber of the pressure vessel is small and would only allow for samples up to 18" in length to be placed inside at any given time. The smaller cable specimens were

(A) Furnace.

(B) Arrangement of samples.

Figure 3.6: An example of a furnace that is used to thermally age cable in a controlled manner (A) and an example of how cable samples are arranged inside of a furnace (B).

Figure 3.7: The Colbalt 60 source irradiation vessel that was used to irradiate the cable samples (image shown is of the Rockbestos Firewall III XLPE cable being irradiated).

hung inside of the chamber and irradiated for their respective amounts of time. This process is costly, difficult to obtain, and time-consuming since only a certain number of samples can be placed inside at one time, and the use of the machine is limited. It was determined that the continuous irradiation of one cable type would provide an adequate understanding of the characteristic changes observed.

3.4 Characterization of Cable

3.4.1 Elasticity Testing

The indenter polymer aging monitor (IPAM) is used to measure the relative elasticity of the cable. The indenter records force, deformation, and velocity as a function of time on a localized point of the cable sample.

This information can be graphed and related to physical changes in the cable's characteristics that result from aging, thermal aging, or irradiation. The cable clamp assembly is connected to the DAQ/power supply which is connected to the handheld PC. The device operates by taking the handheld cable clamp assembly and inserting a cable in the V holder. With the cable inserted the device is turned on and the indenter probe begins deforming the cable, while simultaneously recording the data on the handheld PC. The device uses pure force and deformation sensors to record the data. Figure 3.8 is an image of the indenter used for testing.

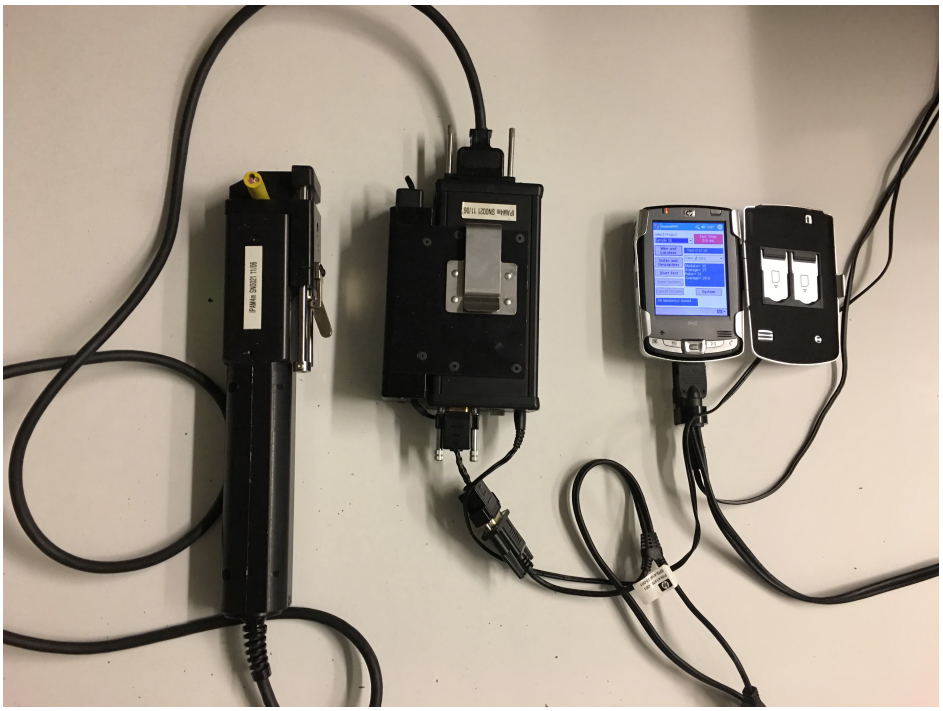

Figure 3.8: Indenter polymer aging monitor used to test elasticity of cable.

The essential parameters to observe from the testing are the force and deformation. The recorded force graph can describe the elasticity of the cable. The modulus of elasticity is a function of the recorded force and deformation at a given point in time. If a sample's force curve reaches its peak faster, it is because the deformation is lower which results in a lower modulus of elasticity (meaning it is not easily deformed and is less pliable). A substantial decrease in the modulus of elasticity is in relation to the jacket of the cable becoming harder, or dehydrated; subsequently, an increase in the modulus of elasticity is in relation to the jacket of the cable becoming softer, or more hydrated. These characteristics can be correlated to aging, thermal aging, or irradiation as these processes directly change the cable jacket's physical characteristics.

3.4.2 Scanning Electron Microscope (SEM)

Scanning electron microscope (SEM) is an ideal tool in creating a virtual representation of the surface of a sample. The SEM can also be used to assess the chemical composition of the sample. These are essential characteristics that can be used to develop an understanding of the sample's physical shape, changes in chemical composition, and morphology.

The SEM works by generating a beam of electrons focused down a column towards the sample. The SEM scans the sample with these electrons, and as the electrons bombard the sample, they are either absorbed or emitted. This process is typically recorded with a cathode ray tube (CRT). The emitted electrons that the CRT picks up are correlated to the electrons emitted by the SEM. This allows a virtual image to be constructed. The chemical composition is also determined by the relative amount of backscattered electrons. The chemical composition of the sample is directly relative to the number of electrons that bounce off the nuclei of the sample's atoms.

The cable samples are tested using the SEM process to determine the physical and chemical characteristic changes that they have undergone. This process helps in explaining how the changes in flammability characteristics are developed and how the aging processes affect the physical characteristics of the samples. The SEM used for testing is a JEOL 5800LV (Spilde & Adcock, 2006) and is shown in Figure 3.9.

3.4.3 Fourier-Transform Infrared Spectroscopy (FTIR)

Fourier-Transform Infrared Spectroscopy is a process used to determine the chemical structure of a sample. The chemical structure of a compound is unique providing a means

Figure 3.9: Image of Scanning Electron Microscope (JEOL 5800LV) used for testing.

of determining even the slightest changes in organic composition. FTIR is typically used to either determine what an unknown sample is made of or how a sample is altered from its original chemical structure (such as additives in the formation of the sample). This can be used to verify the material that the sample is made of and what changes are present between similar samples.

FTIR works by taking an infrared radiation source and running it through a compartment containing the sample. Figure 3.10 shows an image of the model of FTIR that was used.

The amount of infrared radiation (intensity) that passes through the compartment is unique of the chemical structure of the material. The peaks of the wavelength that passes through are related to known compositions, and thus the output can be compared to other samples. The FTIR that was used is a Parkin Elmer Spectrum 1000 with a diamond anvil cell. The diamond anvil cell provides more detail especially with samples that are difficult to read (such as paint, and fiber structures)(Learner, 2002).

Figure 3.10: Image of a Perkin Elmer Spectrum 1000 Fourier-Transform Infrared Spectroscopy (FTIR) used for testing.

3.4.4 Differential Scanning Calorimeter (DSC)

Differential Scanning Calorimeter is a process that observes the material's heat capacity (Cp) as it changes with temperature. The technique looks for significant changes in heat capacity as this signifies points where the material melts, cures, undergoes a phase change or undergoes a glass transition. Most materials will undergo physical transitions when heated, providing excellent details on several aspects of the material ranging from burning characteristics to variations in transition temperatures.

DSC works by measuring and comparing the differences in temperature or time between the sample and reference material, while the samples remain at a preset temperature. The reference material's heat capacity properties are predefined allowing control for the testing. The sample's transition points are easily defined because the sample will either take more or less energy to change its temperature. This increase (exothermic reaction) or decrease (endothermic reaction) in required energy corresponds to transitions such as crystallization

or melting respectively. The DSC process can reveal characteristics of changes in the burning of samples that have undergone various forms of aging or irradiation. Part A of figure 3.11 shows the DSC used for testing and part B shows the reference pan and sample pan used for testing.

3.4.5 Thermogravimetric Analysis (TGA)

Thermogravimetric Analysis is a process that records the changes in weight of a material as a function of temperature while the sample is exposed to increasing amounts of temperature (Earnest, 1988). This is typically performed in an enclosed nitrogen environment or a vacuum. The process typically ranges in temperature from 25°C to around 900°C. Providing an acceptable range for most materials to be studied for changing weight relative to varying temperatures.

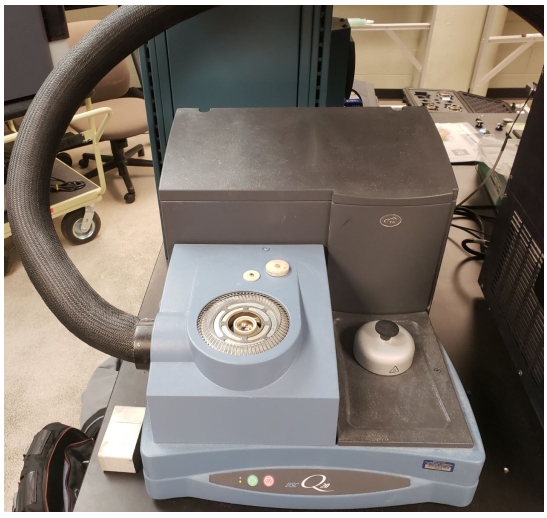

(A) DSC Machine

(B) DSC Pans in Machine

Figure 3.11: An example of a Differential Scanning Calorimeter that is used for testing (A). An example of the DSC pans used for testing where the pan on the left is the reference and the pan on the right is the sample (B).

This is an essential characteristic as it can be related to transition temperatures, ignition temperatures, oxidation temperatures, and any abnormal characteristic temperatures between samples.

TGA works by taking small pieces or powder from a sample and heating the sample while continually measuring the changes in mass of the sample. The TGA performs this operation by hanging a sample from a scale (that measures weight) and lowering it into a furnace that increases in temperature as a function of time where a thermocouple records this change in temperature. This is a relatively simple process to visualize as there are not a lot of variables involved. The key components are the change in temperature, change in mass, and the understanding of how the two correlate to each other. Part A of figure 3.12 shows the TGA used for testing and part B shows a closer view of the sample trays that were loaded for testing.

3.4.6 Cone Calorimeter

The Cone Calorimeter is used as a means to record the heat release of a sample being burned. This device utilizes the understanding that the change in the heat release rate of a burning object is directly proportional to the amount of oxygen used in combustion. The device utilizes a few main components: a sensor to measure the oxygen, a heat source that is set to the desired amount of output, and a fan to exhaust the fumes and keep a steady amount of air flow through the system.

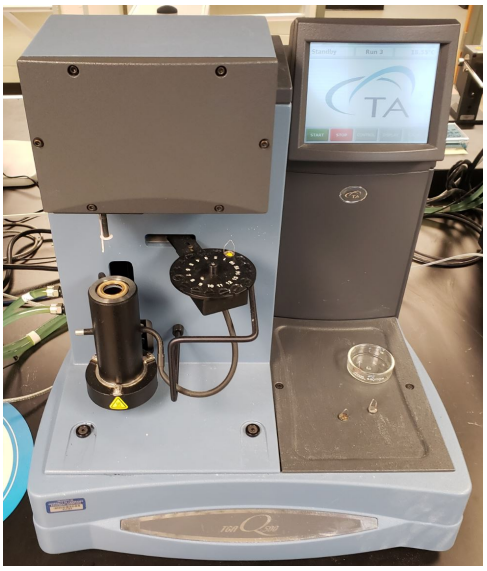

(A) TGA Machine

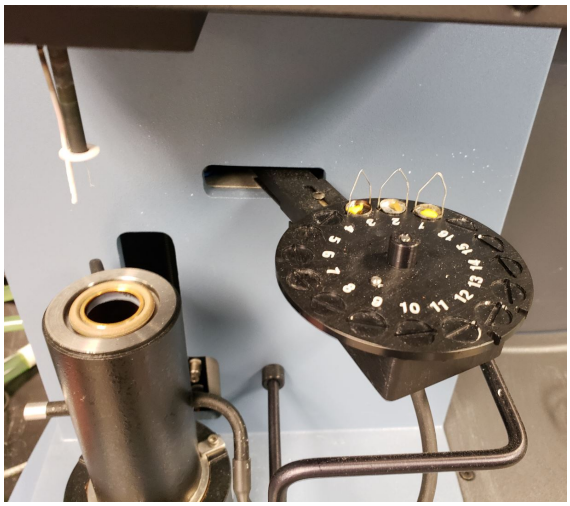

(B) TGA Sample Trays

Figure 3.12: An example of a Thermogravimetric Analysis machine that was used for testing (A). A large view of the furnace and sample trays that were prepared for testing (B).

The Cone Calorimeter requires that samples fit into a metal frame to hold the sample during the test and adequately contain the heat being introduced to the system. The variances in not only the peak heat release but also the time it takes for the heat release to progress before reducing or burning out are essential to understand. In comparison between samples, if one sample ignites and/or reaches its peak heat release faster then it will likely be a hotter and progressively spreading fire. It is also true that if one sample has a longer heat release rate growth then it will likely spread slowly and smolder and may be more difficult to extinguish.

The samples were tested using the Cone Calorimeter to determine changes in heat release characteristics. These changes can be directly related to the way that the material will burn. This information is critical in determining the differences in flammability characteristics between samples. Figure 3.13 shows the Fire Testing Technology's Cone Calorimeter that was used for testing.

3.4.7 UL 94 Flame Spread Test

The UL 94 Flame Spread Test, a standardized test, laid out by Underwriters Laboratories (UL), is used to give materials such as plastics and rubbers a qualification for flammability characteristics (Laboratories, 1997). In many applications, if a material is to be used in practice, the material must meet the UL 94 standard to be considered safe enough to use (as not to be a safety hazard). The test has different levels of certification that are directly dependent on how long the material burns and the potential for material to spread to other materials.

Figure 3.13: Image of the Fire Testing Technology Cone Calorimeter used for testing.

The UL 94 test is an appropriate means of certifying if the samples meet quality standards even after being subjected to various conditions.

The UL 94 Flame Spread Test is performed by setting up a few key components. The test requires a steady flame supplied by a Bunsen Burner, a ring mandrel to hold the test specimen, some cotton, and a stopwatch. The test specimen is secured on the ring mandrel, and the burner is positioned where the open flame is 10 mm below the bottom of the sample. The burner is angled at 45°C to prevent the burned material from falling onto the burner instead of the cotton. The cotton is positioned to catch the dripping material to determine

if the material will catch the cotton on fire or not. Figure 3.14 shows how the UL 94 Flame Spread Test is setup (Laboratories, 1997).

The test is carried out by moving the sample into the open flame for 10 seconds then removing it from the flame. The sample is observed for melting, and dripping until the flame is extinguished. The time the sample is removed from the burner until the flame self-extinguishes is recorded. If the flame is self-extinguished, then the sample is again placed in the open flame of the burner for 10 seconds thus repeating the process an additional time. The time after the sample is removed from the burner until the flame is extinguished is recorded, and the test is then completed. Table 3.3 shows the highest level of classification for the UL94 test and the respective requirements.

The UL 94 test has three levels of classifications V-0, V-1, and V-2. The best classification is V-0 as this means the material is considered to be of the highest basic standard to be used in practice without significant flammability risk.

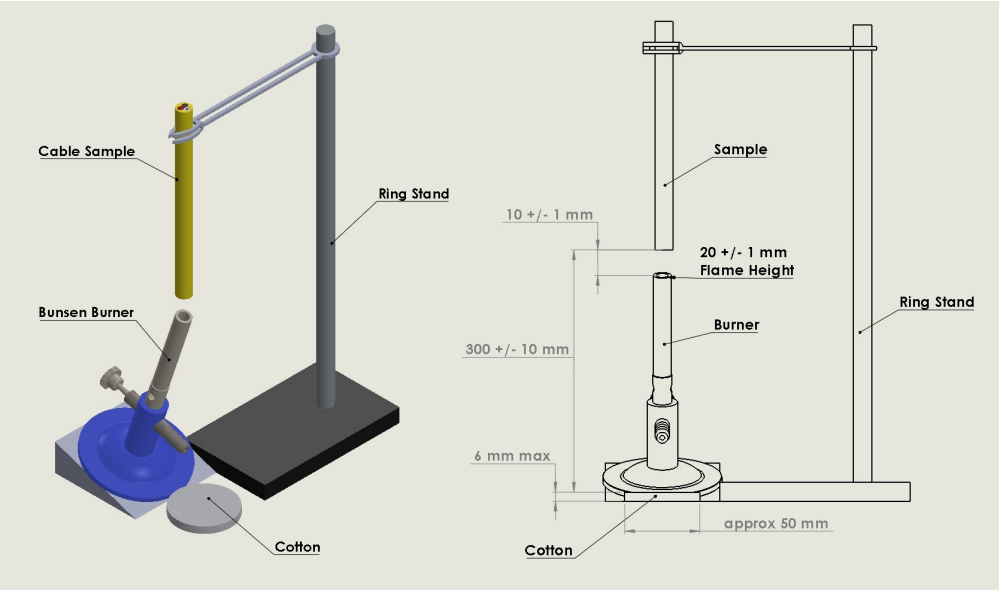

Figure 3.14: Schematic of UL 94 Flame Spread Test .

Table 3.3: Highest Classification of UL 94 flame spread test criteria used for classifying samples.

Criteria Conditions	V-0
Time until flame self-extinguishes t_1 or t_2.	$\leq 10s$
Total flame time after exposure (t_1 plus t_2 for the 5 specimens).	$\leq 50s$
Flame or afterglow time for a specimen after the second flame application ($t_2 + t_3$).	$\leq 30s$
Flame or afterglow of a specimen up to the clamp.	No
Cotton ignition.	No

Note. Testing criteria classification derived from Laboratories (1997).

The main components of the classifications are based on the afterflame time of the first and second exposure to the burner along with the ignition of the cotton. The main differences between classifications V-0 and V-1 are the afterflame time after the first and second exposures to the burner; while the only difference between V-1 and V-2 is the ignition of the cotton below the sample. This test is used to verify that the samples are safe to use (in the industry) after various exposures to certain conditions.

3.4.8 Reactance Measurements

Reactance Characteristics

The capacitive and inductive reactance of a conductor is widely understood as fundamental characteristics of electrodynamics. The capacitive reactance is a direct function of the capacitance of a conductor. Equation 3.1 is used to determine the capacitance of a conductor while Equation 3.2 shows the relation of capacitance to capacitive reactance (Okonite, 2018).

The importance of the capacitance equation is that the changes in capacitive reactance of like cable can be compared by observing the variables that can change between cables during a process such as aging. As such, these equations are only used to provide an understanding of the characteristics that can impact the capacitive reactance curves for a cable.

$$C = \frac{7.35 \times SIC}{\log \frac{D}{d} \times 10^6} \times L \tag{3.1}$$

$$X_C = \frac{1}{2\pi f C} \tag{3.2}$$

Equation 3.1 uses the following variables: SIC - the insulation's dielectric constant, C - conductor capacitance in Farads, d - insulation's smaller diameter, D - insulation's larger diameter, and L - the length of the conductor. The main takeaway from this equation is that the capacitance varies with changes in characteristic diameters (D and d) and changes in the dielectric of the insulation (SIC). This equation is also a function of length which can directly shift the reactance curves. This shift in reactance is something that must be accounted for to evaluate systems of varying lengths. This could be done by essentially dividing out the length and obtaining a curve that is per unit length for the unaged reactance curve and then re-evaluating it at the desired length. A dynamic model could be created to do this for any length of the cable.

The length of transmission lines (when measuring the reactance) also impacts the frequency at which the reactance curve starts or stops due to a shift in the wavelength. To be clear, shifting the wavelength does not change the reactance curve but simply shifts the location along the curve that is first recorded. It is necessary to record the reactance

curves where the first reactance curve is recorded in full from start to stop. This is easily done by leaving the cable open on one end. Then the different lengths will cause either more or fewer resonance curves to be recorded. Equation 3.3 shows the commonly understood equation for wavelength. This equation is important to consider as the wavelength (λ - m), frequency (f - Hz), and the wave speed (c - m/s) will not change as the cable length changes. The changes in cable length simply do not allow the full propagation of the wavelength to occur so only a portion of it is recorded.

$$\lambda = \frac{c}{f} \tag{3.3}$$

This means that a standard value could be determined for a specific brand/model of cable and used to model against an in situ measured cable (regardless of length) by correlation of the wavelength, and normalization of the reactance (in terms of length). This could also be achieved by merely shifting the unaged reactance curve to begin at the same point that the aged reactance curve does (as the general shape of the curve should not change with variances in length unless outside interference is observed). When measuring the capacitive reactance in situ, it is not necessary to consider the impact that the conductor's surroundings have on the final result as the measured capacitance is not easily influenced by its surroundings.

If a baseline for the capacitive reactance is accurately determined then the systematic differences from aged cables can be correlated to two distinct characteristics - the first is the dielectric constant for the insulation and the second is the inner and outer diameters of the insulation. This shows that the physical changes in the insulation are directly proportional to the changes in the reactance of the conductor. This represents the capacitive reactance,

which is only half of the measured reactance curve and provides valuable information on forming an understanding of the subtle variances in cable reactance.

The inductive reactance of the cable should also be considered. It is essential to understand the fundamental variables that define it. One important characteristic of the inductive reactance is the cable's surroundings as this can impact the measured reactance. For instance, if the conductor is routed through a steel tray, it can have a higher inductive reactance. This can be resolved by using a correction factor when normalizing the recorded results. The correction factor (CF) depends on if the conductor is routed by burial (CF of 1), if it is routed by aluminum conduit/tray (CF of 1.2), or if it is routed by steel conduit/tray (CF of 1.5) (Association, n.d.). There are standardized tables that provide insight into how to form a correction factor that is appropriate for the application. If a cable is routed with unique circumstances that cause unforeseen characteristics, it may be necessary to either measure the cable in situ when it is installed or run an unaged conductor the same way to measure and determine a baseline.

The inductive reactance should only change as a result of the distance between the conductors if all other variables are kept constant, such as the correction factor for surroundings. This means that if the insulation changes in size or shape that the inductive reactance will correspondingly change as well. The aging process should cause the inductive reactance to be similar in nature but is still dependent on the amount of exposure. The amount of exposure will cause similar physical changes in the insulation (with other samples exposed to the same conditions) but to a more severe degree. This may lead to patterns forming in the recorded data.

Equation 3.4 is used to determine the inductive reactance of a conductor (Thue, 2003). It can be seen that the variables are as follows: f - frequency, S - the distance between conductor centers (conductor and neutral), r - radius of the center conductor, K - correction factor, and L - Length. The correction factor and radius of the center conductor should remain the same with varying cable samples that have been aged. The inductive reactance will vary with changes in length; however, this will only shift the curve and not change its' shape or size allowing correlation from normalization. Thus, changes in the inductive reactance is a direct function of the distance between the center of the conductor and the center of the neutral (S).

$$X_L = \frac{2\pi f(0.1404 \times \log_{10} \frac{S}{r} + 0.153)}{1000} \times K \times L \tag{3.4}$$

Observation of the changes in inductive and capacitive reactance can be used to correlate the physical characteristic changes of aging cable. The inductive reactance is directly related to the shape and size of the cable's insulation while the capacitive reactance is a direct function of the dielectric constant along with relative changes in the insulation. Well documented changes of these characteristics may prove beneficial to passively measuring the cable's properties.

Reactance Measurement Process

The inductive reactance, capacitive reactance, and resonant frequency of a cable can be measured as a function of frequency to determine critical changes in the cable's characteristics. This testing is done by treating the cable as a transmission line and recording the reactance as a function of input frequency. The change in the cable's reactance can be

quantified and correlated to the flammability characteristics of the cable. Figure 3.15 shows a typical illustration of the reactance measured as a function of frequency.

The reactance graph has three main characteristic points: the reactance below the zero line is the capacitive reactance, reactance measured above the zero line is the inductive reactance, and the point where the capacitive reactance transfers to inductive reactance by crossing the zero line is the resonant frequency of the system (Figure 3.15). As the cable is aged or changes its properties, it subsequently changes the three main points measured from

reactance. Another vital point to consider is the antiresonance of the reactance curve. This is the point where the reactance curve transitions from inductive to capacitive reactance. This point is useful in observing shifts in the reactance curves between samples. Observing the changes and correlating them to the physical modifications of the test specimens produces a better understanding of how the inductive and capacitive reactance can be related.

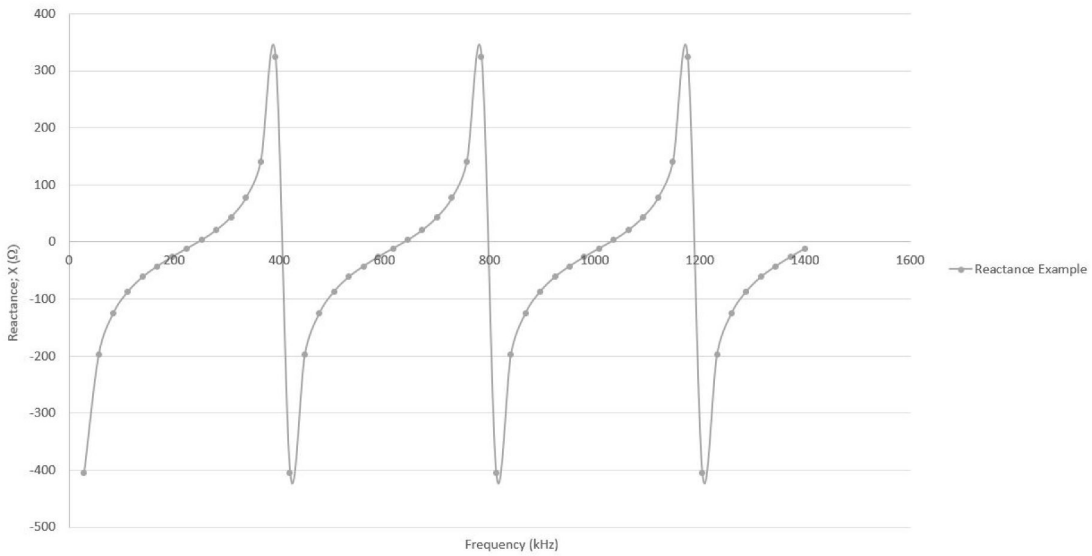

Figure 3.15: Illustration of a typical graph of reactance as a function of frequency for a length of cable.

Figure 3.16 shows the Antenna Analyzer used to measure the reactance of the cables used in this research. The Antenna Analyzer is a RigExpert AA-1400 and can measure accurately up to a frequency of 1.4 MHz (RigExpert, 2014). Each sample was tested individually with the AA-1400. The cable was connected to the antenna analyzer by connecting one conductor to the center pin and another conductor to the outer ring. The cable was open on one side (not connected) when tested. The reactance measurement was recorded for each sample.

The antenna analyzer operates on the theory of magnetic fields.

The center conductor of the cable sends out a low voltage frequency that in turn causes a magnetic field around the conductor. The second conductor (connected to the outer pin) is necessarily a ground and is only influenced by the changes in the magnetic field from the first conductor. The influenced changes are recorded as changes in reactance by the antenna analyzer. The magnetic field is firmly isolated inside the cable and not easily influenced by outside parameters.

Figure 3.16: RigExpert AA-1400 antenna analyzer used for reactance measurements of cable samples.

3.5 Summary of Experimental Procedure

This chapter focused on the methodology behind the research. In the chapter, the cable samples (used for tested) were reviewed to provide an understanding of the different types of samples and how they were conditioned for testing. Additionally, each testing method was expanded to provide a background on how each test was performed. Each test falls into one of three main brackets of determining certain aspects of the cable samples. The first bracket provides an understanding of the changes in physical characteristics of the cable samples: elasticity testing, SEM, and FTIR. The second bracket focuses on the flammability characteristics of the cable samples: DSC, TGA, Cone Calorimeter, and UL 94. The final bracket relates the flammability characteristics with the changes in physical characteristics through the use of reactance measurements. The following chapter will focus on the results of the tests that were performed.

Chapter 4

Research Findings

4.1 Overview

In this research, three cable types were studied, with varying types and amounts of artificial aging. The changes in physical characteristics, flammability characteristics, and in situ characteristics were studied. The resultant analysis is presented in this chapter. The data analysis methods include modulus testing, chemical structure testing, phase transition testing, weight loss testing, standard flammability characterization testing, heat release rate testing, and reactance testing. These methods provide an essential understanding of the characteristic changes that occur from the aging processes that the cables undergo.

4.2 Physical Characterization of Cable Jacket

4.2.1 The Impact of Aging Processes on the Cable Jacket's Elasticity

The Elasticity of a material is a function of the density of that material. The density of the material can be directly altered by the conditions that the material is subjected to. The changes in density of thermally aged and irradiated nuclear cable have been studied to show that these changes can be recorded and an idea of the length of exposure can be determined (Gillen et al., 1999). Observing the changes in density of the cable jacket can divulge not only information about the thermal aging and irradiation that the jacket has been subjected to but also the extent to which those aspects impact the flammability characteristics of the cable. For instance, if the density of the cable decreases and a resultant increase in heat release rate occurs then the change in density can help explain this occurrence.

The cable sample's that were tested had either been subjected to thermal aging or irradiation for a set period of time. The thermal aging causes the outside of the cable jacket to lose water content and essentially "dry up." This results in the surface of the cable jacket becoming extremely rough and effectively shrinking the jacket's size. A somewhat opposite effect occurs when the cable jacket is irradiated. The irradiation heats up the cable jacket from the inside with random areas of higher concentration. This causes the cable jacket to expand and become almost "spongy" in nature.

An indenter test was performed to test aspects of the cables elasticity. The first aspect that was tested focused on the velocity of the probe into the sample as a function of time.

As stated in a previous chapter, the indenter operates by driving a probe into the sample and taking key measurements. One of these measurements is the velocity at which the probe travels before it reaches a peak resistive force and stops moving (as to not damage the cable by puncturing the cable jacket). The velocity is constant until the probe stops. The time until this occurs is recorded. Figure 4.1 shows the velocity versus time for the Firewall III cable samples that are either unaged, thermally aged, or irradiated.

The results from Figure 4.1 show a noticeable deviation in the thermally aged and irradiated cable samples. The unaged sample reaches its peak time at approximately 17.67 seconds. The thermally aged samples (from least amount of thermal aging to the highest amount of thermal aging) have the following times: 16.3 seconds, 16.35 seconds, and 11.92 seconds. The irradiated samples (from least amount of irradiation exposure to the highest amount of irradiation) have the following times: 18.14 seconds, 16.54 seconds, and 27.81 seconds.

The times recorded for the velocity of the probe have distinct grouping and a trending pattern.

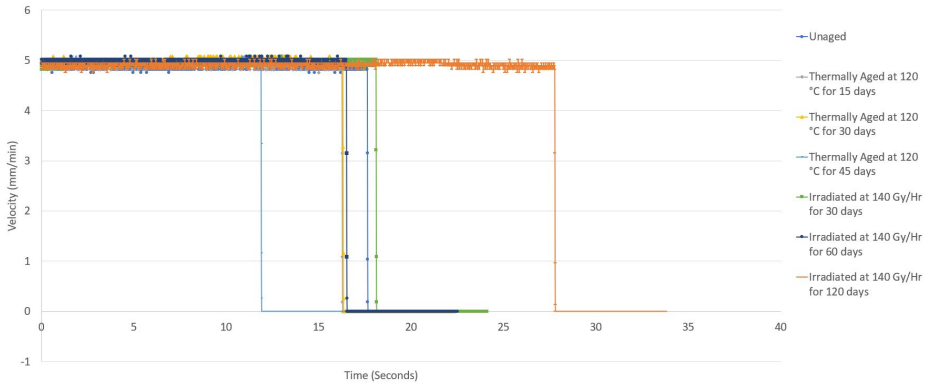

Figure 4.1: Velocity as a function of time for Rockbestos Firewall III XLPE cable that is unaged, thermally aged, and irradiated.

The thermally aged samples all have a shorter time (that the probe travels before stopping) than the unaged sample. This means that the thermally aged samples have become denser and in turn less elastic. The thermally aged samples that were aged for 15 days and 30 days show a closely related time recording while the sample that was aged for 45 days is significantly smaller. It may be that in the thermal aging process there are periods where significant changes occur and periods where small changes occur. It is also possible that the second sample is merely an outlier and does not accurately reflect the amount of thermal aging that it has undergone.

The irradiated samples show a pattern as well but also has a sample that lies outside of the expected results. The trend shows an increase in time (that the probe travels before stopping) over the unaged sample. An increase in time means that the irradiated samples have become less dense and in turn more elastic. As expected, the sample that was irradiated for 30 days shows an increase in time over the unaged sample. The sample that was irradiated for 60 days showed a decrease in time over the unaged sample by over a second. It should be noted that this result is still higher than all of the thermally aged sample times and may be a result of the properties that XLPE have. The XLPE cable is radiation resistant up to a specific dosage and can cause fluctuation in areas along the length of the cable. The final sample that was irradiated (at 120 days) showed a substantial increase in time which shows that once the sample is irradiated heavily, it will begin to become less dense and more elastic.

Figure 4.2 shows the velocity as a function of time for the second cable type, ULTROL 60+. This cable had two samples, one is unaged, and the other is thermally aged. This cable is used to show that other cable types show a similar trend in comparison. The time until

the velocity reaches zero for the unaged cable is 4.71 seconds and the time for the thermally aged cables time is 2.76 seconds. This shows a decrease in time of over 41% and follows the same trend that thermal aging increases the density of the cable and as a result, decreases the elasticity.

Figure 4.3 shows the velocity as a function of time for the third cable type, Boston Insulated Wire (BIW). This cable has two samples - one is unaged and the other is thermally aged at a relatively high temperature to show an extreme example. The unaged cable′s transition time is 14.55 seconds. The thermally aged cable′s transition time is 6.94 seconds.

This shows a decrease of over 52% in transition time. The decrease shows an increase in density and a decrease in elasticity of this cable type as well.

Another indenter test focuses on the force as a function of time that is exerted in opposition to the probe. This test is done by having the probe press into the cable until a fixed resistive force is reached, and then this force is held for a prolonged period of time.

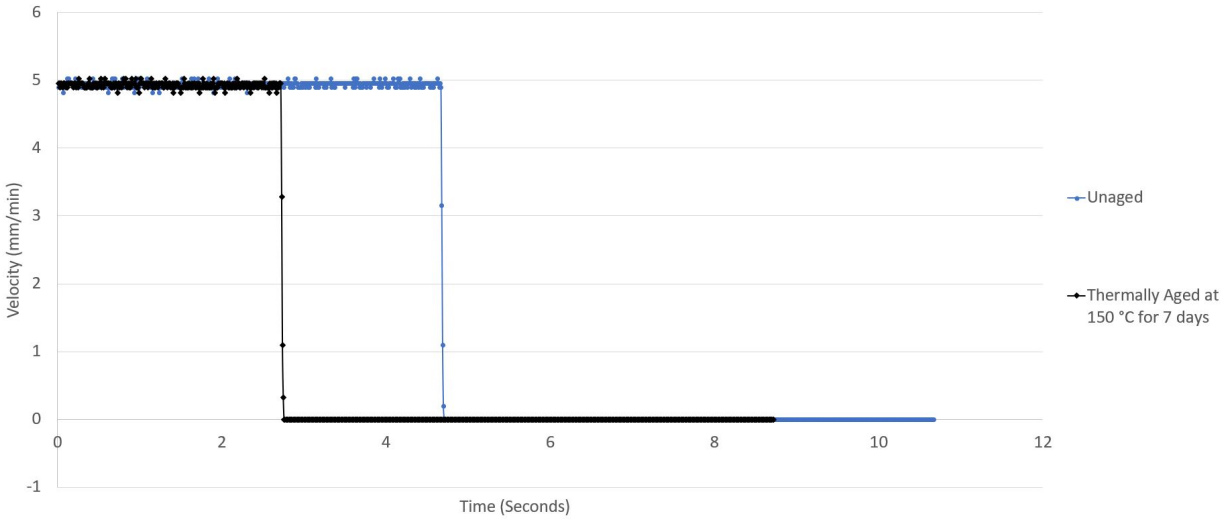

Figure 4.2: Velocity as a function of time for ULTROL 60+ cable that is unaged and thermally aged.

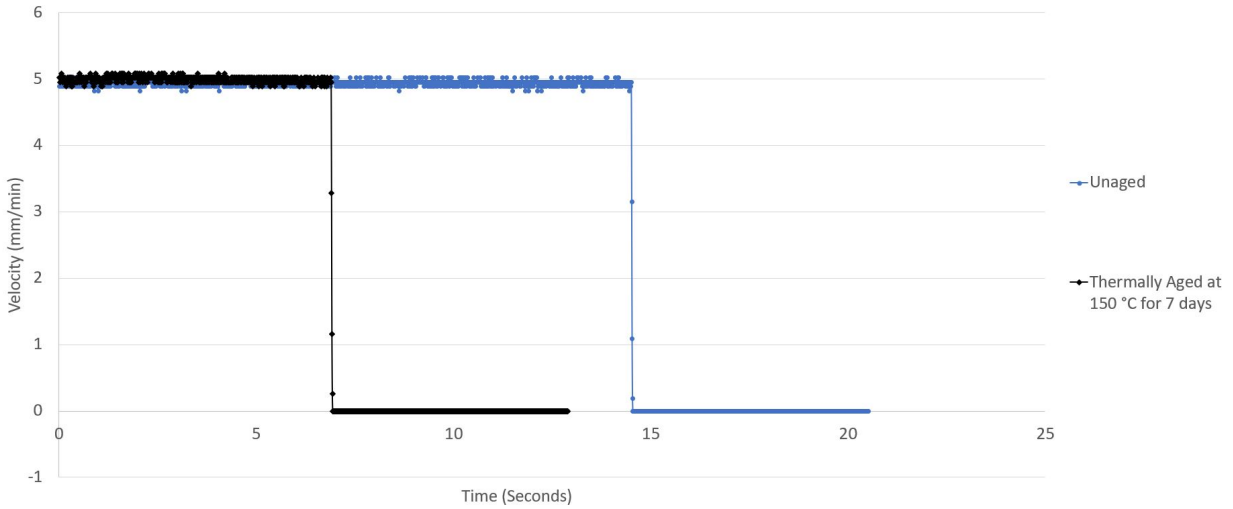

Figure 4.3: Velocity as a function of time for Boston Insulated Wire (BIW) cable that is unaged and thermally aged.

The force graph has three essential aspects to consider: the first is the rate it takes to get to the preset force, the second is the time the preset force is reached, and the third is the rate after the preset force is reached. The rate to the preset force is dynamically moving and is the modulus of elasticity for that sample. The time that the probe reaches the preset force is when the probe stops moving, and the relaxation phase begins. The relaxation phase shows the force required to keep the current probe depth and is useful in understanding the deformation of the material.

The modulus phase is dependent on the elasticity of the material because it requires less force exerted to reach the same probe depth into a sample, on material that is more elastic rather material that is less elastic. There are two main types of deformation. The first is elastic deformation and the second is plastic deformation. Elastic deformation is when an object is deformed but can quickly return to its original state without permanent

deformation. Plastic deformation is when an object is permanently deformed and can't return to its original state. This leads to the relaxation phase as the phase should be consistent across all samples as long as the probe does not cause plastic deformation. If the relaxation phase suddenly decreased drastically, then it would likely be due to plastic deformation of the sample.

Figure 4.4 is a graph of force versus time for the Firewall III cable that is unaged, thermally aged and irradiated at various degrees of exposure. The unaged sample reaches its' preset force at a time of approximately 17.67 seconds. The thermally aged samples (from least amount of thermal aging to the highest amount of thermal aging) have the following times: 16.3 seconds, 16.35 seconds, and 11.92 seconds. The irradiated samples (from least amount of irradiation exposure to the most significant amount of irradiation) have the following times: 18.14 seconds, 16.54 seconds, and 27.81 seconds.

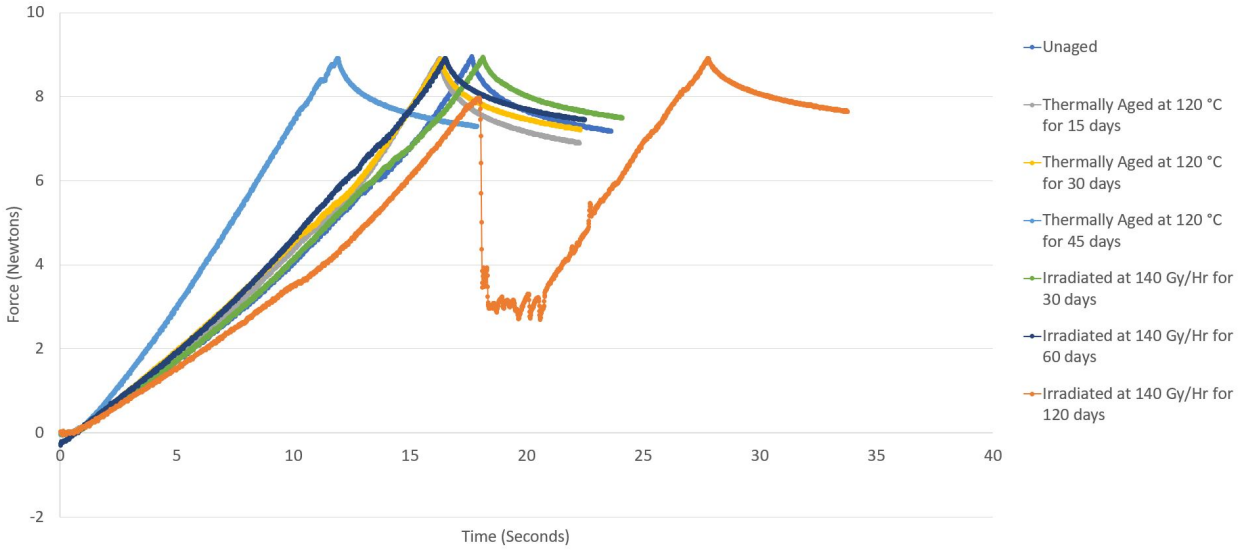

Figure 4.4: Force as a function of time for Rockbestos Firewall III XLPE cable that is unaged, thermally aged, and irradiated.

Figure 4.4 illustrates a similar pattern that the thermal aging reduces the elasticity and irradiation increases the elasticity of the cable samples. There are two aspects that should be noted about the data from the graph. The first is that the sample that was irradiated for 60 days was recorded to have an elasticity measurement below the unaged cable and above all of the thermally aged samples. This is an outlier and does not ideally fit in the trend that irradiated cable increases in elasticity; however, this could merely be an issue with the sample that was tested. The other important aspect about this figure is the sample that was irradiated for 120 days. This sample showed a sudden drop in force during the modulus phase that slowly was regained. This caused the modulus phase to be drastically longer than the other samples; however, this is in direct relation to how the irradiation impacts the samples. The irradiation causes holes to form inside the cable jacket, and it is likely that the probe reached one of these holes during the test. This would result in a sudden drop in force required until the probe reached the other side of the hole in the jacket.

Figure 4.5 shows the force as a function of time for the ULTROL 60+ cable samples. Two samples were used one is unaged, and the other is thermally aged. The time to the preset force for the unaged cable is 4.71 seconds. The time to peak force for the thermally aged cable is 2.76 seconds. This follows the trend that thermally aged cable has a reduction in elasticity of the jacket.

Figure 4.6 illustrates the force versus time for the BIW cable samples. Two samples were used where one is unaged, and the other is thermally aged. The time to the max force for the unaged cable is 14.55 seconds. The time to the max force for the thermally aged cable is 6.94 seconds. This follows the same pattern that thermally aged cable has a reduction in elasticity of the jacket.

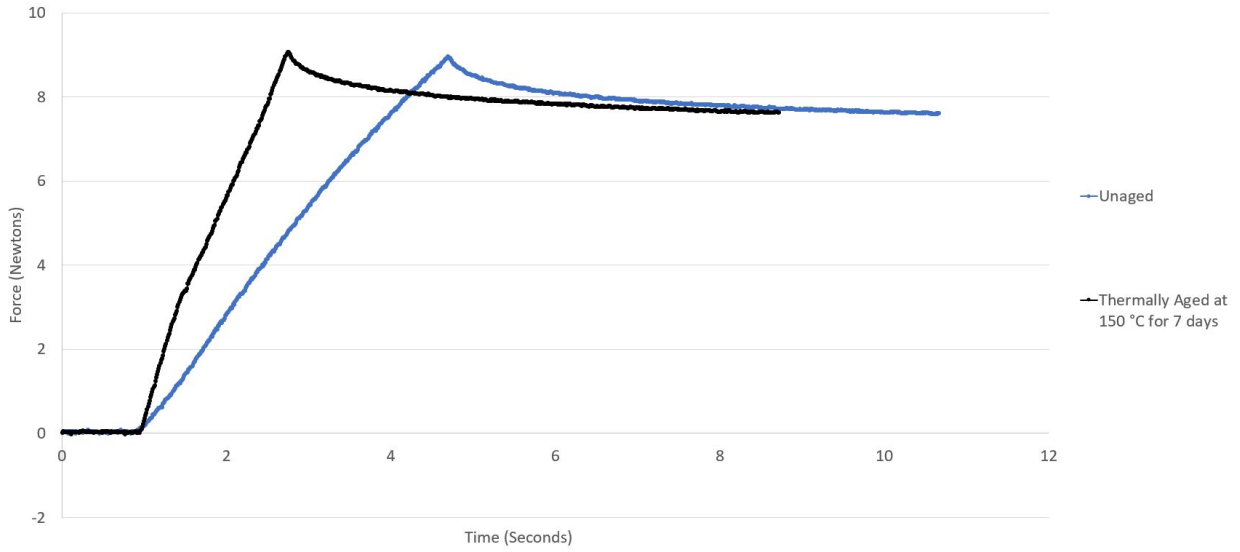

Figure 4.5: Force as a function of time for ULTROL 60+ cable that is unaged and thermally aged.

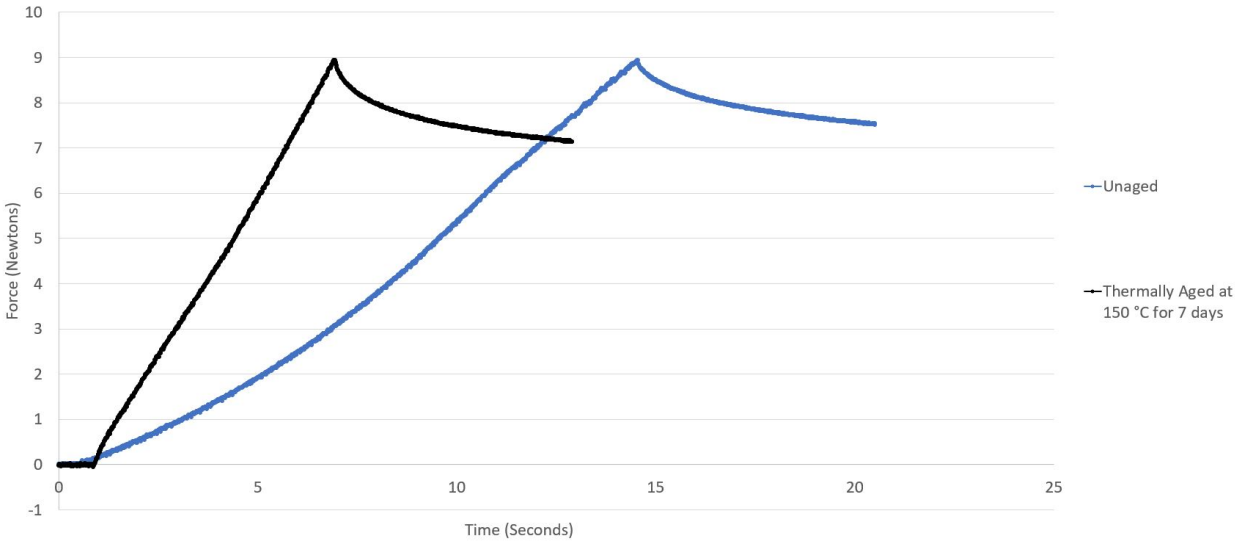

Figure 4.6: Force as a function of time for Boston Insulated Wire (BIW) cable that is unaged and thermally aged.

The final indenter test focuses on the deformation as a function of time. This test is done by having the probe press into the cable until the preset force is reached and the resultant distance into the cable jacket is recorded as the deformation. The deformation graph has a couple of main aspects to consider. The first is the time (s) it takes to reach the deformation plateau and the second is the deformation (mm) at the plateau – the higher deformation (mm) results in a higher elasticity of the material. Figure 4.7 shows the deformation versus time for the Firewall III cable, where the unaged sample reaches its' peak deformation of approximately 1.31 mm. The thermally aged samples have the following amount of deformation: 1.21 mm, 1.23 mm, and 0.87 mm. The irradiated samples have the following amount of deformation: 1.37 mm, 1.24 mm, and 2.12 mm. The recorded deformation is representative of the previous indenter data presented. Figure 4.8 shows the deformation for the ULTROL 60+ cable.

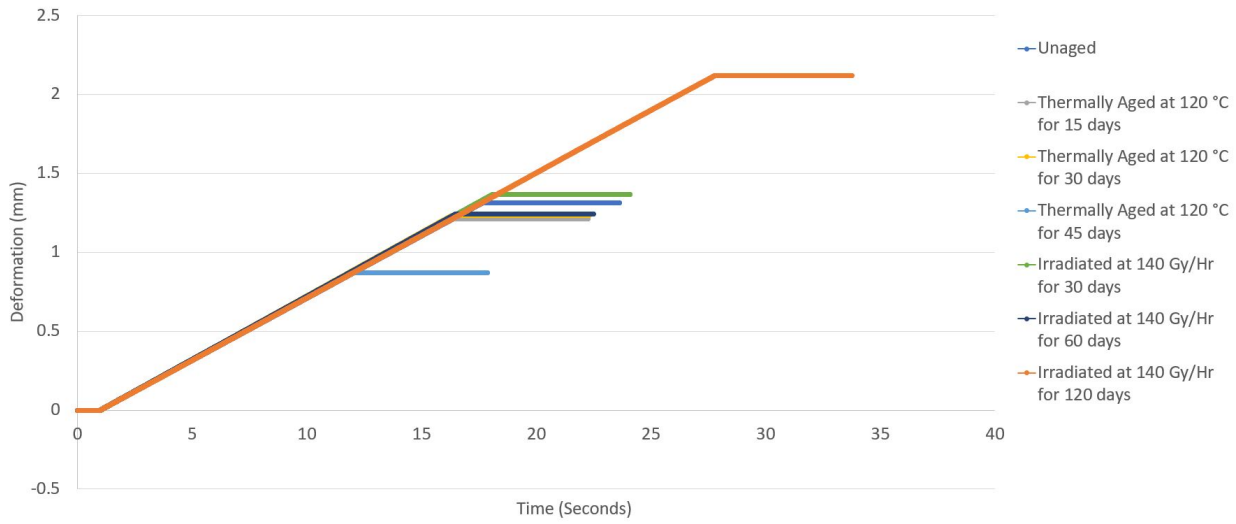

Figure 4.7: Deformation as a function of time for Rockbestos Firewall III XLPE cable that is unaged, thermally aged, and irradiated.

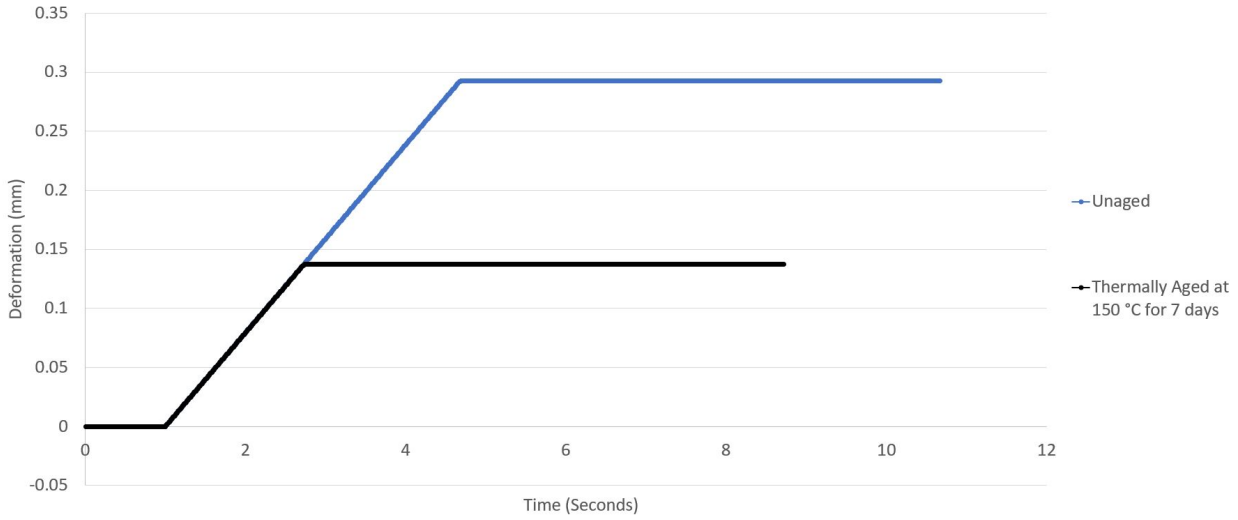

Figure 4.8: Deformation as a function of time for ULTROL 60+ cable that is unaged and thermally aged.

Unaged and thermally aged ULTROL 60+ cables were tested. The resultant deformation of the indenter test is shown in Figure 4.8. The deformation of the unaged cable is 0.30 mm. The deformation of the thermally aged cable is 0.14 mm. The thermally aged cable has a rather substantial reduction in deformation and resultant elasticity. Figure 4.9 shows the deformation of the Boston Insulated Wire (BIW) that is unaged and thermally aged.

The BIW cable showed deformation of 1.08 mm for the unaged cable. The resultant deformation of the thermally aged cable is 0.48 mm. The thermally aged sample shows less deformation than the unaged cable. This correlates to the same pattern observed for the thermally aged data for the previous two types of cable.

The various graphs of deformation, resistive force, and relative velocity provide a visual representation of the trends that occurred from the testing. This is helpful as a visual confirmation but to correctly identify the differences in the samples, statistical correlation is

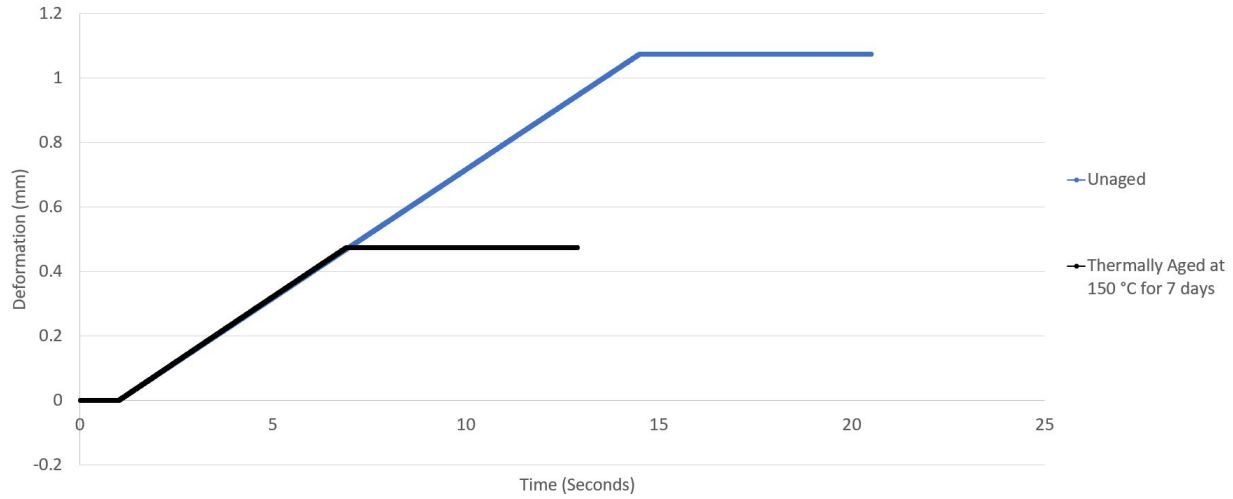

Figure 4.9: Deformation as a function of time for Boston Insulated Wire (BIW) cable that is unaged and thermally aged.

necessary. The resistive force and relative velocity are functions of the deformation and as such a proper evaluation can be made using just the deformation data. Table 4.1 is shown below to evaluate the statistical differences of the recorded deformation between the cable samples and types.

Table 4.1 presents the percent change from unaged for all of the samples. The percent change for samples with the highest exposure to thermal aging are as follows: sample 4 (-33.59%), sample 9 (-51.72%), and sample 11 (-56.48%). The percent change for the sample with the highest exposure to irradiation is sample 7 (61.07%). The data that was recorded from each test showed a trend that the thermal aging of a cable decreases the elasticity, and the irradiation of a cable increases the elasticity. This is important as the

Table 4.1: Peak deformation as derived from Indenter tests

Sample	Cable Type	Aging Characteristic	Peak Deformation	% Change From Unaged
1	RockBestos Firewall III	Unaged	1.31 mm	-
2	”	Thermally Aged (120°C for 15 days)	1.21 mm	-7.63
3	”	Thermally Aged (120°C for 30 days)	1.23 mm	-6.11
4	”	Thermally Aged (120°C for 45 days)	0.87 mm	-33.59
5	”	Irradiated (30 days at 140 Gy/hr)	1.37 mm	4.58
6	”	Irradiated (60 days at 140 Gy/hr)	1.24 mm	-5.34
7	”	Irradiated (120 days at 140 Gy/hr)	2.11 mm	61.07
8	ULTROL 60+	Unaged	0.29 mm	-
9	”	Thermally Aged (150°C for 7 days)	0.14 mm	-51.72
10	BIW	Unaged	1.08 mm	-
11	”	Thermally Aged (150°C for 7 days)	0.47 mm	-56.48

reason behind the changes in elasticity may be a result of changes in material properties or degradation of the material itself.

4.2.2 The Impact that Aging Processes have on the Material Properties of the Cable's Jacket

Making a cable jacket more flame retardant is done in one of two different ways. The first way is to introduce free radicals that act as flame inhibitors such as bromine, chlorine, or phosphorus (Rosser et al., 1958). These free radicals are not bound to a molecule and thus can attach freely to any opening that occurs. The radicals do just that during combustion and this attaching of radicals to molecules help in suppressing the flammability of the polymer. The second method for suppression is to prevent oxygen from reaching the flame. One method to accomplish this is by making the cable jacket thermoset which means the polymer chains are cross-linked with other molecules, hence Cross-Linked Polyethylene-XLPE. This cross-linked pattern does not allow a lot of oxygen to be present inside the cable jacket and means that fire can only propagate by burning on the outer most compromised surface. If the cable is undamaged, then the cable jacket will only burn on the surface until the materials degrade. This leads to a reliable and robust cable jacket that is difficult to ignite and keep burning.

Thermoset cable relies on the uniform lack of oxygen in the polymer structure to have an ideal flame retardancy. The easiest way to reduce the effect of the flame retardant materials is to add a means of oxygen in the system. This can be done by compromising the cable or changing the uniformity of the thermoset material.

When a material is irradiated by a radiation source (such as Cobalt 60), the material is bombarded with ionizing radiation that heats up from the inside and can also cause electrons to be knocked off molecules. The electrons that are knocked off can cause free radicals where oxygen atoms are left without an electron and can even break up cell walls causing localized breakdown of material (Agency, 1973).

Figure 4.10 is a representation of the Firewall III jacket's surface and material makeup. Part A of Figure 4.10 and part C of Figure 4.10 are images of the surface of the cable's jacket for the unaged cable and irradiated cable respectively. Part B of Figure 4.10 and part D of Figure 4.10 show the chemical composition of the unaged and irradiated cable respectively. These figures are useful in determining the changes in material and physical characteristics of the cable.

Figure 4.10 is the compilation of material gathered from SEM for the Firewall III cable. Part A of Figure 4.10 shows the unaged cable's jacket mostly uniform in shape and density. The material does not show any signs of deformation or perforation excepting the slight imperfections that are a result of the original curing process of the jacket's polymers. In comparison, part C of Figure 4.10 shows a lot of porosity in the jacket's surface including localized areas of degradation where holes or vacancies have formed. As mentioned previously, the thermoset cable jacket is dependent on not allowing oxygen to penetrate as to control the reaction. The occurrence of holes and increased porosity throughout the irradiated sample may increase the oxygen content and alter the flammability characteristics.

Part B of Figure 4.10 shows the chemical composition recorded for the unaged sample. The sample mainly consists of carbon, oxygen, aluminum, silicon, and chlorine.

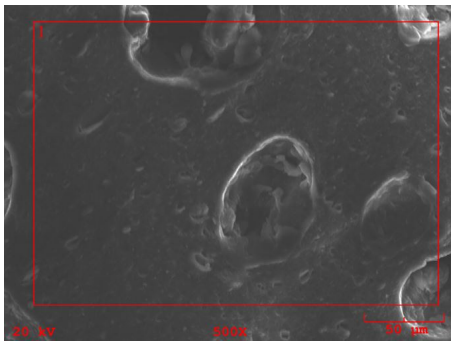

(A) Unaged Jacket.

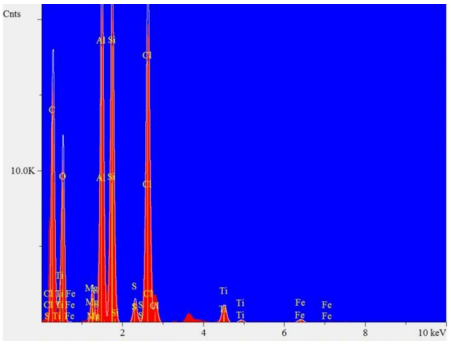

(B) Unaged Jacket.

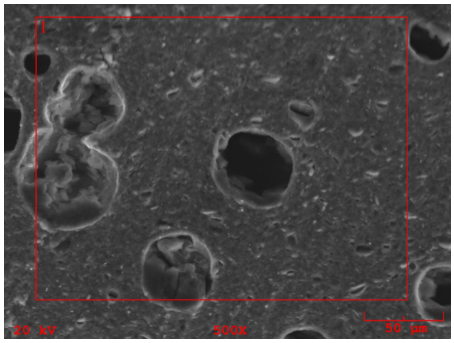

(C) Irradiated Jacket.

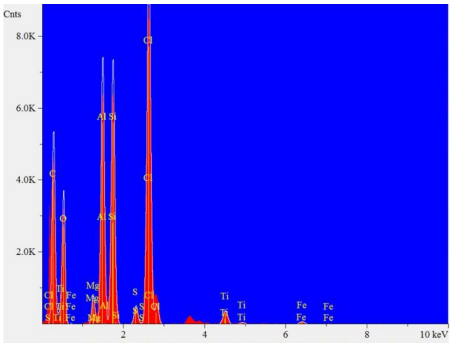

(D) Irradiated Jacket.

Figure 4.10: SEM images (A & C) and chemical analysis (B & D) of Rockbestos Firewall III XLPE cable that has been unaged and irradiated (120 days at 140 Gy/hr).

It is also common knowledge that the carbon in the material acts as a fuel source and the oxygen acts as a catalyst. Part D of Figure 4.10 shows the chemical analysis for the irradiated sample. The analysis for the irradiated cable is similar in nature with very few changes. The two samples consist entirely of the same chemical makeup, and only four elements are recorded to change. The oxygen (1.38% greater), aluminum (0.6% greater), and silicon (0.72% greater) content of the unaged sample is collectively 2.70% greater than the irradiated sample. The irradiated sample contains 2.70% more chlorine then the unaged sample. The recorded differences in percentages are not very high and in turn, may merely be a byproduct of the area of the sample that was measured.

Observation of the chemical analysis presents two main differences between the samples. The first is that the unaged sample shows a higher concentration of oxygen content and aluminum. Oxygen and aluminum should keep the sample burning longer and hotter; while the chlorine from the irradiated sample is not flammable by itself. The second observation (and possibly the most important) is the number of counts recorded for the chemical analysis graphs. The unaged jacket's count is almost twice as high as the irradiated cable's. This is because the SEM test is based on reflected electrons that bombard the test area of the sample. The irradiated cable is porous and contains voids that end up not reflecting the electrons and thus decreases the active surface area of the test. This area is essentially excluded and does not reflect in the chemical analysis. The holes are filled with Air and as such, allow extra oxygen to enter the cable that is not recorded in this test.

Figure 4.11 is a representation of the ULTROL 60+ jacket's surface and material makeup. Part A and part C of Figure 4.11 are images of the surface of the cable's jacket for the unaged cable and thermally aged cable respectively. Part B and part D show the chemical

composition of the unaged and thermally aged cable respectively. These figures are useful in determining the changes in material and physical characteristics of the cable.

The main difference between the two samples is that the thermally aged cable is less porous (the material has shrunk and tightened up). This can be seen as the SEM image of the thermally aged sample shows a lot of lighter colored area (grey and white), which represents a surface area that does not change much in height (the relatively flat surface that has a slight roughness on the surface).

Part B and part D of figure 4.11 show the chemical composition of the unaged and thermally aged jackets respectively. The main elements present in the two samples are carbon, oxygen, aluminum, and antimony. Antimony is a commonly used additive for flame retardancy (Xu et al., 2018). Since antimony is present, that means this cable relies heavily on its composition to provide flame retardant characteristics. The change in percentages from the unaged to the thermally aged cable are as follows: carbon decreased by 7%, oxygen increased by 3.9%, aluminum increased by 3.41%, and antimony decreased by 0.31%. The main difference between the samples is that the thermally aged cable showed an increase in the oxygen and aluminum percentages on the surface of the material.

Figure 4.12 presents the SEM results for the Boston Insulated Wire's (BIW) jacket. Part A and part C of Figure 4.12 are SEM images taken of the surface of the jacket samples. Part B and part D of Figure 4.12 is the resultant chemical composition recorded from the SEM process. The figures presented help in determining the characteristic changes that the samples have undergone as a result of their artificial aging.

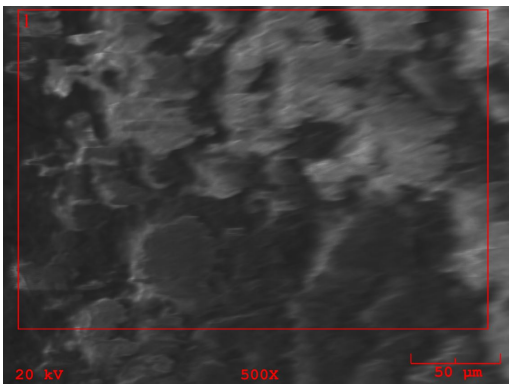

(A) Unaged Jacket.

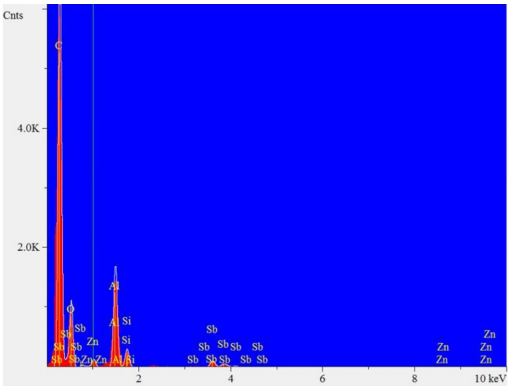

(B) Unaged Jacket.

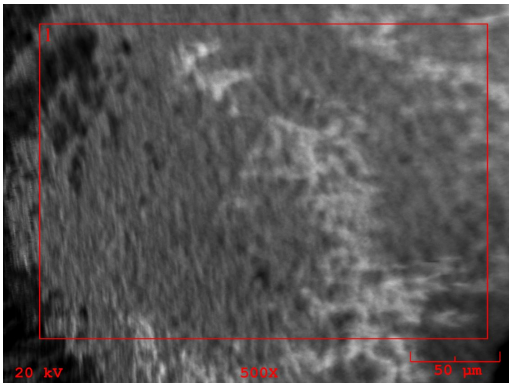

(C) Thermally Aged Jacket.

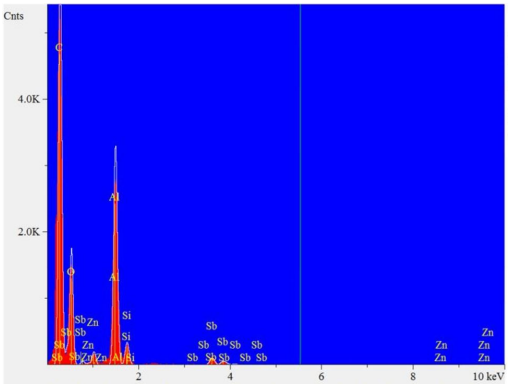

(D) Thermally Aged Jacket.

Figure 4.11: SEM images (A & C) and chemical analysis (B & D) of ULTROL 60+ cable unaged and thermally aged (7 days at 150 °C).

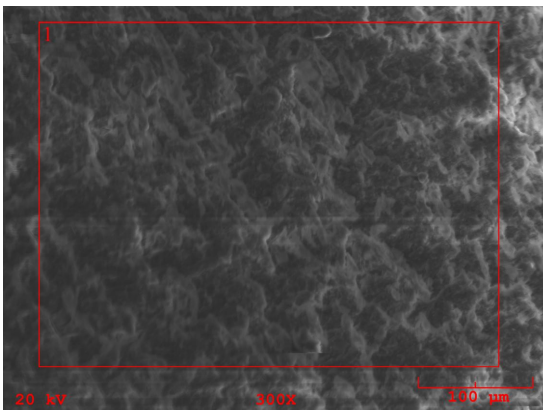

(A) Unaged Jacket.

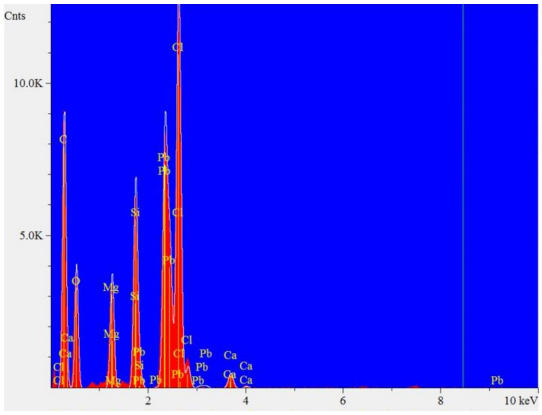

(B) Unaged Jacket.

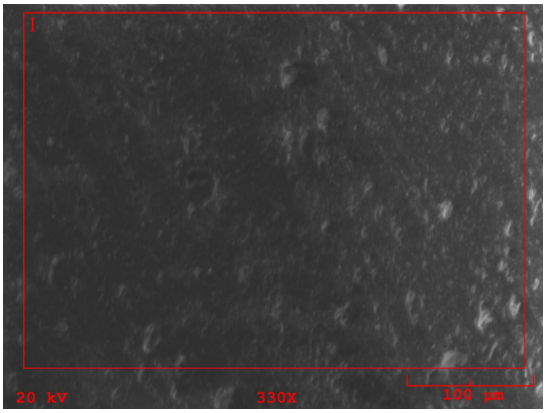

(C) Thermally Aged Jacket.

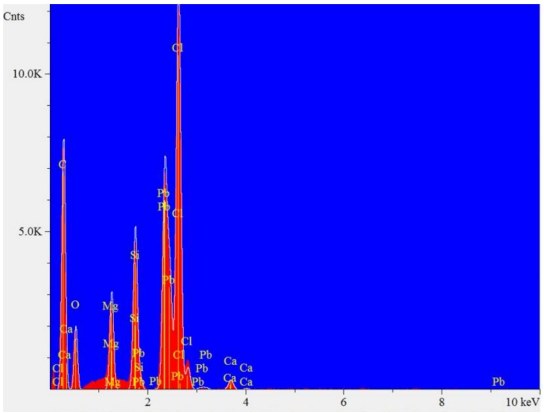

(D) Thermally Aged Jacket.

Figure 4.12: SEM images (A & C) and chemical analysis (B & D) of Boston Insulated Wire (BIW) cable unaged and thermally aged (7 days at 150 °C).

Part A and part C of Figure 4.12 depict the SEM images of the unaged and thermally aged jackets. The apparent difference between the two images is that the thermally aged sample appears smoother with less surface roughness. This is due to the heating of the surface polymers during the thermal aging process which caused the jacket to shrink.

Part B and part D of Figure 4.12 show the chemical composition of the BIW cable samples. The elements present in the samples are: carbon, oxygen, magnesium, silicon, chlorine, calcium, and lead. The main differences in percentages measured between the unaged and thermally aged samples are: 8.02% increase in carbon, 6.30% decrease in oxygen, 0.62% decrease in silicon, 1.87% increase in chlorine and 2.97 % decrease in lead. This cable showed that the major difference was that carbon was less present while oxygen was more present in the thermally aged sample.

The SEM tests record the chemical composition of the cable jacket and are based on the concentration of the elements. The numerical results of the element concentration for unaged and aged samples are compared, to observe high percent changes. This is useful in observing the elements that are most affected by the specific type of aging. The highest percent changes for a specific element are given the most consideration since slight variations can be a result of other factors. These factors may include (but are not limited to) machine error, base differences in sample composition, or the variations in testing areas along the cable samples.

Table 4.2 is a complete compilation of the SEM chemical analysis for each sample and a brief description of the visual changes that were observed. This table provides a clear understanding of the variation in percent change between unaged and aged samples. The Firewall III sample shows the most substantial changes in the presence of chlorine (32.36%

Table 4.2: Chemical and visual variations derived from Scanning Electron Microscope (SEM) tests

	Rockbestos Firewall III			**ULTROL 60+**			**Boston Insulated Wire**		
	Unaged	Irradiated (120 days at 140 Gy/hr)		Unaged	Thermally Aged (7 days at 150°C)		Unaged	Thermally Aged (7 days at 150°C)	
Visual Changes	-	Increased Porosity	-	-	Increase In Surface Density	-	-	Increased Surface Smoothness, Increase in Density	
Element	Concentration (wt %)		% Change	Concentration (wt %)		% Change	Concentration (wt %)		% Change
C	50.39	50.41	0.04	64.73	57.73	-10.81	51.24	59.28	15.69
O	23.69	22.31	-5.83	26.02	29.92	14.99	19.71	13.68	-30.59
Mg	0.79	0.75	-5.06	-	-	-	2.99	2.87	-4.01
Al	7.28	6.68	-8.24	5.86	9.27	58.19	-	-	-
Si	7.64	6.92	-9.42	1.06	1.03	-2.83	4.90	4.31	-12.04
S	0.54	0.51	-5.56	-	-	-	-	-	-
Cl	8.59	11.37	32.36	-	-	-	12.01	13.82	15.07
Ti	0.82	0.78	-4.88	-	-	-	-	-	-
Fe	0.26	0.27	3.85	-	-	-	-	-	-
Zn	-	-	-	0.01	0.04	300.00	-	-	-
Sb	-	-	-	2.32	2.01	-13.36	-	-	-
Ca	-	-	-	-	-	-	0.60	0.45	-25.00
Pb	-	-	-	-	-	-	8.55	5.59	-34.62

increase) for the irradiated sample. This is likely due to a reduction in the presence of other materials. The ULTROL 60+ sample shows significant changes in the amount of aluminum (58.19% increase), carbon (10.81% decrease), and oxygen(14.99% increase). There is also a massive change in the amount of zinc present; however, this is a trace element and can easily just be a result of the testing variance. The BIW sample shows a bit of an opposite change in the oxygen (30.59 % decrease), carbon (15.69% increase), and the other large variances come from the calcium (25.00 % decrease) and lead (34.62 % decrease) concentrations.

The main takeaways from the SEM data are that the thermally aged cable shrunk and the surface became relatively smooth while the irradiated cable became more porous and created voids. The chemical composition of the irradiated cable showed a significant change only in the amount of chlorine present. The chemical composition of the thermally aged samples showed significant changes in the amount of carbon and oxygen present along with changes in the aluminum, calcium, and lead concentrations.

4.2.3 Polymer Degradation as a Result of Aging Processes

The modern high voltage cable insulation basic polymer is crosslinked low-density polyethylene (XLPE). This polymer has excellent insulation properties such as low permittivity and dielectric losses. This material can withstand operating temperatures up to 110 °C without melting, is chemically inert and aging resistant and also is low cost in comparison to other polymers.

XLPE is the most used cable insulation in practice today (Liu et al., 2016). The crossed-linked polymers in XLPE are susceptible to the formation of new chemical bonds such as C=C carbon bonds and C=O carbonyl. This can occur from a variety of processes such as irradiation or oxidation (Glass et al., 2015). The formation of new polymers can change the characteristics of a material. It is essential to understand how thermal aging and irradiation can impact the basic polymer structure of the material.

The XLPE is usually not the sole component in the insulation. The compound typically contains peroxide, antioxidants (Ho et al., 2014), fillers or extenders (making the formulation more cost-effective), and compatibility stabilizers. These components make the degradation process analysis more difficult; however, this also allows an accurate estimate of the product properties to be observed.

The XLPE is obtained from LDPE during the manufacturing process by reacting with active low-molecular compounds containing peroxide or silane groups, which are known as strong oxidizing units. During this reaction, the chemical composition of the polymer is changed. New chemical groups, containing oxygen are introduced into the resultant polymer, and the number of vinylidene groups (containing double bonds) is reduced. The polar reaction by-products usually stay inside the material during the peroxide cross-linking (Hussin & Chen, 2010).

An XLPE aging insulation study is possible with different techniques: differential scanning calorimetry (DSC), X-ray structural analysis, absorption analysis and FTIR spectroscopy (Boukezzi et al., 2008). Each of these techniques is applicable for a separate aspect of aging as a complex study process. The covered area of FTIR is the study of chemical changes based on the transformation of inter-element chemical bonds of respective

atom groups. Infrared spectroscopy is a unique method for polymer degradation and cross-linking detection.

The chemical changes in cable insulation materials were studied on the commercially available samples: 1) Rockbestos Firewall III and 2) ULTROL 60+. The XLPE part of the composition from the Firewall III unaged and irradiated samples are represented by the absorption bands shown in Table 4.3.

Other bands in the samples are represented by additional components of compositions. The Firewall III material bands with coordinates 3695, 3653 and 3620 cm^{-1} can be attributed to OH vibrational stretching of alumosilicates, probably of asbestos type (Rodica, 2008). The band 3405 cm^{-1} is a vibrational stretch of O-H bond of absorbed water, which is also characteristic of such fillers. Si-O-Si stretching vibration is represented by bands 1116, 1039 and 915 cm^{-1} and the 748 cm^{-1} band can be attributed to silicate chain vibration. It is surprising that this sample does not contain bands with coordinates in the region 1700-1800

Table 4.3: Absorption bands of XLPE in the Unaged and Irradiated Firewall III samples.

Band Frequency (Unaged), cm^{-1}	**Band Frequency (Irradiated), cm^{-1}**	**Functional Group Assignment**
748	728	Methylene Rocking
1377	1373	CH_2 Wagging
1460	1468	CH_2 Bending
2852	2854	Methylene Bond Symmetric Stretch
2926	2927	Methylene Bond Asymmetric Stretch

Note. Understanding of band absorption to functional group assignment derived from (Kochetov et al., 2017).

cm^{-1}, which are typical for PE polymers treated with peroxide cross-linker. However, it can be suggested that bands at 1652 and 1670 cm^{-1} are attributed to the ketone C=O stretch vibration (Gulmine & Akcelrud, 2006).

The ULTROL 60+ XLPE, on the contrary, contains C=O links in different variations. The quantity of such groups in unaged material is unusually high. The 1773 cm^{-1} band may be attributed to γ -lactone groups, while the 1739 cm^{-1} and 1711 cm^{-1} bands are attributed to aldehyde (or ester) and ketone carbonyl groups respectively. The presence of bands 1243, 1164, and 1080 cm^{-1} cannot be attributed to XLPE but instead are indications of an inorganic filler introduced into the composition.

In such conditions, typical applications for the XLPE insulation aging analysis methods are not applicable. For example, the carbonyl index change calculation (Hyvnen, 2008) and unsaturated part change techniques are not sufficient: the unaged sample does not contain peaks in the area 1700-1800 cm^{-1} even after aging procedure, and the irradiated sample's peaks are too strong initially; however, in the latter case, they are changed after aging. Further analysis will be conducted by comparing XLPE characteristic bands, which changed during the aging procedure.

The best way to determine the characteristic changes in the cable samples is to compare the FTIR curves for the unaged and aged samples. The Unaged Firewall III FTIR is shown in part A of Figure 4.13 and the Irradiated Firewall III FTIR is shown in part B. The circles on the unaged FTIR denote cable specific characteristics, and the arrows on the irradiated FTIR denote essential changes between the samples.

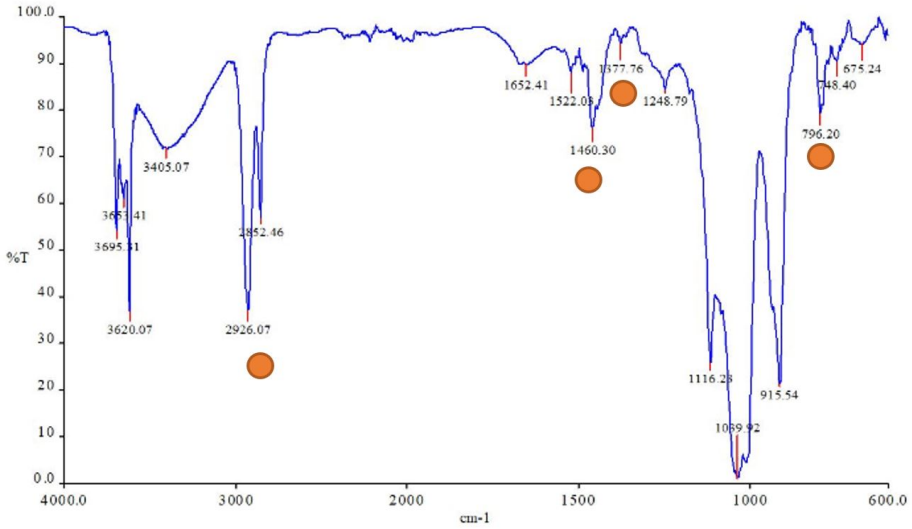

(A) Unaged Cable.

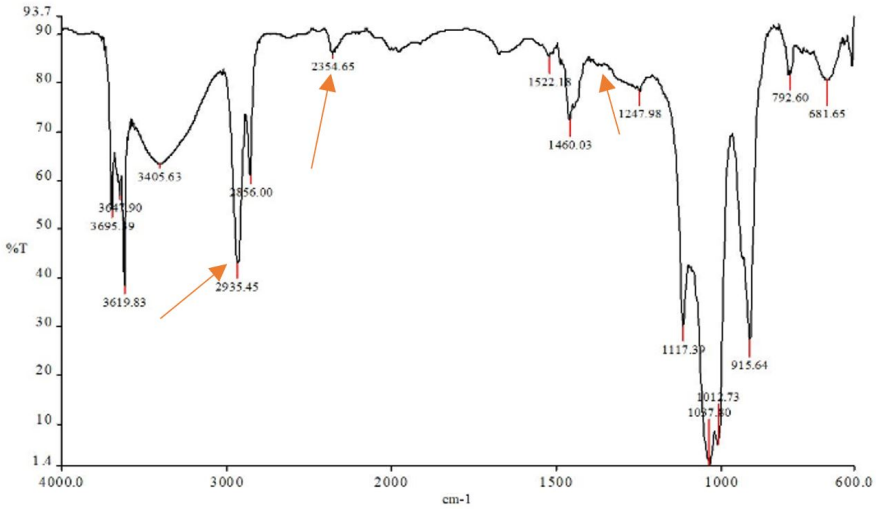

(B) Irradiated Cable

Figure 4.13: Fourier transform infrared spectroscopy (FTIR) of Rockbestos Firewall III XLPE cable that is unaged (A) and irradiated (B, 120 days at 140 Gy/hr).

It is essential to understand the characteristics from Figure 4.13 for both the unaged and irradiated Firewall III samples. The Rockbestos Firewall III sample shows a peak at 1039 cm^{-1}, that is referenced as alumosilicate.

It should be noted that a Si-O-Si bond is considered far more resistant to aging than the polymer part of the composite. A ratio of respective bands absorption before and after aging is used to determine the indexes of the XLPE bands. The peak absorbance at 2926 cm^{-1} decreased, and the resultant index is 0.87, for 2852 cm^{-1} the index is also close to 0.87, indicating the CH2 bonds were conversed by oxidation. Bands 1460 and 1377 cm^{-1} also decrease showing the occurrence of oxidation and their respective indexes are 0.9 and 0.95. The recent peak became hindered which made the determination difficult. The same may be stated for the 748 cm^{-1} peak, which was lost between other bands and its index is small in comparison at 0.67. Also, the absorbance of O-H vibrational stretching in absorbed water increased and the result index is 1.08, which indicates the accumulation of the water in the sample material during the aging procedure.

The observed characteristics of XLPE polymer destruction and the porosity increase after aging is described in a number of works (Hvidsten & Larsen, 2009) (Ross & Smit, 1992). It may be assumed that the process affects the polymer-alumosilicate interface and decreases the contact between these two components, which leads to the accumulation of water on this boundary.

The Unaged ULTROL 60+ FTIR is shown in part A of Figure 4.14 and the thermally aged ULTROL 60+ FTIR is shown in part B. The circles on the unaged FTIR denote cable specific characteristics and the arrows on the thermally aged FTIR denote important changes

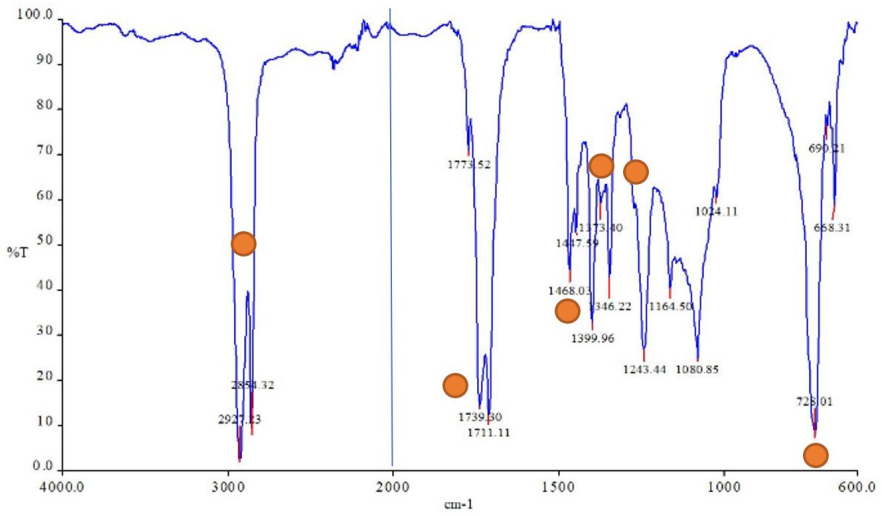

(A) Unaged Cable.

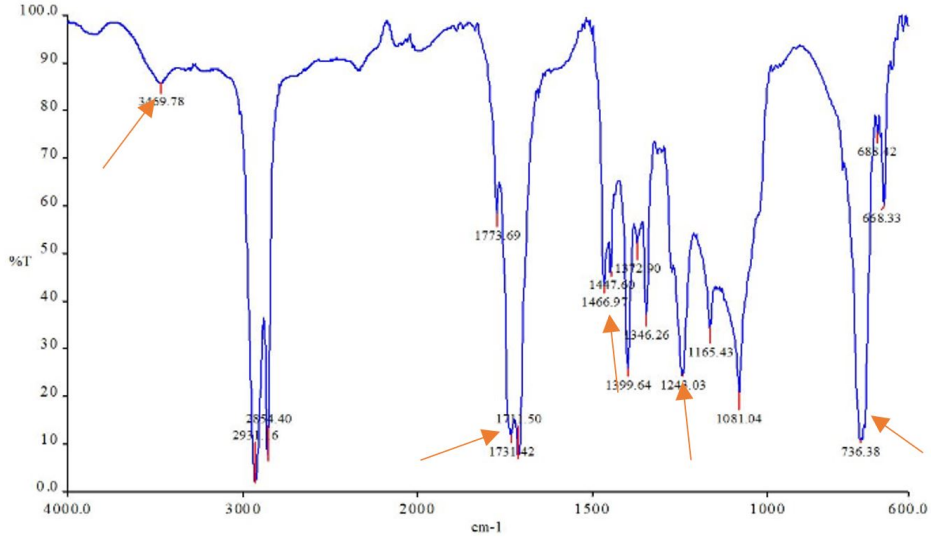

(B) Thermally Aged Cable

Figure 4.14: Fourier transform infrared spectroscopy (FTIR) of ULTROL 60+ cable that is unaged (A) and thermally aged (B, 7 days at 150 °C).

between the samples. The two FTIR figures are compared to observe changes in the aging process.

Figure 4.14 is used to compare the characteristic changes before and after the aging process. The filler band , 1080 cm^{-1}, is taken as a reference point for the ULTROL 60+ sample. It is assumed that this band remains unchanged during the aging process and polymer indexes are calculated based upon it. It was found that the absorption bands at 2927 and 2856 cm^{-1} decreased slightly, and their respective indexes were found to be 0.96 and 0.94 respectively. This showed a decrease of CH_2 bond quantity and a confirmation of the oxidation process. The bands, which correspond to carbonyl groups, were observed to change in a nonuniform manner: the band 1773 cm^{-1} increased its absorbance with an index 1.26, the band 1739 cm^{-1} slightly decreased with index 0.98 and the band 1711 cm^{-1} decreased with index 0.97. This may be interpreted as the oxidation of material that leads to the formation of γ -lactone groups primarily, while all other types remain almost unchanged or converted to this type. Other bands such as 1468 and 728 cm^{-1} also decreased with indexes of 0.93 and 0.91 respectively. The band 1374 cm^{-1}, on the other hand, increases which means there is a change of the materials crystallinity during the aging process and the respective index is 1.08. Another important marker of aging is the appearance of the band at 3469 cm^{-1}, which corresponds to a vibrational stretch of OH links. The index of this band is 1.13, which shows significant polymer destruction and an increase in its polarity. This fact can also be attributed to an increase in the materials density and expectable decrease of electrical insulation ability.

The carbonyl index increase is related to the decrease in dielectric properties as presented in the work (Hyvnen, 2008). The carbonyl index (C.I.) for the ULTROL 60+ samples is

calculated for separate bands. The C.I. is a measure of carbonyl groups of the different kinds of ratios in the polymer, which remained during aging in the composition.

T The reference band 1468 cm-1, corresponds to the CH_2 methylene band (Boukezzi et al., 2010). It should be noted that in this case carbonyl groups are most likely contained as cross-linker residues or copolymers. This may explain the unusually high quantities which cannot be explained by process destruction (aging) of the primary polymer.

The C.I. increases from 0.4 to 0.77 in the case of lactone carbonyl, which is 1.9 times more than the initial. For the aldehyde/ester band at 1739 cm^{-1}, the C.I. slightly increases from 1.48 to 1.56 (1.05 times). The ketone band at 1711 cm^{-1} also increases from 1.55 to 1.61 (1.04 times).

Table 4.4 is a collective representation of the most important bands that were observed for the various samples. For each sample, the important wavenumbers are shown, and the resultant index fraction is shown. The index fraction is based on the transmission percentage of the unaged sample relative to the transmission percentage for the aged sample. This provides a representation of either the increase or decrease of the permittivity of the respective band. An interpretation of each band is also presented to provide an understanding of the polymer bond variations between the samples.

The FTIR analysis results showed that the cable insulation in both cases is composed of polymer composites with mineral fillers and other functional additives. During the aging process, the materials increased their affinity to water, which is proven by respective bands at 3400 and 3600 cm-1 increasing in their absorbance. The increase in water content and the increase of porosity can explain the decrease of the materials dielectric properties and the increase in the polarity.

Table 4.4: Infrared absorption as derived from Fourier Transform Infrared Spectroscopy

Rockbestos Firewall III				**ULTROL 60+**			
Unaged	Irradiated (120 days at 140 Gy/hr)			Unaged	Thermally Aged (7 days at 150°C)		
Wavenumber cm^{-1}		Index Fraction (Unaged/Irradiated)	Interpretation	Wavenumber cm^{-1}		Index Fraction (Unaged/Thermally Aged)	Interpretation
3695, 3653, 3620	3695, 3647, 3620	1.02, 1.08, 0.95	Stretching O-H	3660	3660	1.13	Vibrational Stretch of OH Links
3405	3405	1.13	Stretching O-H of Water	2927, 2856	2931, 2854	0.96, 0.94	Decrease in CH_2/ Confirmation of Oxidation
2926	2935	0.87	Methylene Bond Asymmetric Stretch	1773	1773	1.26	Aldehyde (or Ester)
2852	2856	0.87	Methylene Bond Asymmetric Stretch	1739	1711	0.98	Ketone Carbonyl
1652	1652	1.05	Stretching $C = O$	1468	1467	0.93	CH_2 Methylene Vibration
1460	1468	0.90	CH_2 Bending	1373	1372	1.08	Increased With Aging (Change In Crystallinity)
1377	1373	0.95	CH_2 Wagging	1243, 1164, 1080	1243, 1165, 1081	1.18, 1.17, 1.22	Inorganic Filler
1116, 1039, 915, 796	1117, 1037, 915, 792	0.89, 0.86, 0.85, 0.97	Silicate Chain Vibration	-	-	-	-
748	728	0.67	Methylene Rocking	-	-	-	-

This data cannot be used to compare composition performance, but can accurately be used to compare the evidence of the respective destruction processes that took place.

In both cases, the quantity of methylene groups in the polymer part of the composition decreases together with the increase of polar groups quantity. This shows the destruction of XLPE chains during the exposure process. Considering that the conditions of the tests were not the same, it can be assumed that for the Firewall III sample's destruction grade (from the absorbance at 2926 and 2852 cm-1) is near 12-13% and for the ULTROL 60+ sample's only near 6%.

4.3 Changes in Flammability Characteristics for Aged Cable

4.3.1 A Look Into The Variation Of The Working Operational Range Determined Through Thermo-Gravimetric Analysis

The thermal aging under evaluated temperatures and the irradiation of cable insulation was studied using TGA analysis. The thermal analysis is a standard method for polymer composite research frequently used to estimate the operational range of materials and define the processes that the polymer undergoes during the working cycle. It also can be helpful in the determination of the inorganic content of the composition and the ratio between polymer and low molecular constituents. In this research, the unaged cable sample of insulation Firewall III was taken as the reference, and two other samples of the material: aged under irradiation and thermally aged at elevated temperatures were examined by the aforementioned method.

The general shape of the TGA curves remains typical for the material and shows two transition steps (Figure 4.15). This is not typical for the pure cross-linked low-density polyethylene, as it has an only one-step curve with the onset temperature of the step approximately at 430 °C (Liu et al., 2013) (Mo et al., 2013). This corresponds to the second step of the considered materials curves. A similar case was described in (Melo et al., 2013), where commercial cable insulation samples were taken. The authors explained two-step curves by the occurrence of destruction processes during manufacturing and splitting the step due to the molecular weight fractioning of XLPE.

It is also important to notice that all samples have significant residue which can be attributed to the inorganic part of the composition, namely an alumosilicate extender. The first step of curves is interpreted to belong to a modifier of XLPE, which temperature stability is significantly lower than of said polymer. This modifier is significantly affected by aging conditions, which can be seen from the curves.

The TGA curve of each material was conditionally divided into three regions: a) before the first step onset; b) between the first and second step onsets (modifier thermal degradation); c) between the second step onset and the curve end (XLPE degradation). Temperatures of curve step onsets for all analyzed materials are similar in comparison. Thus the temperature regions are: from room temperature to 240°C for the first one; 240 to 433°C for the second one and 433 to 900°C for the third.

For the aged materials, the thermally aged sample (Figure 4.15 C) and the irradiated sample (Figure 4.15 B) the weight loss in the first region is near 4.7 % wt, and the unaged sample (Figure 4.15 A) is at approximately 2.07 % wt. This can be attributed to the releasing of absorbed water from aged materials (Ross & Smit, 1992) and with the possible evaporation of low-molecular products of polymer destruction, which took place during the aging process (C. Kim et al., 2006).

The first step for the unaged material (Figure 4.15 A) starts at 240°C, and the weight loss of this step is 27.5 % wt. The irradiated material (Figure 4.15 B) shows the start of the transition to be closely related to the unaged material - 240°C but resulted in less quantity of modifier left 26.4 % wt and the thermally aged material (Figure 4.15 C) started the transition at 234°C with the lowest modifier content 22.12 % wt.

The second step starts at 433°C for the unaged material and the weight loss, which corresponds to XLPE destruction, is 30.6 % wt. For the irradiated material the onset temperature is similar at 434°C, but the weight loss is slightly more 31.0 % wt.

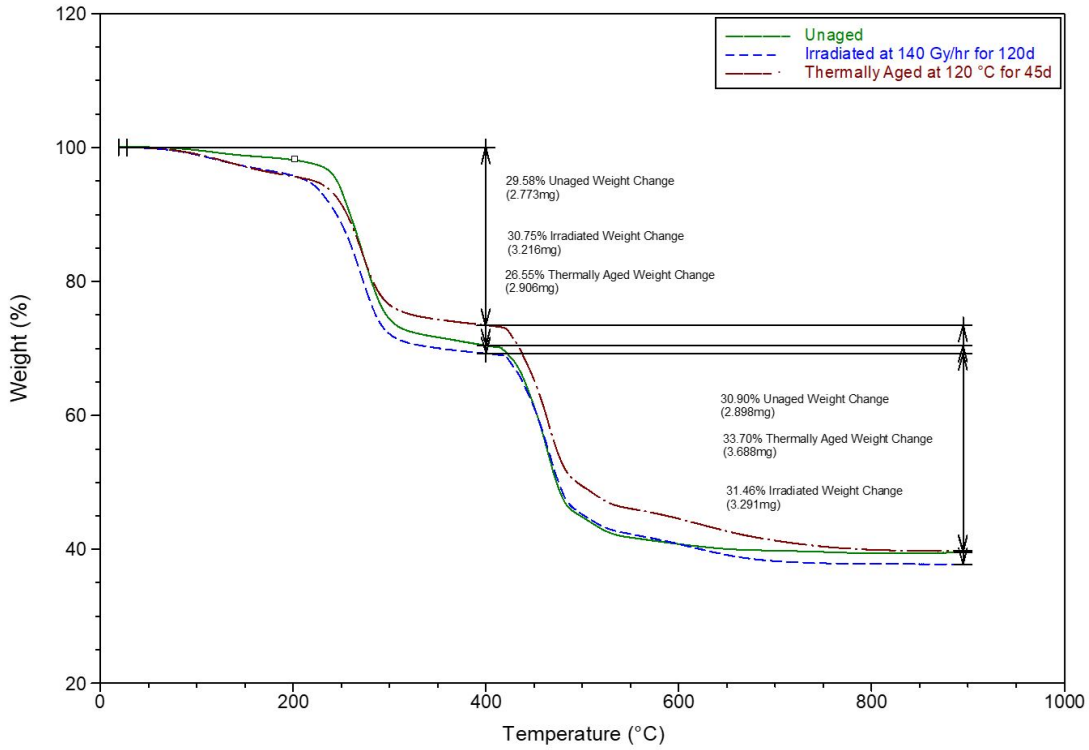

Figure 4.15: Weight Changes From Thermo-Gravimetric Analysis of Rockbestos Firewall III XLPE cable that is unaged (A), irradiated (120 days at 140 Gy/hr) (B), and thermally aged (45 days at 120°C) (C).

The thermally aged material shows another close onset point - 432°C, but increased the content of XLPE fraction 33.4 % wt.

The inorganic content of the composite remains at the same level for unaged and thermally aged sample 39.8 % wt but is reduced for the irradiated sample to 37.9 % wt. The probable explanation for this difference is the deviation of the inorganic extender content in the composition during production.

The aging process grade becomes evident from the comparison of the ratio of losses at the second and first step, which correspond to the modifier to XLPE content ratio. For the unaged material, it is 0.9, for irradiated it is 0.85, and for the thermally aged it is 0.66. Therefore, it can be assumed that the thermal aging in the selected conditions is a far more

destructive factor than the irradiation. Figure 4.16 shows each individual TGA curve for the three samples along with a graphical representation of the derived weight change percentage.

The comparison of the derivative curves of unaged material (part A of Figure 4.16) to the irradiated (part B of Figure 4.16) and thermally aged (part C of Figure 4.16) samples shows that the maximum speed of volatile fraction evaporation is gained at temperatures near 115°C, which is typical for the water, entrapped in structural defects of the material. Also, the oxidative peak of XLPE on DTA changes its configuration, splitting into 3 merged, but distinguishable sub-peaks, indicating a supramolecular structural change of the material during the degradation.

Table 4.5 is a compilation of the three main temperature ranges where the transitions occur for the samples. Each temperature range has a regular weight loss that corresponds to the respective sample. The thermally aged and irradiated samples measured weight loss was compared with the unaged samples to determine the percent change for each transition. Both the thermally aged and irradiated samples showed a substantial percent change for the first transition period (127.05%). The second transition showed a higher loss for the thermally aged sample (-19.56%) over the irradiated sample (-4.00%). Finally, the last transition showed less of a regular weight loss over the unaged sample (9.15% for thermally aged and 1.31% for irradiated). This shows a higher weight loss for the first and third transition for the thermally aged and irradiated samples, with an overall more significant weight loss at the end of the test.

It can be concluded from the TGA results that the cable insulation contains the following constituents: the inorganic extender (39.8 % wt), XLPE polymer (30.6 % wt), modifier (27.5 % wt) and the rest volatile components (2.07 % wt).

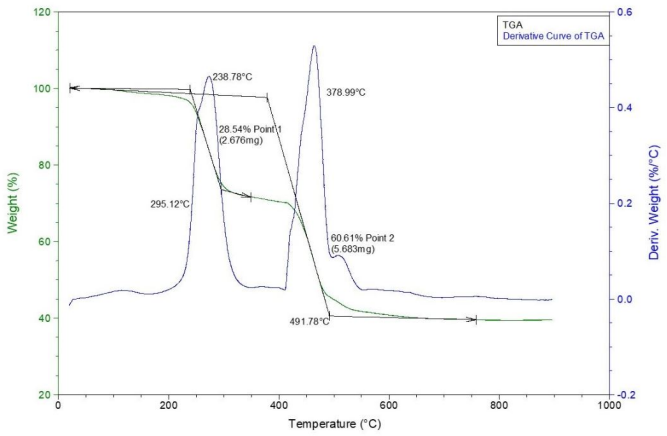

(A) Unaged Cable.

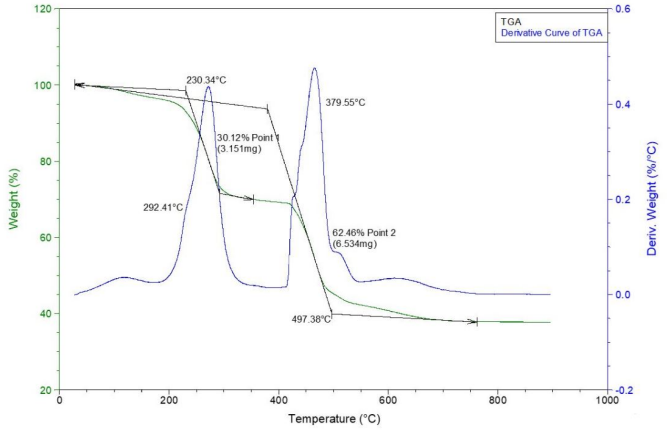

(B) Irradiated Cable

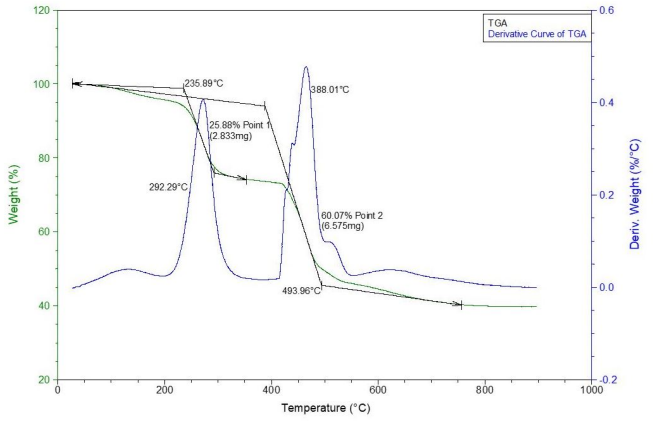

(C) Thermally Aged Cable

Figure 4.16: Thermo-Gravimetric Analysis of Rockbestos Firewall III XLPE cable that is unaged (A), irradiated (120 days at 140 Gy/hr, B), and thermally aged (45 days at 120°C, C).

Table 4.5: Variations in weight change as a function of temperature, derived from Thermogravimetric Analysis tests

Sample	Cable Type	Aging	Temperature	Measured Weight Loss	% Change (From Unaged)
1	Rockbestos Firewall III	Unaged	0°C ~240°C	~2.07%	-
"	"	"	240°C ~433°C	~27.5%	-
"	"	"	433°C ~900°C	~30.6%	-
2	"	Thermally Aged (120°C for 45 days)	0°C ~240°C	~4.7%	127.05
"	"	"	240°C ~433°C	~22.12%	-19.56
"	"	"	433°C ~900°C	~33.4%	9.15
3	"	Irradiated (120 days at 140 Gy/hr)	0°C ~240°C	~4.7%	127.05
"	"	"	240°C ~433°C	~26.4%	-4.00
"	"	"	433°C ~900°C	~31.0%	1.31

During the aging, the fraction of the latter increases to 4.7 % wt, and the fraction of modifier decreases to 26.4-22.1 % wt due to its degradation. The relative fraction of XLPE thus increases, and the inorganic extender content remains unchanged. These changes are most evident in the case of the irradiated sample followed by the thermally aged sample.

4.3.2 A Look Into The Heat Related Transition Phases Using Differential Scanning Calorimetry

The DSC analysis of the samples was used for the estimation of molecular weight and crystallinity changes in samples as a result of the aging. It was stated previously (C. Kim et al., 2006) that during the oxidative aging XLPE polymers undergo two contrary processes: cross-linking and chain scissoring (Sorin & Radu, 2009). Both change the molecular weight of material increasing and decreasing it correspondently, which can be monitored by the broadening of the DSC melting peak. The shifting of the peak onset to lower temperatures

indicates the appearance of polymer fraction with smaller molecular weight the product of chain scissoring process and by the change of supramolecular crystals structure by de-ordering of transition areas between crystals and thus increasing their surface energy (Rabello & White, 1997).

The unaged material (Figure 4.17) has a relatively sharp and non-symmetrical peak with an onset at 246°C and the maximum heat flow at 255°C. The melting enthalpy of the material is 119.4 J/g comparable to data from (Boukezzi et al., 2007). In this article, authors note that during the aging this parameter non-uniformly changes: at the first stages of the process it increases (probably due to the additional cross-linking) and then decrease due to the molecules destruction. It can be deduced that for the case considered; the aging process had overcome the stage of the cross-linking process and prevailing in annealing/re-ordering thus shifting to the destruction phase.

The irradiated sample showed that the crystallinity decreased (Figure 4.18). The decrease in crystallinity is reflected in the change of melting enthalpy to 99.5 J/g, which is 83 % of initial. The peak onset temperature is shifted to 228°C indicating the appearance of low molecular fractions of polymer, probably from XLPE side chains scissoring.

The thermal aging changes showed a more significant appearance (Figure 4.19). The melting enthalpy decreased to 62.3 J/g, which indicated the lowering of crystallinity by almost twice as much to 52.4 % of the initial. The melting onset shifted to 240°C and showed the maximum process speed to 261°C. It can also be noted that a small shoulder appeared at a temperature of 254°C, which is probably connected to the prevailing polymer backbone dissociation mechanism.

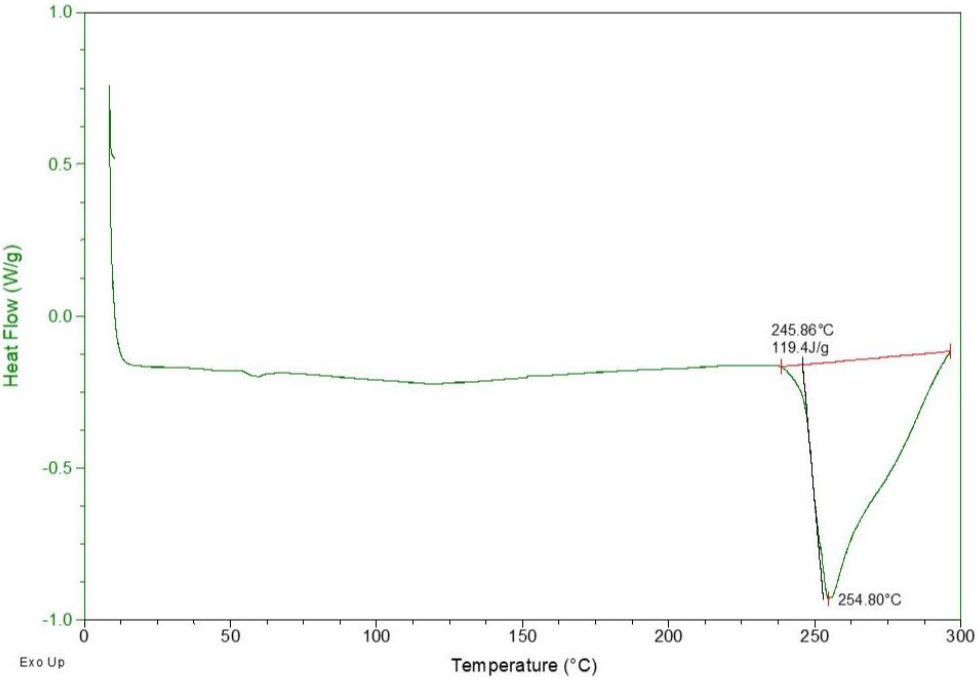

Figure 4.17: Differential Scanning Calorimetry of Rockbestos Firewall III XLPE cable that is unaged.

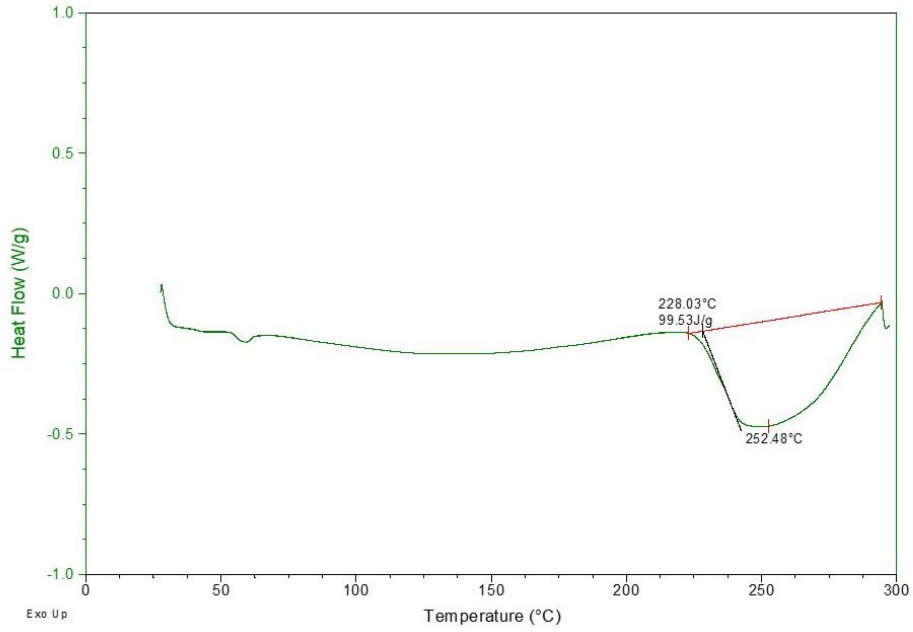

Figure 4.18: Differential Scanning Calorimetry of Rockbestos Firewall III XLPE cable that has been irradiated (120 days at 140 Gy/hr).

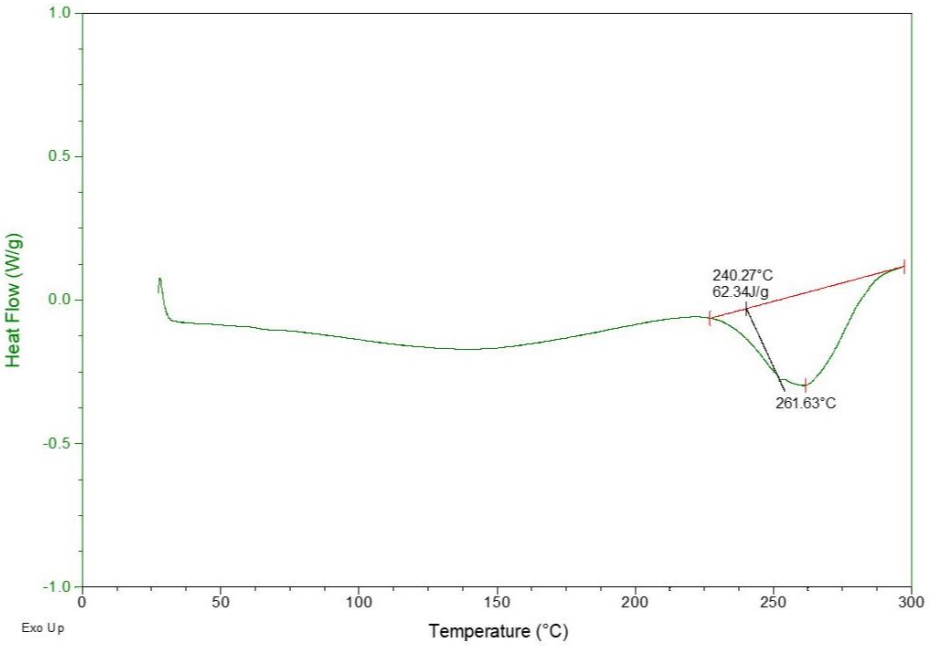

Figure 4.19: Differential Scanning Calorimetry of Rockbestos Firewall III XLPE cable that has been thermally aged (45 days at 120°C).

The DSC results indicate the destruction of polymer crystal structures associated with the re-distribution of its molecular weight due to the oxidative degradation processes. Phase melting temperatures decreased by 18 degrees in the case of irradiation aging and by 6 degrees in the case of the thermal aging. This can be explained by a more significant influence from irradiation on increasing the amorphous phase content. However, the change in the crystallinity of the samples materials is more evident in the case of thermal aging. Melting enthalpy decreased to 52 % of the initial value for the thermally aged sample, and the irradiated sample showed a more significant decrease of 83% over the original.

Table 4.6 shows all of the essential parameters recorded for the unaged, thermally aged, and irradiated samples that were tested using DSC. The main focus for the DSC tests is

the transition characteristics. This includes the onset, peak, and endset temperatures along with the energy required for the transition to occur. These values are presented in

Table 4.6: Glass transition characteristics as derived from Differential Scanning Calorimetry tests

Parameter	**Unaged (Control)**	**Thermally Aged** (45 days at 120°C)	**Irradiated** (120 days at 140 Gy/hr)
Onset (°C)	∼246	∼240	∼228
Peak (°C)	∼255	∼262	∼252
Endset (°C)	∼297	∼298	∼294
ΔH (J/g)	119.4	62.3	99.5
Percent Change in ΔH (%)	-	-47.8	-16.7

the table along with a percent change comparison between the aged samples and the unaged sample.

It can be surmised that the considered cable material is a composition, which consists of the two-component polymer fractions (modifier and XLPE) and an inorganic extender. During the aging process in conditions of irradiation and evaluated temperature treatment the modifier fraction is degraded significantly, which is evident from the fraction weight loss analysis being 1.1 and 5.4 % wt respectively. The degradation effect is underlined by DSC study results, which indicates the decrease of material crystallinity by 17 and 48 % for irradiative and thermal aging. The latter conditions are proven to be harsher for sample testing, and the temperature factor is more significant in terms of cable conditioning.

4.3.3 Variation in Heat Release Rate as a Result of Aging Processes

It is essential to understand the heat release rate when considering the flammability characteristic of a material. The heat release rate is based on the amount of energy released

from the material during combustion as a function of time. This characteristic is important because an increase in the heat release rate of a material can increase the temperature of the fire reduce nearby oxygen content, and alter the rate of temperature increase thus accelerating the spread and intensity of the fire (Babrauskas, 1996).

Peak heat release (PHR) and the total heat release (THR) of a material determines the duration and progression of the resultant flame propagation during combustion. The peak heat release directly impacts the temperature of the fire, and the instantaneous radiative/conductive/convective heat given off. This sudden increase in HR can cause rapid growth of local flame propagation, and can also cause material that is not in contact, to ignite due to high levels of radiative heat transfer. The total heat release is significant because some materials will burn slowly and smolder. This can result in prolonged burning and an overall higher increase in HR that merely is spread out over a more extended time period. Controlled testing was done to observe these changes in the samples.

The cable samples were tested using a Cone Calorimeter to determine the time to ignition for the sample, and the heat release as a function of time. The Cone Calorimeter test works by exposing the sample to a set amount of heat flux (HF) and waiting until the sample self-ignites. The point that the sample ignites is recorded as the time to ignition. Once the sample is ignited, the oxygen content begins to change due to combustion. This change in oxygen content directly determines the amount of HR that the sample is giving off. The resultant HR is recorded as a function of time. Figure 4.20 shows the heat release versus time for the Firewall III cable that is unaged, thermally aged, and irradiated. This data is derived from the Cone Calorimeter test where the heat flux for each test was set at 50 $\frac{kW}{m^2}$.

Figure 4.20 presents the HRR for the seven Firewall III cable samples that were tested. The unaged sample's ignition time was recorded to be 344 seconds with a Peak Heat Release (PHR) recorded to be 650 $\frac{kW}{m^2}$ at time 395 seconds. The Total Heat Release (THR) is recorded to be 70.1 $\frac{MJ}{m^2}$. The time to ignition for the unaged cable is the longest recorded with the smallest PHR (excluding the samples that burnt out prematurely). The reason that the unaged cable sample has the longest time until the ignition is likely due to the expansion that occurred. During the test, the sample absorbed the heat flux and began expanding in size which delayed the time that it took for ignition. This is how the cable should operate, as it is designed to expand significantly and not melt but rather burn on the surface until it degrades enough to expose the next polymer layer of the cable jacket.

The thermally aged samples were recorded to have the following PHR and times (least thermal aging to greatest): 380 $\frac{kW}{m^2}$ at time 225, 777 $\frac{kW}{m^2}$ at time 390, and 881.93 $\frac{kW}{m^2}$ at time 340. The thermally aged samples increased in peak heat release in relation to the increase in thermal aging exposure. The THR for the thermally aged samples (in order of exposure)

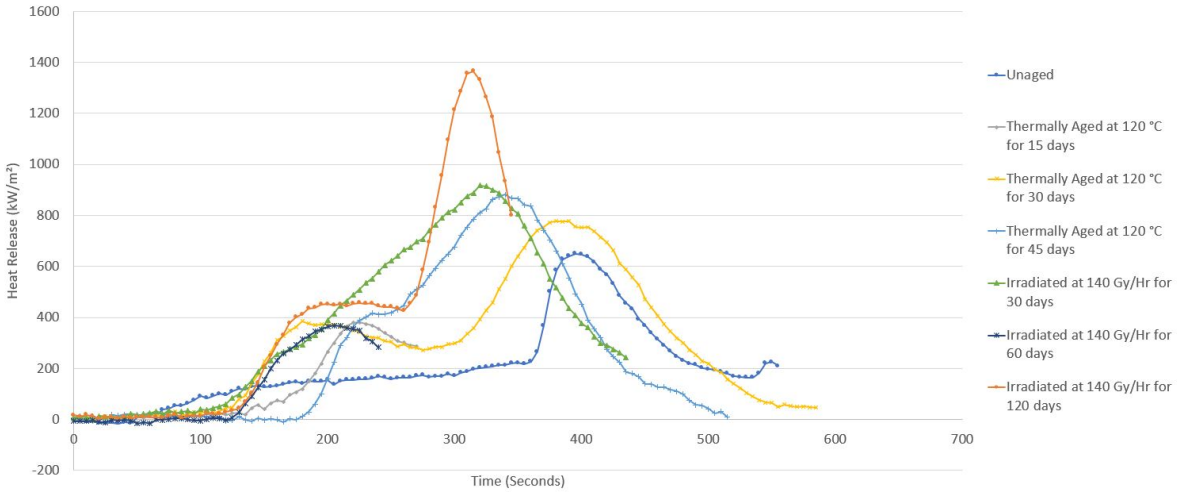

Figure 4.20: Cone Calorimeter Heat Release Rate for Firewall III Cable that is unaged, thermally aged, and irradiated.

are as follows: 31 $\frac{MJ}{m^2}$, 169.5 $\frac{MJ}{m^2}$, and 123.5 $\frac{MJ}{m^2}$. The THR is low for the sample aged for 15 days because it self-extinguished early in the test run, and the 30-day sample has a larger THR than the 45-day samples because it didn't take as long to reach half of its THR.

The irradiated samples were recorded to have the following time and PHR from least to most irradiated: 917.66 $\frac{kW}{m^2}$ at time 320 seconds, 368 $\frac{kW}{m^2}$ at time 205 seconds, and 1365.68 $\frac{kW}{m^2}$ at time 315 seconds. Two of the irradiated samples showed a large increase in PHR. The cable that was irradiated for 60 days, self-extinguished but appeared to be trending towards the same pattern as the rest of the samples. The THR for the irradiated samples (in order of exposure) are as follows: 156.8 $\frac{MJ}{m^2}$, 21.8 $\frac{MJ}{m^2}$, and 128.3 $\frac{MJ}{m^2}$. The higher THR for the 30-day sample is based on the high heat release and a prolonged period of burning. The small THR for the 60-day sample is again related to the self-extinguished flame that occurred, but it is likely that it would have fallen in line with the rest.

Figure 4.21 shows the Cone Calorimeter data recorded from the ULTROL 60+ test samples. Two samples were tested for this cable, the first sample is unaged and the second sample is thermally aged. The test was conducted by using twelve pieces of cable cut to length and fitted into the Cone Calorimeter. The test was conducted with a heat flux of 50 $\frac{kW}{m^2}$. The results show that the unaged cable ignited quickly and burned out while the thermally aged cable took longer to ignite and burned for a longer period of time.

Figure 4.21 provides a vital understanding of the changes in heat release for unaged and thermally aged cable. This understanding is greatly expanded by the use of many samples tested to demonstrate a clear difference in the results. The unaged cable sample's ignition time is 94 seconds while the thermally aged samples is 71 seconds. This shows that the unaged cable can absorb more heat flux before it ignites.

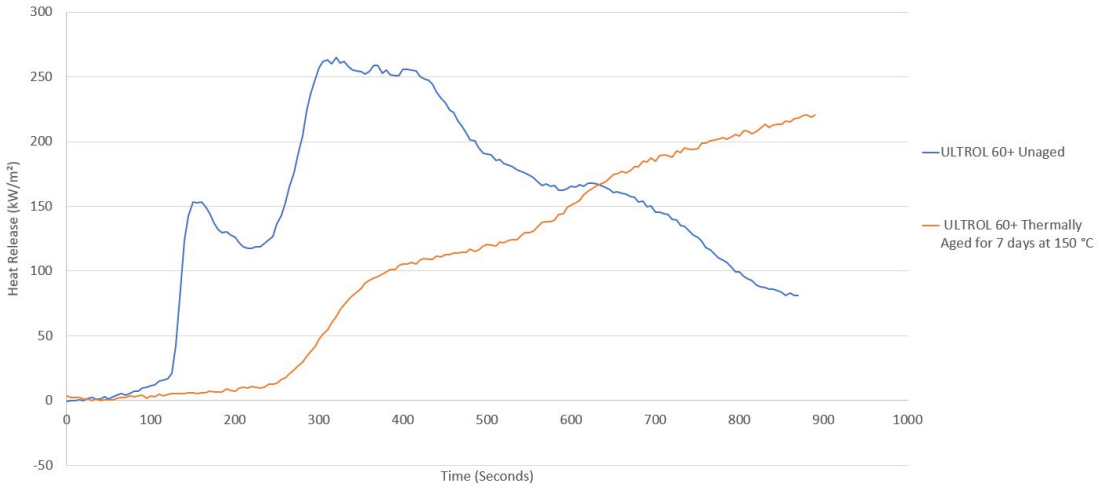

Figure 4.21: Cone Calorimeter Heat Release Rate for ULTROL 60+ Cable that is unaged and thermally aged (7 days at 150 °C). The test was performed using 12 pieces of cable (for each sample) to form a layer in the Cone Calorimeter.

Another consideration is the peak heat release (PHR) for the cable samples. The PHR is recorded to be 265 $\frac{kW}{m^2}$ at time 320 seconds for the unaged cable and 220 $\frac{kW}{m^2}$ at time 890 seconds for the thermally aged cable. This infers that the unaged cable burned hotter and faster than the thermally aged cable. The thermally aged cable ignited faster but burned slowly and steadily while reaching towards the max HR for the sample. The total heat release (THR) for the unaged sample is recorded to be 126.0 $\frac{MJ}{m^2}$, and the thermally aged sample has a (THR) of 91.3 $\frac{MJ}{m^2}$. This shows that for the time shown on the figure the unaged cable has produced a more significant amount of THR.

Table 4.7 is a high-level overview of the numerical data recorded for the cone calorimeter tests. The time until peak heat release and the resultant peak heat release for each sample is presented in the table. The table also offers the percent change recorded between each individual sample and the unaged sample. The first and second highest PHR recorded was for the most irradiated and third most irradiated samples. The third, fourth, and fifth

Table 4.7: Peak Heat Release as derived from Cone Calorimeter tests

Sample	Cable Type	Aging Characteristics	Time of Peak Heat Release (sec)	Peak Heat Release ($\frac{kW}{m^2}$)	% Change From Unaged	Observation
1	Rockbestos Firewall III	Unaged	395	650	-	Lowest HR (Besides Self-Extinguished)
2	"	Thermally Aged (120°C for 15 days)	225	380	-41.54	Self-Extinguished
3	"	Thermally Aged (120°C for 30 days)	390	777	19.54	Fourth Highest HR
4	"	Thermally Aged (120°C for 45 days)	340	882	35.69	Third Highest HR
5	"	Irradiated (30 days at 140 Gy/hr)	320	918	41.23	Second Highest HR
6	"	Irradiated (60 days at 140 Gy/hr)	200	363	-44.15	Self-Extinguished
7	"	Irradiated (120 days at 140 Gy/hr)	315	1366	110.15	Highest HR
8	ULTROL 60+	Unaged	320	265	-	Early Peak HR
9	"	Thermally Aged (150°C for 7 days)	880	220	-16.98	HR Still Rising

highest was recorded for the thermally aged samples in order of exposure (from highest to lowest exposure). A couple of samples self-extinguished before their PHR was reached and as such, they do not provide much insight.

The Cone Calorimeter testing provides an understanding of a sample's ignition time, burn time, peak heat release, time that PHR occurs, and total heat release.

The Firewall III cable showed a trend where the thermal aging increased in heat release and peak heat release over the unaged cable. The irradiated Firewall III cable samples also showed an increase in heat release and peak heat release over both the thermal aged and unaged samples. The ULTROL 60+ cable that was thermally aged showed a faster ignition time and the possibility of a higher heat release over the unaged cable if the test would have gone longer (a direct result of using twelve samples instead of one).

4.3.4 Industry Standard: A Look Into UL94 Flame Spread Testing

The standard test for determining the flammability of plastic parts is the UL94 vertical flame spread test (Laboratories, 1997). This test is useful in setting a standard for what is considered acceptable for the flammability characteristics of a material that is to be used in practice. As a result, if a sample passes this test, then it is reasonable to assume that its flammability characteristics do not compromise its continued use in practice. Some of the samples that are tested have undergone irradiation and thermal aging that is considered to be past the expected exposure that would occur during the normal lifetime of the cable. These conditions provide a means of assessing if, during the normal operating lifespan, irradiation or thermal aging can cause the cable to become unsafe or unfit for use due to degradation in the cable's flammability characteristics.

Six cable samples were tested using the UL 94 Vertical Flame Spread Test. The six samples consisted of three cable types where the best and worse case scenarios were selected for each cable type. The two Firewall III samples consisted of an unaged sample and the sample that was irradiated for 120 days at 140 Gy/hr. The two ULTROL 60+ samples consisted of the unaged sample and the sample that was thermally aged for 7 days at 150°C. The Boston Insulated Wire samples consisted of an unaged sample and a sample exposed to 7 days of thermal aging at 150°C. The testing of these samples provides an acceptable standard showing whether or not the flammability characteristics are acceptable during the average lifespan of cable that is exposed to such conditions.

The UL 94 test is conducted by using a Bunsen Burner to expose the sample to a constant flame source for a duration of 10 seconds, at which point the sample is removed from the flame source. If the sample is still burning after it is removed, then the time until the flame is extinguished is recorded. If the flame self-extinguishes then the sample is exposed to the

flame again for 10 seconds, and the process is repeated. It is also noted if any flaming pieces are dripped onto the cotton and if the cotton gets ignited. Part A and B of Figure 4.22 show the cable samples at the last second of the tests before the flame is removed while part C and D show the same moment recorded with a thermal imaging camera.

The Firewall III cable samples that were tested are shown in Figure 4.22. The Firewall III cable samples that were tested both received a rating of V-0, the highest rating given for the UL 94 vertical flame spread test. The samples that were tested were both exposed to the flame for 10 seconds and removed. The samples immediately self-extinguished. Both samples were again subjected to 10 seconds of flame exposure. When the samples were again removed they both immediately self-extinguished. This meant that both the unaged and irradiated Firewall III samples passed the UL 94 test with a V-0 rating.

The samples passed but observations of the tests can still be made. During the test, the unaged sample showed expansion and charring of the cable jacket. The cable jacket also had small pieces of the jacket fall off from degradation.

This process is intentional as thermoset cable is not supposed to melt but burn away and degrade over time. The irradiated sample showed little signs of charring and expansion. This sample absorbed more of the heat and displayed a larger flame during the exposure to the Bunsen Burner. While both samples passed the test with a high rating, the samples both displayed different characteristics.

The ULTROL 60+ cable samples were tested in the same manner as the Firewall III samples. The ULTROL 60+ unaged and thermally aged samples were tested.

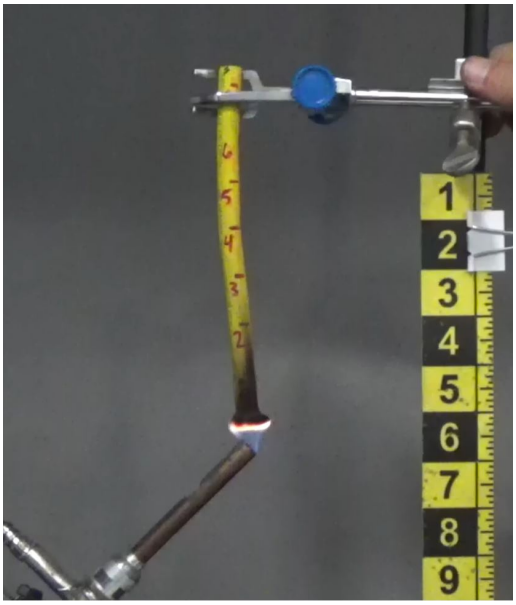

(A) Unaged Jacket.

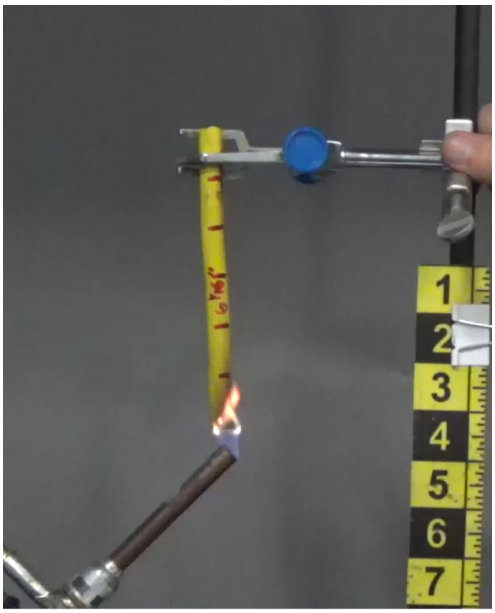

(B) Irradiated Jacket.

(C) Unaged Jacket

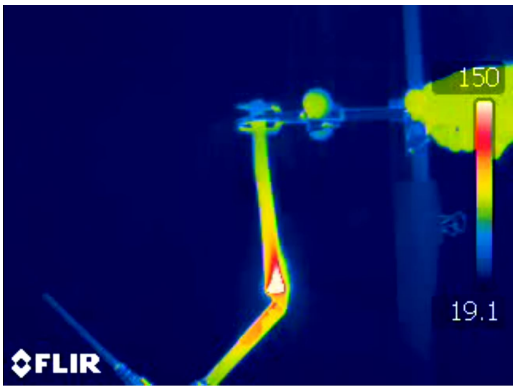

(D) Irradiated Jacket.

Figure 4.22: UL94 Flame Test of Rockbestos Firewall III XLPE cable that is unaged (A & C) and irradiated (120 days at 140 Gy/hr, B & D) (Images taken at last second of UL 94 tests before flame was removed).

Part A and part B of Figure 4.23 show the ULTROL 60+ samples at the last second, before the flame was removed, of the UL 94 test. Part C and part D of Figure 4.23 show the thermal imaging recorded at the end of the test before the flame was removed.

The ULTROL 60+ cable samples that were tested are shown in Figure 4.23. Two of the cable samples were tested to determine if thermally aging, past the average lifespan, would compromise the cable's safety standard. Both ULTROL 60+ samples were subjected to 10 seconds of flame exposure and both samples self-extinguished once the flame was removed. This process was repeated immediately following with the same result. The two samples both received a UL 94 vertical flame spread test rating of V-0 since the samples self-extinguished immediately after being removed from the flame.

The unaged ULTROL 60+ sample showed very minimal changes during the exposure to the flame. The sample slowly charred on the surface of the cable jacket but no flame propagation or falling pieces were observed. The thermally aged sample showed similar charring with minimal flame propagation. The thermally aged sample did not show any falling pieces of material during the test. The two samples displayed a similar amount of absorption of the flame heat with minimal dissipation of the heat. This behavior is acceptable and is typical for a cable that utilizes additives to provide adequate flammability suppression.

The final samples that were tested using the UL 94 test were the Boston Insulated Wire samples that were unaged and thermally aged past the average lifespan of the cable. Part A and B of Figure 4.24 show the two samples during the last moments of the UL 94 test before the flame was removed from the samples. Part C and D of Figure 4.24 show the thermal imaging that was recorded at the last moments before the flame was removed. These figures help in showing how the cable was reacting during the test.

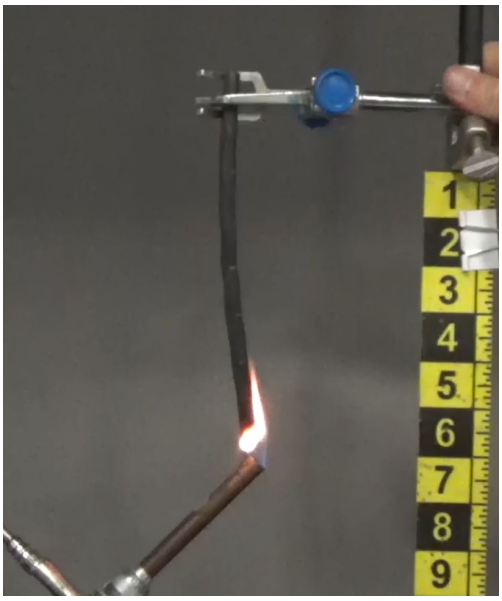

(A) Unaged Jacket.

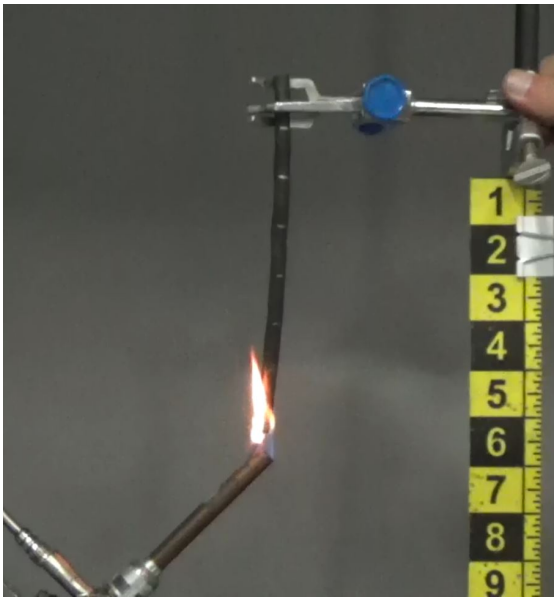

(B) Thermally Aged Jacket.

(C) Unaged Jacket

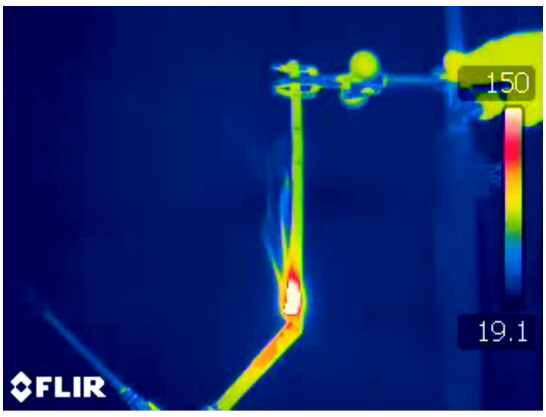

(D) Thermally Aged Jacket.

Figure 4.23: UL94 Flame Test of ULTROL 60+ cable that is unaged (A & C) and thermally aged (7 days at 150 °C, B & D) (Images taken at last second of UL 94 tests before flame was removed).

Figure 4.24 is a compilation of the UL 94 tests performed on the Boston Insulated Wire samples. Two samples were tested where one was unaged, and the other was thermally aged past its typical lifespan. The two both self-extinguished immediately after the flame was removed from the samples. This means that both samples also received a rating of V-0.

The unaged BIW sample showed expansion of the cable jacket and charring and also showed a much faster transfer of heat through the cable. The thermally aged cable showed no expansion and minimal charring. The heat transfer through the cable was not as fast as the unaged jacket sample. The two samples both showed acceptable flammability characteristics.

Table 4.8 is a compilation of the data recorded from the UL94 tests. The primary questions raised were if there was any flammable dripping, the time to self-extinguish after first exposure, and time to self-extinguish after the second exposure. Every sample that was tested showed no dripping, and a very fast extinguish for both sets of exposures. All of the samples received a rank of V-0.

The UL 94 tests that were performed on the three different cable types showed favorable results. The Firewall III cable samples showed that irradiation, past the normal lifetime exposure, of that cable type did not compromise the safety of the cable's flammability characteristics (as suggested by industry standards). The ULTROL 60+ cable samples and the Boston Insulated Wire cable samples showed that thermal aging, past the normal lifetime exposure, did not compromise the safety of the cable's flammability characteristics (as suggested by industry standards).

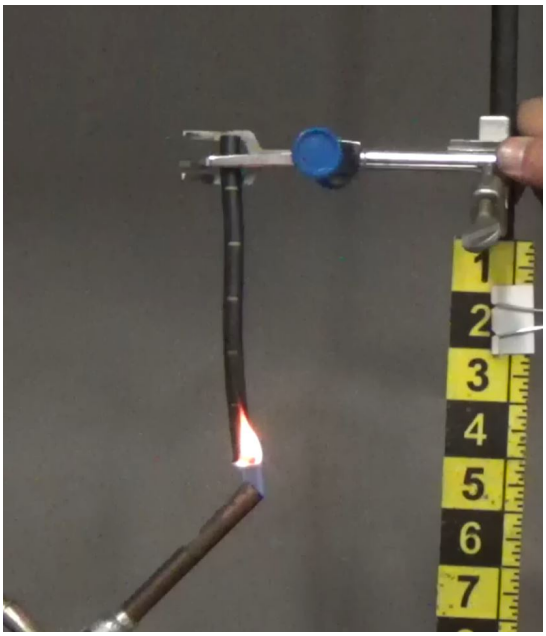

(A) Unaged Jacket.

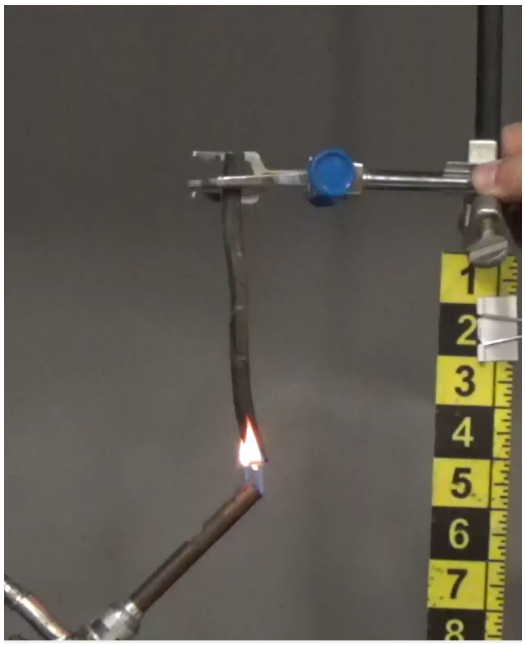

(B) Thermally Aged Jacket.

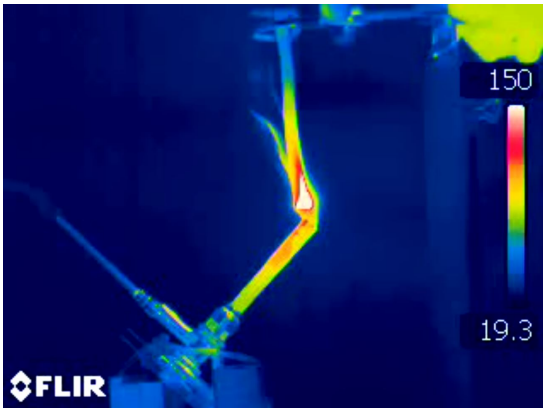

(C) Unaged Jacket

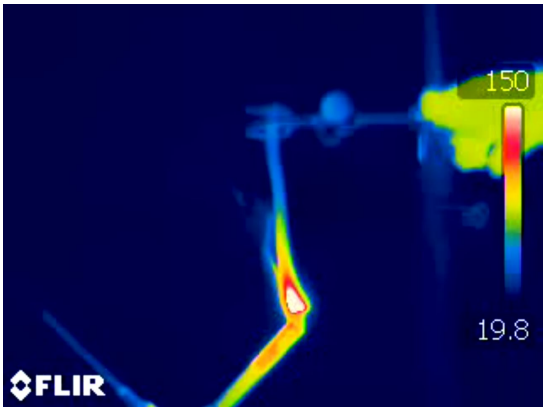

(D) Thermally Aged Jacket.

Figure 4.24: UL94 Flame Test of Boston Insulated Cable (BIW) cable that is unaged (A & C) and thermally aged (7 days at 150 °C, B & D) (Images taken at last second of UL 94 tests before flame was removed).

Table 4.8: UL 94 classifications for cable samples

Sample	Cable Type	Aging Characteristics	Dripping	T1	T2	Rank
1	Rockbestos Firewall III	Unaged	No	< 1 sec	< 1 sec	V-0
2	”	Irradiated (120 days at 140 Gy/hr)	No	< 1 sec	< 1 sec	V-0
3	ULTROL 60+	Unaged	No	< 1 sec	< 1 sec	V-0
4	”	Thermally Aged (150°C for 7 days)	No	< 1 sec	< 1 sec	V-0
5	Boston Insulated Wire	Unaged	No	< 1 sec	< 1 sec	V-0
6	”	Thermally Aged (150°C for 7 days)	No	< 1 sec	< 1 sec	V-0

4.4 In Situ Reactance Measurements In Relation To Aging Processes

Similar to cable used in nuclear power plants, cable in industry is typically constructed with multiple conductors inside a single cable jacket and separated by individual jackets. This allows one cable to have multiple conductors that can run different signals to different components. This also introduces the ability to measure the reactance of two conductors that run parallel to each other but are separated by an insulator (the single conductor jackets). In electrical practices, a *transmission line* is any two conductors that run parallel to each other and are insulated by some medium. It is well known that transmission lines impact each other because of their changes in electric and magnetic fields that result from the transmission of AC current and voltage. This means that electrical cable used in industry can be treated as a transmission line and the resultant changes in reactance can be observed to provide an understanding of the physical changes of the cable.

To measure the reactance of the different cable samples, it was necessary to use an antenna analyzer that had the capability to record the inductive and capacitive reactance. This allowed the reactance for each sample to be measured where at least 2 resonant frequencies were recorded. It was necessary to have the ability to measure at high enough frequencies to be able to record multiple resonant frequencies to develop proper deviations in the data between the samples. Seven different samples for the Firewall III cable were tested ranging from irradiated to thermally aged and unaged. Two ULTROL 60+ and two BIW samples were tested that were unaged and thermally aged to provide an additional understanding of the results.

The Firewall III samples were the first to be tested. The samples consisted of one unaged sample, three thermally aged samples, and three irradiated samples. Each sample was connected the same way, and the antenna analyzer was left in the same location throughout the tests. Each cable was tested where there was no connection at the far end of the cable. Each cable was prepared to be as close as possible to the same length. Changes in length result in changes in both the wavelength and the reactance curve; however, these changes would essentially only cause the reactance curve to shift in one direction or the other but retain the same shape. Each of the Firewall III samples was tested, and the resultant reactance that was recorded is displayed in Figure 4.25.

The reactance that is recorded has four integral components that are important to understand. The first is the rising curve that starts as a negative reactance and goes to zero reactance; this curve represents the capacitive reactance. The continuation of that curve from zero to its max positive value is considered the inductive reactance. At this point, an asymptote occurs and the inductive reactance transitions back over to capacitive

reactance. The transition point from capacitive reactance to inductive reactance (at zero reactance) is the series resonance. This resonant point is when the effective capacitance and inductance of the cable is in series and equal. The final point to consider is when the inductive reactance transitions to the capacitive reactance. This point represents the antiresonance for the cable. This resonance is essential because the difference between the inductive and capacitive reactance will become apparent at this point. This will separate the samples that differ in capacitive and inductive reactance resulting in trends.

The inductive and capacitive reactance for the thermally aged and irradiated samples formed separate groupings as shown in Figure 4.25. The thermally aged samples show a clear reduction and shift in inductive reactance for the first resonance. The irradiated samples show a close relation to the original sample in the first resonance but significantly deviated in the second resonance. It is also noticeable that the thermally aged samples deviated

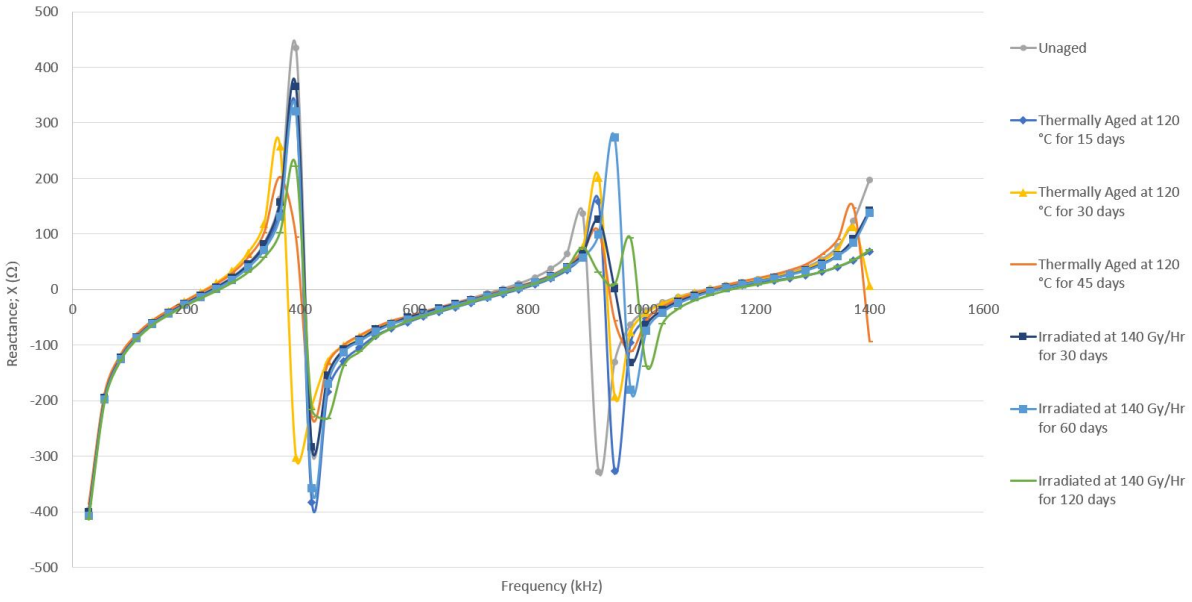

Figure 4.25: Reactance as a function of frequency of the Rockbestos Firewall III XLPE cable for varying amounts of thermal aging and irradiation.

more in the second resonance. This is likely due to compounding separation of inductive and capacitive curves. It may also be noted that, at the second resonance, the shift is the greatest to least in the order of the irradiated samples, the thermally aged samples, and the unaged sample. The thermally aged and irradiated sample measurements are broken up and graphed to provide a clearer understanding of their characteristics. Figure 4.26 shows the reactance measurement for the thermally aged samples in comparison to the unaged sample.

The thermally aged samples showed a reduction in inductive reactance and a lower frequency shift in peak inductive reactance for the first resonance. The second resonance shows a lined-up grouping of inductive reactance where the most aged sample has the smallest inductive reactance. Noticeably, the capacitive reactance is uniquely distinct and characteristic of the amount of thermal aging that the samples had undergone. The least aged sample shifted right from the unaged sample with a slight decrease in capacitance. The second most aged sample reduced its capacitive reactance by about 30% over the unaged

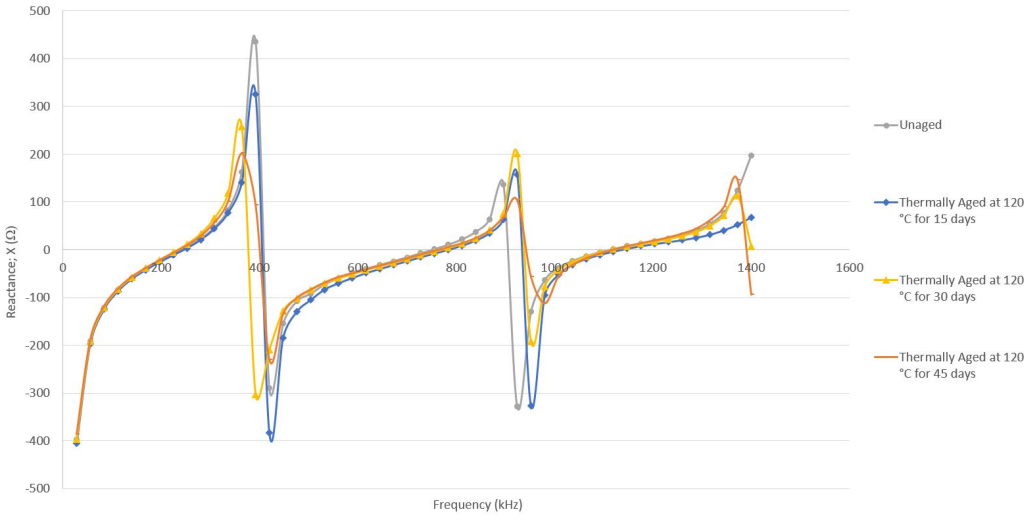

Figure 4.26: Reactance as a function of frequency of the Rockbestos Firewall III XLPE cable for varying amounts of thermal aging.

sample. The most aged sample showed a reduction of almost 60% over the unaged sample. This apparent shift caused the third resonance to follow the same pattern with the inductive reactance as what occurred with the capacitive reactance. The most aged sample reached its peak inductive reactance first followed by the second most aged sample and so on.

Figure 4.27 shows the reactance measurement for the irradiated samples in comparison to the unaged sample. The irradiated samples showed some truly unique characteristic reactance curves. The inductive reactance peaks for each sample lined up for the first resonance. Interestingly, the max inductive reactance for each sample decreased as the irradiation exposure increased for the first resonance. The capacitive reactance for the first resonance showed a similar behavior with the exception of the least irradiated sample, as it had the highest capacitance. The second resonance once again displayed a significant shift in the characteristics of the different sample. The inductive reactance shifted right (increased peak frequency) for each sample in the progression of irradiation exposure. The capacitive

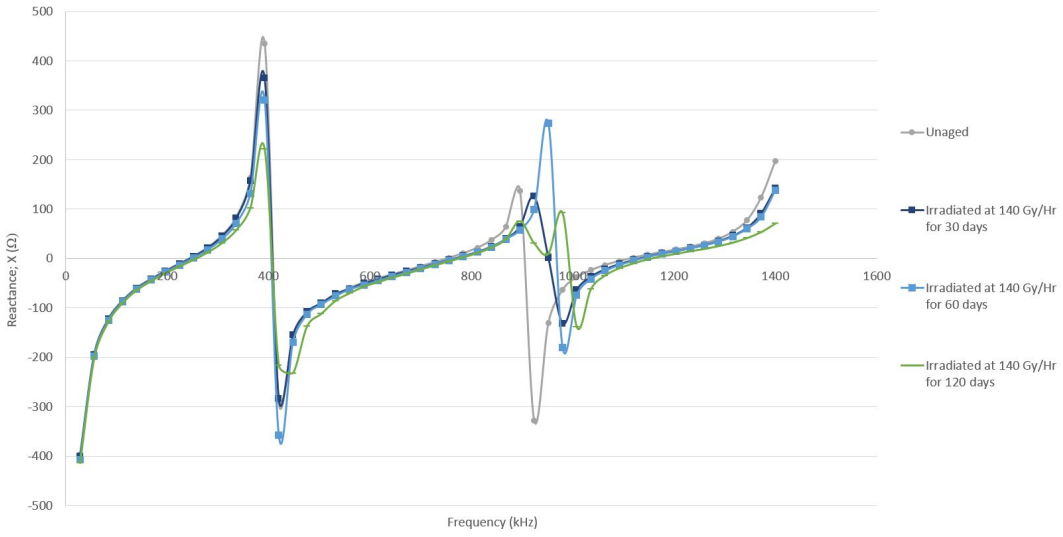

Figure 4.27: Reactance as a function of frequency of the Rockbestos Firewall III XLPE cable for varying amounts of irradiation.

reactance also showed a right shift with the most capacitive reactance being the unaged sample (which was the same case for the thermally aged samples). The most irradiated sample displayed a unique characteristic where the inductive reactance had two peaks and caused a drastic shift in the second antiresonance frequency. The third resonance shows a similar trend as the unaged appears to be the first to transition followed by the least to most irradiated samples. Figure 4.28 shows the reactance measurement for the thermally aged and unaged samples for the ULTROL 60+ cable.

The ULTROL 60+ samples recorded many more resonant frequencies across the same frequency range as the previous cable. The additional resonant frequencies are likely due to the physical differences in the cable types. The main difference is that this cable has a copper sheath around the conductors that acts as a neutral. The two samples were both measured the same way as the previous cable samples.

The inductive and capacitive reactance for the thermally aged and unaged samples formed separate groupings as shown in Figure 4.28. This particular sample was thermally aged for 7 days at 150 °C, a high temperature to be exposed to that can cause more damage at a faster pace over the other samples. The thermally aged sample shows a clear separation from the unaged sample's curve. The thermally aged sample's inductive reactance shifted left in peak frequency and periodically changes its peak inductive reactance from a higher value to a lower value over the unaged sample. The capacitive reactance is more significant for the first three resonances, but the fourth to the sixth capacitive reactance is much smaller over the unaged samples. Figure 4.29 shows the reactance measurement for the thermally aged and unaged samples for the BIW cable.

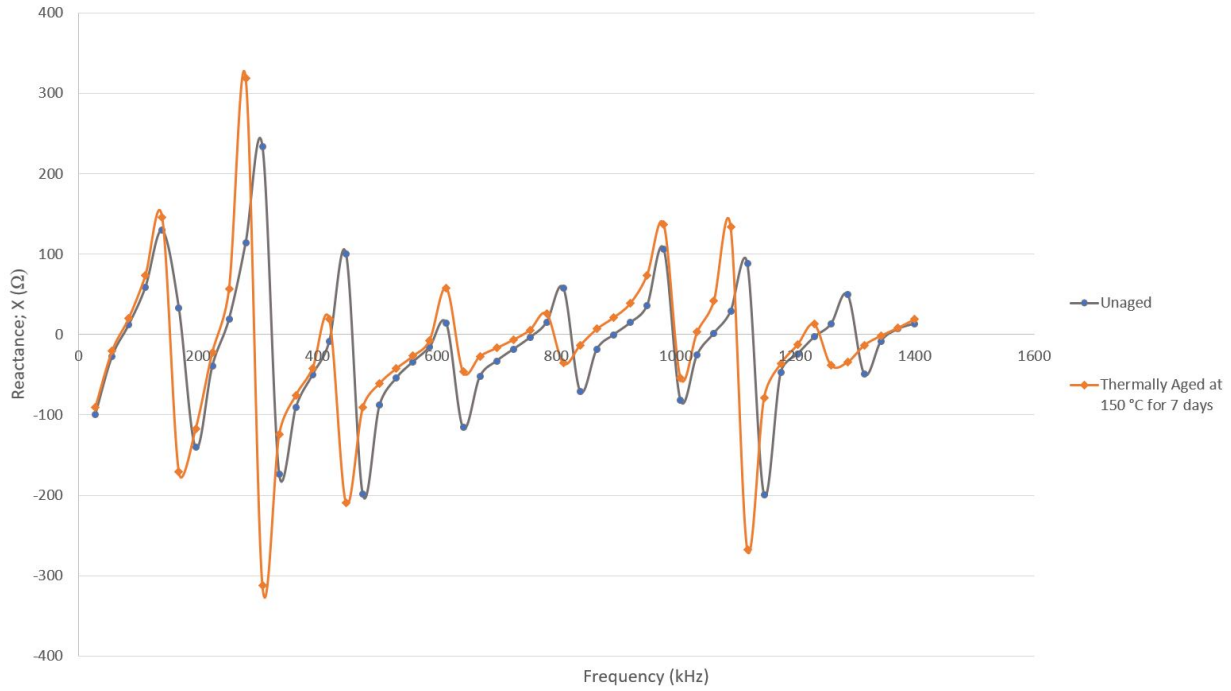

Figure 4.28: Reactance as a function of frequency of the ULTROL 60+ cable (unaged and thermally aged).

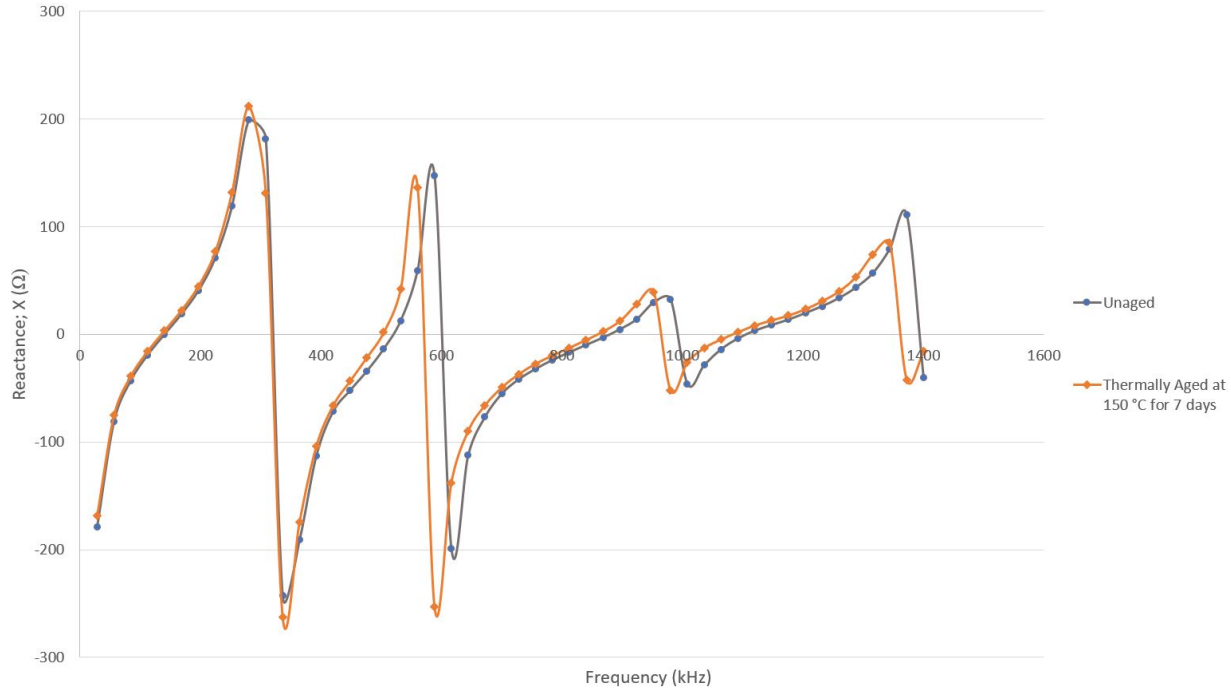

Figure 4.29: Reactance as a function of frequency of the Boston Insulated Wire (BIW) cable (unaged and thermally aged).

The Boston Insulated Wire (BIW) samples recorded four distinct resonances. Similar in design to the ULTROL 60+ cable, Boston Insulated Wire also has a sheath type neutral around the conductors. The thermally aged BIW sample also shows similar characteristics of the ULTROL 60+ cable. There is a clear left shift of the resonant frequency for the thermally aged sample. This particular cable did not show any significant variations in inductive or capacitive reactance until the fourth resonant point where the inductive reactance begins to reduce in size. It is possible that a higher frequency range for this cable could provide additional information, but a clear deviation can still be observed by the second resonance.

Table 4.9 provides a numerical representation of all of the key points from the reactance graphs that were recorded. The table shows the series resonance, antiresonance, peak inductive reactance, and peak capacitive reactance for the first, second, and third resonances of each sample. Observation of this data shows little variation between samples for the first resonance. The second resonance provides the clearest deviation and understanding between samples. There is particular interest in the series resonance and antiresonance for the second resonance of the system. A clear pattern is formed for both of these points where the series resonance shows a massive spike with a gradual decrease for the thermally aged samples and a slight spike with a gradual increase for the irradiated samples. The antiresonance shows a gradual increase for thermally aged and for irradiated Firewall III samples.

The peak capacitive reactance for the second resonance is also useful to observe. The thermally aged samples showed less capacitive reactance as a function of exposure, and the irradiated samples showed less capacitive reactance with a slight increase as a function of exposure. The ULTROL 60+ and BIW samples showed a significant increase with thermal aging exposure. Basic observation suggests that a right shift in the second resonance

Table 4.9: Frequency resonance, inductive reactance, and capacitive reactance recorded for Firewall III cable, ULTROL 60+ cable, and Boston Insulated Wire (BIW) cable.

			First Resonance				Second Resonance				Third Resonance			
Sample	Cable Type	Aging Characteristic	Series Resonance (kHz)	Antiresonance (kHz)	Peak Inductive Reactance	Peak Capacitive Reactance	Series Resonance (kHz)	Antiresonance (kHz)	Peak Inductive Reactance	Peak Capacitive Reactance	Series Resonance (kHz)	Antiresonance (kHz)	Peak Inductive Reactance	Peak Capacitive Reactance
1	Rockbestos Firewall III	Unaged	244	409	435	-290	752	904	137	-328	1113	NR	≥198	NR
2	”	Thermally Aged (120°C for 15 days)	246	405	325	-383	784	933	157	-326	1137	NR	≥68	NR
3	”	Thermally Aged (120°C for 30 days)	233	377	257	-303	770	938	202	-192	1117	NR	≥113	NR
4	”	Thermally Aged (120°C for 45 days)	236	400	202	-231	764	942	104	-112	1119	1389	147	≤ -94
5	”	Irradiated (30 days at 140 $\frac{Gy}{hr}$)	245	408	366	-284	767	952	125	-132	1132	NR	≥142	NR
6	”	Irradiated (60 days at 140 $\frac{Gy}{hr}$)	250	405	321	-358	770	969	274	-180	1138	NR	≥138	NR
7	”	Irradiated (120 days at 140 $\frac{Gy}{hr}$)	258	406	222	-232	777	991	92	-139	1158	NR	≥70	NR
8	ULTROL 60+	Unaged	76	173	129	-141	243	324	234	-174	423	458	100	-199
9	”	Thermally Aged (150°C for 7 days)	70	153	146	-171	232	294	318	-312	412	422	19	-210
10	BIW	Unaged	140	320	199	-243	518	600	148	-199	879	992	33	-46
11	”	Thermally Aged (150°C for 7 days)	135	317	212	-263	502	570	136	-253	859	964	40	-52

combined with a reduction of capacitive reactance is a direct function of the exposure to thermal aging and irradiation. Where the two differ only by the degree of variance (more massive shift and less capacitive reactance trends toward irradiation over thermal aging).

The results from each of the cable samples showed a clear deviation from the unaged sample. The Firewall III samples showed a right shift and reduction in both capacitive and inductive reactance for both the thermally aged and irradiated samples where the two aging process formed independent groupings. The ULTROL 60+ samples showed a left shift and increase/decrease (depending on resonant point) in both the capacitive and inductive reactance for the thermally aged sample. The BIW samples showed a left shift and a slight reduction in inductive reactance for the thermally aged sample. In every case, the deviations from the unaged samples did not become significantly apparent until the second resonant frequency.

4.5 Summary of Research Findings

This chapter explored and presented the data recorded from each aspect of the research. The physical characterization of the cable jacket was examined to identify changes that resulted from the aging processes. The indenter modulus testing, SEM, and FTIR were evaluated to provide an understanding of the physical changes. To provide an understanding of the changes in flammability characteristics the following data were evaluated: TGA, DSC, UL94, and Cone Calorimetry. Finally, to determine a measurable relation between the aging processes and changes in flammability characteristics, the reactance testing was performed.

These tests give an evaluation for the main three topics of how the aging processes impact the cable's characteristics. The purpose of this chapter is to analyze the data without forming an opinion about the outcome of the data. The following chapter will go into the implications of the data and what it entails.

Chapter 5

Discussion and Implications

5.1 Overview

The aim of this study was to find out the flammability characteristic changes of aging cable used in industry. Irradiated and thermally aged cable was studied where the physical property changes and flammability characteristics were observed and recorded. A passive method to measure the characteristic differences was also proposed.

This research conducted experiments on different types of cables. The samples were exposed to a various amount of thermal aging or irradiation. Each cable type had a control sample that was used to compare against for each test. The first set of tests focused on providing an understanding of the physical changes that resulted in each cable as a result of either thermal aging or irradiation. The second set of tests focused on determining the impact that thermal aging or irradiation had on the flammability characteristics of the samples. Finally, a method of testing the cable to determine the changes in flammability characteristics as a function of thermal aging or irradiation was explored. The various

research methods provide an excellent top-down approach to understanding the impact that thermal aging and irradiation have on the cable used in industry.

This chapter focuses on the discussion and implications obtained from the empirical results. The previous chapter included some brief observations of the data but did not provide an in-depth understanding. The aim of this chapter is to lay out the theory and implications of the results. The research and findings will also be compared to any existing literature to explore contradictions or agreements that arise. In addition, this research provides an expansion on current knowledge and a foundation for future understanding of aging cable used in industry.

5.1.1 Significant Factor: Physical Characteristics

The results of the deformation, SEM, and FTIR analysis on the physical changes, that occurred from the aging processes, showed specific alterations in the jacket materials including an increase in water affinity, oxidation, changes in density, changes in porosity, and polymer destruction. An increase in water affinity is typically a result of polymer degradation where the polymer structure forms gaps that allow foreign substances to enter. The occurrence of polymer destruction from thermal aging is a result of the vibrational stretching of the OH links due to sustained heat exposure. The irradiated sample showed similar polymer destruction from vibrational stretching of the OH links that significantly degraded the alumosilicate polymer bonds. The prolonged heat exposure caused changes in the material crystallinity for the thermally aged samples that resulted in an increase in density. The irradiated samples showed a reduction in the methylene bonding combined

with the polymer degradation that resulted in increased porosity and a decrease in relative density. Oxidation is a common occurrence for material that has been subjected to thermal aging or irradiation as free electrons are formed during these processes. The oxidation can create layers of varying characteristics along the jackets material and is a sign of material degradation.

The physical changes during aging can alter a couple of critical characteristics of the cable. The first characteristic that is considered is the dielectric constant for the jacket material. The dielectric constant is a measure of how much a material can be polarized and subsequently determines the insulative properties of the material. The increase in water affinity, oxidation, and changes in porosity directly impact the dielectric properties of the cable jacket. An increase in density causes an increase in the polarization and subsequent dielectric constant that is seen for the thermally aged sample. While an increase in porosity decreases the dielectric constant, which is seen for the irradiated samples, both aging types showed an increase in water affinity and oxidation which should increase the dielectric constant. This shows that the most significant differentiating factor for characteristic physical changes from thermally aged and irradiated samples is the relative density.

The relative change in density is a direct function of the elasticity of the cable jacket. The testing revealed that the thermally aged samples caused a decrease in the elasticity of the material and that the irradiated samples showed an increase in the elasticity. The decrease in elasticity, for the thermally aged samples, is consistent with the physical variations that were observed. The thermally aged cable shrunk in size, became denser, and some surface smoothing was observed. The irradiated cable became more elastic, increased in porosity,

and a decrease in density was observed. These physical changes are reflective of the aging processes that the cables were subjected to.

Figure 5.1 summarizes the physical changes that are observed in the thermal and irradiative aging processes. The thermally aged process results in an increase in density and less deformation. The irradiated process results in an increase in porosity and higher deformation.

The irradiated sample exhibited greater degradation and polymer destruction (12%) than the thermally aged samples (6%). This research aims to determine the changes in flammability characteristics with different amounts of thermal aging or irradiation. Evaluating the physical alterations that occur from the aging processes provides an

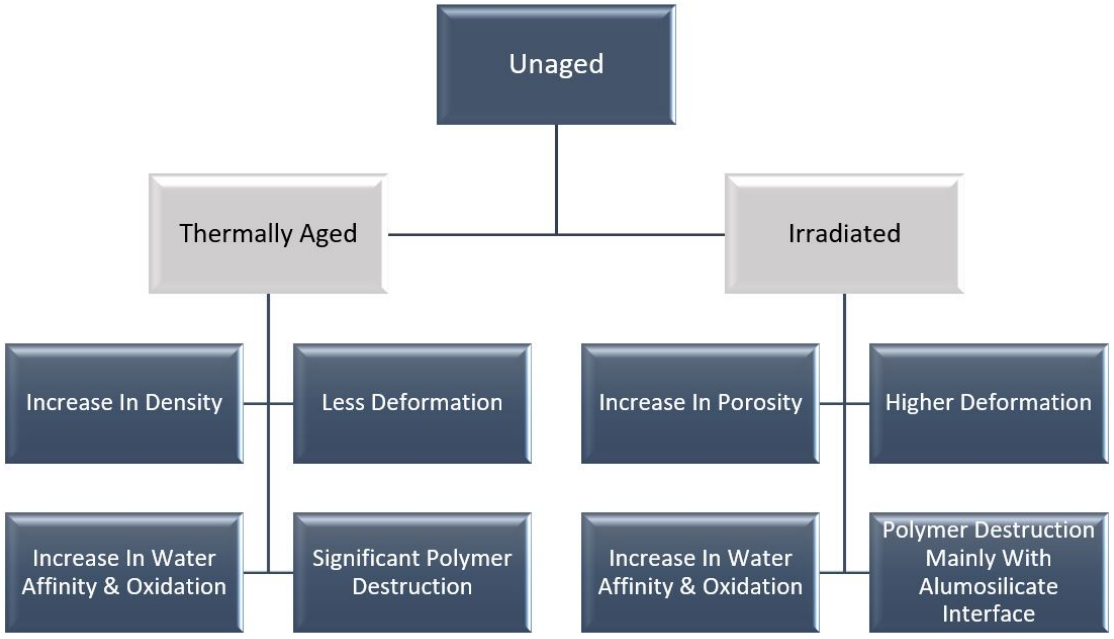

Figure 5.1: Flow chart illustration to show the main physical changes for thermal aging and irradiation.

understanding of the relative differences in the flammability characteristics between samples. These two aspects will be compared in the following sections.

5.1.2 Significant Factor: Flammability Characteristics

The results of the TGA, DSC, Cone Calorimeter, and UL 94 analysis, on the flammability characteristics of thermally aged and irradiated samples, revealed specific alterations in their properties including an increase in peak heat release, lower glass transition temperatures, faster degradation from burning, and less energy required for glass transition. The results from these tests show that the cables remain within industry standards for flame spread ratings. An increase in the peak heat release is significant. Heat release directly contributes to the possible spread of fire. Every material has a certain amount of energy required to combust and the heat release is the energy given off by a material that is burning. The glass transition temperature is the temperature required for the material to undergo a phase change (begin to degrade or melt). The glass transition temperature is the beginning of the cable being compromised and is related to degradation. Finally, to determine if any of the samples were compromised and did not meet industry standards (as a result of aging) the samples underwent the UL 94 flammability test.

The first aspect to consider is the heat release rate that was recorded for each sample. The thermally aged samples (that did not self-extinguish) demonstrated a higher heat release rate than the unaged samples for the Firewall III cable. The irradiated Firewall III samples (that did not self-extinguish) resulted in the highest heat release of all of the samples. The peak heat release for both the thermally aged and irradiated samples also occurred faster

than the unaged sample. If the heat release is higher and occurs quicker, then it will cause the fire to propagate faster. This presents the notion that the thermally aged and irradiated samples are more volatile than the unaged sample.

The second consideration is the working operational range and degradation as observed by Thermo-Gravimetric Analysis (TGA). The TGA analysis looks at the weight loss as the temperature exposure increases. This directly relates to the temperature range to which the material can be subjected before degradation starts to occur; this is known as the operational working range. The TGA graph showed two transition steps that relate to three different phases during the test. The thermally aged and irradiated samples showed a higher degradation for the first phase, a lower degradation for the second phase, and a higher degradation for the third phase. The final weight loss % resulted in the most degradation for the irradiated sample with the thermally aged and unaged samples ending with the same weight loss. The thermally aged sample was the slowest to lose weight with the increasing temperature. Thus, the degradation with increasing temperature from best to worst is thermally aged, unaged, and irradiated.

The third characteristic is the glass transition phase derived from the Differential Scanning Calorimeter test (DSC). The DSC test measures the relative heat flow from the sample as a function of temperature and is used to determine when the sample changes phases, in this case, begins to degrade. This is important as the cable will begin to degrade and become compromised at this point. Therefore, the lower the transition temperature and the less energy required, the easier it is for the cable to be compromised. The thermally aged sample showed a lower onset temperature with less energy required for the transition. The irradiated sample resulted in an even lower onset temperature but required a little more

energy than the thermally aged sample, but still less than the unaged sample. Thus, the thermally aged sample will transition first followed by the irradiated and unaged samples.

The final characteristic is the UL 94 vertical flame spread test. This test is performed to determine if the various aging subjugation compromises the standard flammability safety rating for the cable. The UL 94 flame spread test only has three classifications which are a result of the variable testing credentials. The thermally aged and irradiated sample all showed immediate self-extinguish of the flame after exposure. This resulted in every sample passing the standard with the highest rating of V-0.

Figure 5.2 summarizes the flammability characteristics for the thermally aged and irradiated exposures. From the comparison chart, it can easily be seen that the irradiated samples showed the highest changes in the flammability characteristics. These changes directly decrease the effectiveness of the cable's resistance to burning. Similar characteristics were observed for the thermally aged samples but were not as severe as the irradiated samples. Both forms of aging resulted in less favorable flammability characteristics over the unaged sample. Even though the aged samples showed degraded flammability characteristics, all of the samples passed the UL 94 vertical flame spread test. This signifies that the cables can be used past their intended lifespan without compromising their flammability characteristics.

5.1.3 Significant Factor: Relation of Reactance to Flammability Characteristics

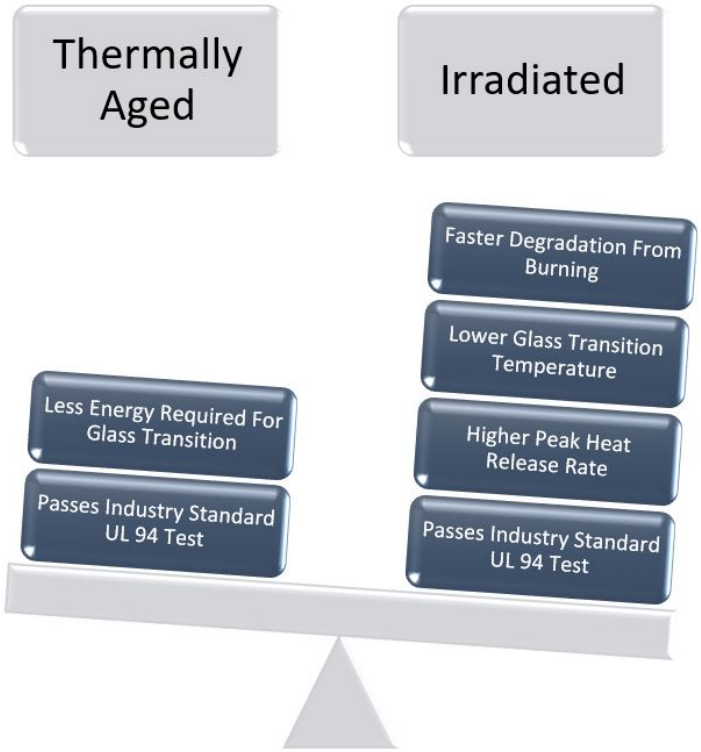

Figure 5.2: Comparison chart showing the main flammability characteristics for each of the two aging processes.

To begin to understand a means of correlating the flammability characteristics to the reactance of a cable it is first necessary to determine the substantial differences that occurred. The four main aspects to consider for the reactance are capacitive reactance, inductive reactance, resonance, and anti-resonance. Each aspect will be observed in detail, starting with the capacitive reactance. The capacitive reactance is a function of the dielectric constant, diameter of the conductor, diameter of the insulation, and the length of the conductor. The length can be accounted for by normalizing the reactance as a function of length. This was resolved by using samples that were all cut to the same length to make

it easier to correlate the data. Another variable that can be accounted for is the diameter of the conductor. This variable does not change between samples. The conductor could vary in diameter as a result of the manufacturing process but the diameter is assumed to be consistent. This leaves only two main factors that contribute to alterations in the capacitive reactance between samples: the diameter of the insulation, and the dielectric constant.

Each of these aspects was most prevalent after the first resonance as the developing characteristics began to deviate and show the patterns. All four of the reactance aspects will be evaluated with the second resonance data. The capacitive reactance that was recorded for the second resonance is shown in Table 5.1 below.

The capacitive reactance for the thermally aged Firewall III samples shows an increase that corresponds to the amount of thermal aging. 15 days of thermal aging show only a slight increase (0.61 %), 30 days of thermal aging shows a much more significant increase (41.46 % and 45 days of thermal aging shows the largest increase (65.85 %). The three irradiated

Table 5.1: Capacitive reactance from second resonance recorded for Firewall III cable, ULTROL 60+ cable, and Boston Insulated Wire (BIW) cable.

Second Resonance					
Sample	Cable Type	Aging Characteristic	Frequency of Peak Capacitive Reactance (kHz)	Peak Capacitive Reactance	% Change From Unaged
1	Rockbestos Firewall III	Unaged	924	-328	-
2	”	Thermally Aged (120°C for 15 days)	952	-326	0.61
3	”	Thermally Aged (120°C for 30 days)	952	-192	41.46
4	”	Thermally Aged (120°C for 45 days)	980	-112	65.85
5	”	Irradiated (30 days at 140 $\frac{Gy}{hr}$)	980	-132	59.76
6	”	Irradiated (60 days at 140 $\frac{Gy}{hr}$)	980	-180	45.12
7	”	Irradiated (120 days at 140 $\frac{Gy}{hr}$)	1008	-139	57.62
8	ULTROL 60+	Unaged	336	-174	-
9	”	Thermally Aged (150°C for 7 days)	308	-312	-79.31
10	BIW	Unaged	616	-199	-
11	”	Thermally Aged (150°C for 7 days)	588	-253	-27.14

samples show a closely related grouping where two samples are -132 (59.76% change) and -139 (57.62% change) while one is -180 (45.12% change). This shows that as the thermal aging increases so does the capacitive reactance and the irradiated samples seem to increase uniformly to approximately 60% over the unaged.

The ULTROL 60+ and BIW thermally aged samples both showed a decrease in peak capacitive reactance. This is the opposite of the characteristics shown for the Firewall III samples and can be easily explained. The ULTROL 60+ and BIW cables both have a grounding sheath around the insulated conductors. This sheath limits the inner conductor's exposure to thermal aging while also shrinking in size. The compression of the sheath results in variations of the relative capacitance between the two individual conductors of the cable. This causes the capacitive reactance to vary with frequency. The sheath can alter the effective dielectric constant and sheath diameter by absorbing some of the energy in the system which can cause a decrease in relative capacitance. This translates to an increase in the relative capacitive reactance and results in a left shift of the reactance curve. An initial left shift results in compounding differences seen with each resonance. This leads to varying deviations in the curve compared to the original unaged curve.

Lastly, the frequency that the peak capacitive reactance occurs at is vital to consider. The Firewall III samples resulted in three separate frequency groupings. The peak capacitive reactance for the unaged sample occurred at 924 kHz. The resultant frequency for the samples that were thermally aged for 15 and 30 days is 952 kHz. This shows a right shift for the first two thermally aged samples and is likely a direct result of the diameter of the insulation decreasing in size (D). The sample that was thermally aged for 45 days along with the samples that were irradiated for 30 and 60 days showed a peak occurrence at 980

kHz. The right shift for the thermally aged sample is due to a more substantial decrease in insulation size (D). The right shift for the irradiated samples is a result of a significant decrease in the dielectric of the insulation, caused by an increase in the insulations porosity. The final sample that was irradiated for 120 days showed a peak occurrence at a frequency of 1008 kHz and is a result of an even more significant decrease in the dielectric constant of the material.

The second aspect to consider is the inductive reactance that was recorded. The inductive reactance is a direct function of the distance between the arranged conductors (S). This arrangement can be altered as a result of the various types of aging. The inductive reactance that was recorded for the second resonance is shown in Table 5.2 below.

The inductive reactance for the thermally aged Firewall III samples shows a collective grouping. The three thermally aged samples showed a peak inductive reactance at a frequency of 924 kHz which is higher than the unaged sample. This is likely due to a decrease in the distance between the conductors (S) which causes a reduction in inductive reactance and shifts the curve to the right. The sample that was irradiated for 30 days also showed a peak inductive reactance at 924 kHz. This is a secondary result of the right shift that was induced by the change in capacitive reactance that was observed with the first resonance. The other two irradiated samples showed the same result, where the shift in capacitive reactance from the first resonance caused the inductive reactance to shift right for the second resonance.

The inductive reactance is more complicated for the ULTROL 60+ and the BIW cables due to their grounding sheath.

Table 5.2: Inductive reactance from second resonance recorded for Firewall III cable, ULTROL 60+ cable, and Boston Insulated Wire (BIW) cable.

Second Resonance					
Sample	Cable Type	Aging Characteristic	Frequency of Peak Inductive Reactance (kHz)	Peak Inductive Reactance	% Change From Unaged
1	Rockbestos Firewall III	Unaged	896	137	-
2	”	Thermally Aged (120°C for 15 days)	924	157	15
3	”	Thermally Aged (120°C for 30 days)	924	202	48
4	”	Thermally Aged (120°C for 45 days)	924	104	-24
5	”	Irradiated (30 days at 140 $\frac{Gy}{hr}$)	924	125	-9
6	”	Irradiated (60 days at 140 $\frac{Gy}{hr}$)	952	274	100
7	”	Irradiated (120 days at 140 $\frac{Gy}{hr}$)	980	92	-33
8	ULTROL 60+	Unaged	308	234	-
9	”	Thermally Aged (150°C for 7 days)	280	318	36
10	BIW	Unaged	588	148	-
11	”	Thermally Aged (150°C for 7 days)	560	136	-8

The thermal aging causes the jacket to shrink in size and compresses the grounding sheath around the insulated conductors. This makes the variable for the distance between the conductors more complicated because the grounding sheath directly impacts the effective inductive reactance. It is assumed that the grounding sheath causes the inductive reactance to increase which results in a left shift of the curve. As a result, the first curve shift from the capacitive reactance causes the curve to shift more dramatically.

It is more challenging to try and observe the peak inductive reactance to correlate to the aging characteristics as it is dependent on the spacing between the conductors. This spacing will become smaller with thermal aging or slightly larger with irradiation; however, the inductive reactance is also dependent on the shift observed by the capacitive reactance.

The third and fourth aspects to consider are the resonant and antiresonant frequencies. These two frequencies are primarily dependent on the curve shifts that are observed from the

capacitive and inductive reactance measurements. The resonant and antiresonant frequencies for the second resonance are shown in Table 5.3 below.

The resonant frequency shows an increase in both the thermally aged and irradiated sample for the Firewall III cable. This corresponds to the right shift observed from the capacitive reactance discussed previously. The thermally aged samples decrease in resonant frequency with exposure while the irradiated samples increase with exposure. The resonant frequency is a result of the correlation between the capacitive and inductive reactance for each sample. The thermally aged ULTROL 60+ and BIW samples show a decrease in resonant frequency which again corresponds to the left shift observed from the previously discussed capacitive reactance.

The antiresonant frequency for the second resonance of the system most efficiently relates to the type of aging and the amount of exposure that is observed. The antiresonance is a concise representation of the relation between the inductive and capacitive reactance as this value is dependent on the resultant shift of the reactance curve. The lowest value for the

Table 5.3: Resonant and Antiresonant frequencies from second resonance recorded for Firewall III cable, ULTROL 60+ cable, and Boston Insulated Wire (BIW) cable.

Second Resonance					
Sample	Cable Type	Aging Characteristic	Resonant Frequency (kHz)	Antiresonant Frequency (kHz)	% Change From Unaged
1	Rockbestos Firewall III	Unaged	752	904	-
2	”	Thermally Aged (120°C for 15 days)	784	933	3.21
3	”	Thermally Aged (120°C for 30 days)	770	938	3.76
4	”	Thermally Aged (120°C for 45 days)	764	942	4.20
5	”	Irradiated (30 days at 140 $\frac{Gy}{hr}$)	767	952	5.31
6	”	Irradiated (60 days at 140 $\frac{Gy}{hr}$)	770	969	7.19
7	”	Irradiated (120 days at 140 $\frac{Gy}{hr}$)	777	991	9.62
8	ULTROL 60+	Unaged	243	324	-
9	”	Thermally Aged (150°C for 7 days)	232	294	-9.26
10	BIW	Unaged	518	600	-
11	”	Thermally Aged (150°C for 7 days)	502	570	-3.09

Firewall III antiresonant frequency is the unaged sample at 904 kHz. The thermally aged samples increase as a function of exposure from 933 kHz to 942 kHz. The irradiated samples increase with exposure from 952 kHz to 991 kHz. The ULTROL 60+ is unaged to thermally aged sample shows a decrease in antiresonance (324 kHz to 294 kHz) that corresponds to the left curve shift that was observed. The BIW unaged to thermally aged samples shows the same behavior (600 kHz to 570 kHz).

The Firewall III samples show a 3.2% to 4.2% change in antiresonance for lifetime exposure to thermal aging. Lifetime exposure to irradiation for the Firewall III cable's antiresonance shows a 5.31% to 9.62% change. The ULTROL 60+ and BIW thermally aged samples show a reduction in antiresonance by 9.26% and 3.09% respectively.

The reactance measurements are useful in evaluating the type of aging and the amount of exposure. This is most easily evaluated by observing the changes in capacitive reactance and anti-resonance. It is more beneficial to observe these changes after the first resonance so that deviations are more apparent. The capacitive reactance will shift to the right and decrease in amplitude for increases in exposure and variation in aging types. The opposite may occur for a cable that has a grounding sheath around the conductors. It may also be useful to observe the antiresonance as thermal aging shows an increase of around 3% while irradiation shows an increase of around 6%. A flow chart is shown in figure 5.3 to help illustrate the determination process that is being utilized.

Figure 5.3: Evaluation process for measuring and correlating reactance data.

The reactance data shows a clear correlation of antiresonance with increasing exposure to thermal aging and irradiation. It is also shown that, from the previous section, the highest flammability characteristic degradation (as a function of exposure) corresponds to the amount of irradiation and thermal aging respectively. Considering these two pieces of information, it is obvious to consider that as the antiresonance shifts more to the right, that the resultant degradation of the flammability characteristics will also increase. It is also possible that the opposite should be considered for a cable that has a grounding sheath around the conductors. This type of cable showed a left shift that corresponded to an increase in the degradation of the flammability characteristics.

5.2 Summary of Discussions and Implications

This chapter looks into the following three main questions that this research intended to study:

1) How does thermal aging and irradiation alter the physical characteristics of the samples? The thermal aging showed increased density, decreased insulation diameter, increased water affinity, oxidation, and significant polymer destruction. The irradiated samples showed an increase in porosity, higher deformation, increased water affinity, oxidation, and alumosilicate polymer destruction. The increased water affinity, oxidation, and polymer destruction resulted in an increase in the dielectric constant for both types of aging. The most considerable contributing difference between the two types of aging resulted in the increase in density for the thermal aging and increase in porosity for the irradiated samples.

2) What impact does aging have on the flammability characteristics? The flammability characteristics for the thermally aged samples showed: higher peak heat release, faster time to peak heat release, less energy, and temperature required for glass transition, and a higher affinity for degradation when burning than the unaged sample. The irradiated samples all showed the same characteristics but were more significant than even the thermal aging. Thus, irradiation exposure showed the highest degradation of flammability characteristics of all the samples tested. To verify that none of the samples were compromised by their respective aging process, each sample was subjected to the UL 94 Vertical Flame Spread Test. This test provided an industry standard flammability certification. All of the samples passed the test with a rating of V-0 which means that during the average lifetime exposure the aging processes do not compromise the cable.

3) What means can be used to measure the amount of aging or degradation and correlating that to the flammability characteristics? The intention is to provide a passive method to measure the degradation of flammability characteristics. The reactance testing

showed that the comparison, of at least the data from the second resonance, of antiresonance and capacitive reactance provides a means of determining the amount of aging the cable has undergone. This can be directly correlated with the flammability degradation observed from aged samples. The result is that as the antiresonance increases (the curve shifts right) so does the degradation of the flammability characteristics. This is also true for a cable that has a grounding sheath around the conductors with the exception that the curve shifts to the left with increased flammability degradation. Considering either scenario, an increasing shift in the reactance curve corresponds to an increasing amount of flammability characteristic degradation.

Chapter 6

Conclusions

6.1 Research Overview

This research investigated the impact that thermal aging and irradiation have on the flammability characteristics of cable used in industry. This was done by observing the physical changes of the samples using FTIR, SEM, and indenter testing. Then the flammability characteristics were determined by TGA, DSC, Cone Calorimeter, and UL 94 testing. Finally, a means of passively measuring the changes in flammability characteristics was evaluated using reactance measurements from the cable samples. These aspects provide a complete analysis of how the aging characteristics impact the cable used in industry and provide a means of measuring the cable's degradation without having to remove it.

The physical characteristics were evaluated using FTIR, SEM and indenter testing. The indenter testing was used to evaluate the modulus of elasticity for each sample where the result provided an understanding of the relative density of the material. The FTIR testing provided an understanding of how the polymer degradation was affecting the material's

performance. The SEM test showed specific interactions such as the alumosilicate polymer degradation that caused a decrease in the silicate and an increase in the presence of aluminum in the material. This showed how the aging material increased its affinity for water intake. Another important aspect of the SEM test was the ability to take images at highly increased magnifications. This provided an understanding of the increase in porosity observed for the XLPE cable insulation.

The flammability characteristics were showcased by the TGA, DSC, Cone Calorimeter, and UL 94 tests. The TGA test inherently showed weight loss as a result of the changing temperature for the system. The TGA is useful in determining the operational range for the material that is being evaluated. This range is critical to consider since exceeding it can cause the cable jacket to begin to degrade causing structural deterioration and possibly compromising (to some extent) the inherent properties of the cable. This test shows that as the material is aged, it causes the weight loss as a function of temperature to increase and progress faster; however, by the upper-temperature limits, minimal end result differences are observed. The DSC test is useful in determining the transitional phase of the material, usually referred to as the glass transition. This transition is the point where the material begins to change its phase (in this case melt). This period is when the material begins to degrade away and corresponds to the weight change that was observed with the TGA tests. The DSC test allows the observation of the beginning of the transition temperature along with the energy required to change the phase of the material. This showcases that as the material is aged either by thermal aging or irradiation, the onset temperature, and energy required for the transition to occur decreases.

The Cone Calorimeter testing is used to determine the heat release rate, ignition time, and specific subcategories such as the peak heat release of the material. This is important when considering the propagation of a potential cable fire and how it could be impacted by aging. The heat release rate curves showed that the unaged cable took longer to increase its heat release rate and the peak heat release was smaller than other thermally aged and irradiated samples. The thermally aged samples showed two peaks that suggest the idea that the top layer of the jacket contained heavy oxidation that burned quicker causing a small peak. The thermally aged material inevitably reached a higher peak heat release and it occurred quicker than the unaged sample. The irradiated sample reached its peak heat release first and had the highest peak heat release. This presents the idea that the flame propagation of an irradiated cable would be higher than any of the others.

Since this research needs to consider the impact that degrading flammability characteristics of irradiated and thermally aged cables has on the industry, it is necessary to determine if these changes compromise the safety of the cables. Essentially, since the cable can burn faster and hotter does that mean that it is not safe to use after a certain period of time? A few of the samples were exposed to thermal aging or irradiation that exceeds normal exposure for the life of cable used in practice. These samples are used to evaluate whether or not the exposure compromises the flammability ratings of the cable. The flammability ratings are determined from standardized testing. The UL94 Vertical Flame Spread test is used to evaluate each one of these samples. This test is an industry standard for characterization of flammability ratings for plastics, and rubber components. Each one of the samples passed this test with the highest flammability rating that is given (V-0). This essentially means that even though the thermally aged and irradiated cable burns faster and hotter, it is still within

industry standards and should not impact the average lifespan of cables in industry. This statement should hold true for the types of cable jackets that were tested in this research.

Finally, researching a method for determining the changes in aging characteristics without removing the cable was performed. This is important as removing a cable to test it defeats the point of testing the cable in the first place since the significant cost is installing the cable. The reactance of the cable was measured to evaluate the changes in resonance and capacitive reactance to correlate them to the aging characteristics of the cables. The testing showed that the reactance curve shifted to the right, decreased the capacitive reactance, and increased the antiresonance with increased exposure to thermal aging and irradiation where each produced independent groupings. The thermal aging shifted to the right from the unaged and decreased in capacitive reactance. The irradiated samples did the same but to a higher degree. The cable that contained a grounding sheath around the conductors resulted in a left shift of the reactance curve due to an increase in the dielectric constant and decrease of the conductor's diameter. Evaluating the reactance of a cable may prove useful in evaluating the aging characteristics of cable used in industry.

It is important to evaluate the changing flammability characteristics that resulted from varying exposures to the aging processes. The thermal aging showed an increase (over the unaged samples) in peak heat release, time to peak heat release, glass transition temperature, and weight loss with temperature. Cable exposed to this type of aging showed a right shift and reduction in capacitive reactance. The irradiated samples showed the same results as the thermally aged but to a higher degree. The irradiated samples were impacted more than the thermally aged samples. Comparing the flammability characteristics to the reactance measurements shows a trend where an increasing shift in reactance corresponds to higher

levels of flammability characteristics degradation. The research results adhere to common understandings of the impact that these types of aging have on cable. The measured flammability characteristics were expected and do not directly go against what is currently understood in practice today.

6.2 Contributions

This research 1) laid the groundwork for understanding the impact that thermal aging and irradiation have on the flammability characteristics of cable used in industry and nuclear power plants today, and 2) developed a method of correlating the reactance of a cable to degradation of flammability characteristics for in situ testing of cable. There was plenty of research that looked into the physical degradation of cable exposed to various forms of aging, and separate research that looked into flammability characteristics of cable jackets but none of the research correlated aging to changes in the flammability characteristics of the cable jacket. Researchers also evaluated several methods for in situ measuring of cable, but there was not much focus on the reactance of the cable, and there was no correlation to the changes in flammability characteristics. Since little research had previously been done on aging exposure and degrading flammability characteristics, comparison to previous research proved not resourceful.

The cone calorimeter tests provided a valuable understanding of the differences in flammability characteristics of the aging cables. This, in correspondence with the SEM and indenter testing, provided an understanding of the correlation of physical changes to changes in the flammability characteristics. Utilizing this and evaluating the differences in

reactance, provided a rubric for measuring the changes of cable that is exposed to various forms of aging.

The numerical results indicate the critical factors surrounding aging cable used in the industry. Understanding how aging degrades the flammability properties of the cable's jacket can provide meaningful insight into the evaluation of certifying cable for continued use in industrial and nuclear plants. When certifying cable for continued use, it may prove beneficial to reference this research to evaluate the impact and possibly even quantify it. This could be done by just evaluating the predicted aging (based off of location and known aspects) and correlating it to data produced here. It could also be done by measuring the reactance of the cable to determine the approximate aging and resultant flammability characteristics. Either way, being able to predict this without destruction of the cable can contribute to cost reduction from prolonged use of the cable.

Several empirical studies reported that irradiation and thermal aging degraded the cable jacket, but none provided a high-level evaluation of the impact in relation to the flammability characteristics (Maier & Stolarz, 1983) (Nowlen, 1991) (Mecheri et al., 2013). This type of research proposed that irradiation and thermal aging of cable can cause degradation in many forms that are yet to be fully developed. According to this theory, fully understanding the characteristic changes of cable exposed to various forms of aging, is essential in adequately evaluating their continued use in practice today. This research used data to evaluate the impact that irradiation and thermal aging have on the degradation of the flammability characteristics to improve the current understanding and can be used to provide theoretical support for evaluating the continued use of aging cable.

6.3 Limitations

Several limitations could affect the generalization of this research's conclusions:

1) The different types of cables were limited to two types and three brands. The two types are differentiated by containing a grounding sheath or not. Also, the only type that contained irradiated samples was the Firewall III cable. This provided a foundational understanding but may be improved on by adding more cable types.

2) The samples size was limited to eleven different samples. These samples contained three different cable types that were either thermally aged or irradiated to varying degrees. Including additional samples with increased variety could be beneficial, but procuring these samples is hugely time-consuming and costly without a proper foundation for acquiring them.

3) The tested samples were from the same stock but were not the same sample. In short, it may be beneficial to age the sample and actively measure the differences. This may help in measuring the changes in reactance but will be futile in determining the changes in flammability characteristics unless the physical sample size is large enough to remove sections for destructive testing.

4) Each sample was tested individually in isolated spaces. This is beneficial when considering the specific changes of the sample but may not accurately represent the routine use of the cable.

6.4 Future Research

This study presents some issues that are worth additional research.

First, the types of cables (brands and material) can be increased to provide a broader evaluation of the characteristics changes.

Second, the sample size can be increased with more variation in samples. The more samples, with finer iterations of aging, will narrow the specific results. This may help in precisely correlating the data to some additional factor.

Third, each cable type could have one sample that is tested with no form of aging and tested again after some amount of aging. This could be done over and over until the cable is well past the average lifespan exposure. This may only provide a subtler understanding of the already evaluated characteristics but inevitably will narrow the results.

Fourth, this type of cable is typically run in cable trays with large bundles of additional cables. It may be useful to evaluate flame propagation of aged cable in cable trays or other typical arrangements.

Fifth, the reactance testing was performed in an isolated space with identical conditions. It is well understood that reactance can vary by the situational placement of the cable. Future testing could take long lengths of cable (with various forms of aging) and run them through a facility where the reactance could actually be measured "in situ." This would provide a proper evaluation of the ability of such a method.

6.5 Summary of Conclusion

This research expanded on the current knowledge of flammability characteristics of cable that is exposed to varying amounts of irradiation or thermal aging. It also provided a means of measuring this degradation by monitoring the changes in reactance of a cable.

This is something that could be done passively to approximate a cable's characteristics without removing or destroying the cable. Determination of the aging cables was evaluated by observing the physical changes, flammability changes, and reactance changes with varying amounts of exposure.

This study reported that aging cable (thermally aged or irradiated) results in degrading loss in flammability characteristics. This loss is represented by an increased Heat Release Rate, quicker burn time, and increased physical degradation resulting in possible compromising of the cable. It should also be noted that these heavily aged cables still meet or exceed basic industry standards for flame spread. This corresponds to the original hypothesis where it was assumed that increased exposure to irradiation or thermal aging would result in degrading flammability characteristics. The findings from this research can provide insights and suggestions for future evaluation of aging cable used in industry.

Bibliography

Adl-Zarrabi, B., & Kakavand, A. (2015). Introduction of possible inspection methods for evaluating thermal aging status of existing pre-insulated district heating systems. *Chalmers University of Technology*. Retrieved from https://energiforskmedia.blob.core.windows.net/media/22929/delrapport-7-possible-measuring-methods.pdf.
26

Agency, I. A. E. (1973). Improvement of Food Quality by Irradiation. *Joint FAO/IAEA Division of Atomic Energy in Food and Agriculture*. Retrieved from https://inis.iaea.org/collection/NCLCollectionStore/_Public/06/162/6162937.pdf.
70

Agency, I. A. E. (2012). IAEA Annual Report 2012. *IAEA*. Retrieved from https://www.iaea.org/sites/default/files/publications/reports/2012/anrep2012_full.pdf.
26

Association, T. A. (n.d.). Engineering Design as Related to Cable Applications. *Section III Insulated Aluminum Conductors*. Retrieved from https://www.aluminum.org/sites/default/files/aecd9.pdf.
51

ASTM. (2017). Standard Specification for Modified Concentric -Lay- Stranded Copper Conductors for Electrical Conductors. *ASTM B784-01*. doi: 10.1520/B0784-01R17E01
9

Babrauska, V. (2008). Research on Electrical Fires: The State of the Art. Proceedings of the Ninth International Symposium. *Fire Safety Science*, 3-18. doi: 10.3801/IAFSS.FSS.9-3 15

Babrauskas, V. (1996). Heat Release Rate: A Brief Primer. *Fire Science and Technology Inc.*. Retrieved from http://www.interfire.org/features/heat_release.asp. 98

Berg, H., Piljugin, E., Herb, J., & Roewekamp, M. (2012). Comprehensive Cable Failures Analysis for Probabilistic Fire Safety Assessments. *RT&A #01, 1(24)*, 1-14. Retrieved from https://www.researchgate.net/publication/266412175_COMPREHENSIVE_CABLE_FAILURES_ANALYSIS_FOR_PROBABILISTIC_FIRE_SAFETY_ASSESSMENTS. 10

Board, N. T. S. (1996). In-flight Breakup Over the Atlantic Ocean Trans World Airlines Flight 800, Boeing 747-141, N93119. *National Transportation Safety Board*. Retrieved from https://www.ntsb.gov/investigations/AccidentReports/Reports/AAR0003.pdf. 14

Botha, T. (2017). The Hidden Fire Risk - Electrical Cables. *Fire Engineering Consultant*. Retrieved from http://gnedenko-forum.org/Journal/2012/012012/RTA_1_2012-02.pdf. 13, 16

Boukezzi, L., Boubakeur, A., & Lallouani, M. (2010). Oxidation Evaluation of Cross-linked Polyethylene (XLPE) under Thermal Degradation : FTIR Study.

5th International Symposium on Hydrocarbons and Chemistry ISHC 5, At Algeria, Volume: 1. Retrieved from https://www.researchgate.net/publication/282657951_Oxidation_Evaluation_of_Cross-linked_Polyethylene_XLPE_under_Thermal_Degradation_FTIR_Study.

86

Boukezzi, L., Boubakeur, A., Laurent, C., & Lallouani, M. (2007). DSC Study of Artificial Thermal Aging of XLPE Insulation Cables. *2007 IEEE International Conference on Solid Dielectrics*. doi: 10.1109/icsd.2007.4290774

94

Boukezzi, L., Boubakeur, A., Laurent, C., & Lallouani, M. (2008). Observations on structural changes under thermal aging of cross-linked polyethylene used as power cables insulation. *Iranian Polymer Journal 17*, 611-624. Retrieved from https://www.researchgate.net/publication/228616116_Observations_on_structural_changes_under_thermal_ageing_of_cross-linked_polyethylene_used_as_power_cables_insulation.

79

Bowler, N., & Liu, S. (2015). Aging Mechanisms and Monitoring of Cable Polymers. *International Journal of Prognostics and Health Management, 29*, 1-12. Retrieved from https://www.phmsociety.org/sites/phmsociety.org/files/phm_submission/2015/ijphm_15_029.pdf.

23

Cable, G. (2013). ULTROL 60+ Cable Solutions. *General Cable Technologies*. Retrieved from https://cdn.generalcable.com/assets/documents/information-center/downloads/brochures/16$NuclearULTROL60Plus_Catalog.pdf?ext=.pdf.

31

Campbell, C., McConkey, J., Hashemian, H., Sexton, C., & Cummins, D. (2012). Result of Recent DOE Research on Develoment of Cable Condition Monitoring and Aging Management Technologies. *IAEA-CN*. Retrieved from https://inis.iaea.org/collection/NCLCollectionStore/_Public/43/070/43070832.pdf.

4, 25

Chaudhary, A., Gupta, S., Gupta, A., Kumar, R., & Gupta, A. (2015). Burning Characteristics of Power Cables in a Compartment. *Procedia Earth and Planetary Science, 11*, 376-384. doi: 10.1016/j.proeps.2015.06.075

13, 14

Corporation, A. (2015). Frequency Domain Reflectometry (FDR) - Electrical Testing to Locate and Monitor Cable Aging. *AMS*. Retrieved from http://www.ams-corp.com/wp-content/uploads/2011/04/FDR.pdf.

26

Earnest, C. M. (1988). Compositional Analysis by Thermogravimetry. *ASTM*. doi: 10.1520/STP997-EB

42

Fifield, L., & Duckworth, R. C. (2016). LWRS Cable Aging and Cable NDE. *Pacific Northwest National Laboratory*. Retrieved from https://www.energy.gov/sites/prod/files/2016/10/f33/12-Fifield%20LWRS%20Cables%20MaterialsXCutCoord%208-16-16%20PNNL-SA-120274.pdf.

30

Fifield, L., & Shin, Y. (2017). Tracking Aging in Nuclear Electrical Polymers. *Transaction of the American Nuclear Society*, 631-633. Retrieved from http://answinter.org/wp-content/2017/data/polopoly_fs/1.3879861.1507849337!/fileserver/file/822710/filename/199.pdf.

22

Gillen, K., Celina, M., & Clough, R. (1999). Density measurements as a condition monitoring approach for following the aging of nuclear power plant cable materials. *Radiation Physics and Chemistry 56*, 429-447. doi: 10.1016/S0969-806X(99)00333-3

57

Gillen, K., Clough, R., & Jones, L. (1982). Investigation of Cable Deterioration in the Containment Building of the Savannah River Nuclear Reactor. *Albuquerque, NM: Sandia National Laboratories*. Retrieved from https://www.osti.gov/servlets/purl/7094253.

22

Glass, S., Fifield, L., Dib, G., Tedeschi, J., Jones, A., & Hartman, T. (2015). State-of-the-Art Assessment of NDE Techniques for Aging Cable Management in Nuclear

Power Plants. *FY2015*. Retrieved from https://www.pnnl.gov/main/publications/external/technical_reports/PNNL-24649.pdf.

79

Glass, S., Fifield, L., Jones, A., & Hartman, T. (2017). Frequency Domain Reflectometry NDE for Aging Cables in Nuclear Power Plants. *Pacific Northwest National Laboratory*. doi: 10.1063/1.4974640

4, 23, 24, 26

Gulmine, J., & Akcelrud, L. (2006). FTIR characterization of aged XLPE. *Polymer Testing. 25*, 932-942. doi: 10.1016/j.polymertesting.2006.05.014

81

Hampton, N., Hartlein, R., Lennartsson, H., Orton, H., & Ramachandran, R. (2007). Long Life XLPE Insulated Power Cable. *Jicable '07*, 1-6. Retrieved from https://www.neetrac.gatech.edu/publications/jicable07_C_5_1_5.pdf.

11

He, F., & Brazis Jr., P. (2012). *Influence of Damage and Degradation on Breakdown Voltage of NM Cables Final Report.* Retrieved from https://library.ul.com/wp-content/uploads/sites/40/2015/02/Investigation_of_Damage_and_Degradation_of_NM_Cables.pdf.

3, 13

Hernandez-Mejia, J. (2016). Time Domain Reflectometry. *Cable Diagnostic Focused Initiative (CDFI) Phase II*. Retrieved from https://www.neetrac.gatech.edu/

publications/CDFI/5-TDR_17_with-Copyright.pdf.

25

Ho, C., Logakis, E., Ghoul, C., & Krivda, A. (2014). *Patent application WO2014075726A1.* Retrieved from https://patents.google.com/patent/WO2014075726A1.

79

Hussin, N., & Chen, G. (2010). Space charge accumulation and conductivity of crosslinking byproducts soaked LDPE. *2010 Annual Report Conference on Electrical Insulation and Dielectic Phenomena, West Lafayette, IN*, 1-4. doi: 10.1109/CEIDP.2010.5724002

79

Hvidsten, R., Kvande, & Larsen. (2009). Severe degradation of the conductor screen of service and laboratory aged medium voltage XLPE insulated cables. *Dielectrics and Electrical Insulation, IEEE Transactions on, 16(1)*, 155-161. doi: 10.1109/TDEI.2009.4784563

83

Hyvnen, P. (2008). Prediction of insulation degradation of distribution power cables based on chemical analysis and electrical measurements. *TKK Dissertations, 126*. Retrieved from http://urn.fi/URN:ISBN:978-951-22-9403-9.

81, 85

Jones, S., Wraith, J., & Or, D. (2002). Time Domain Reflectometry Measurement Principles and Applications. *Hydrological Processes*. doi: 10.1002/hyp.513

24

Kim, C., Jin, Z., Jiang, P., Zhu, Z., & Wang, G. (2006). Dielectric behavior of thermally aged XLPE cable in the high frequency range. *Polymer Testing. 25*, 553-561. doi: 10.1016/j.polymertesting.2006.03.009

89, 93

Kim, M., & Chung, S. O. (2011). Effect of AC Electric Fields on Flame Spread Over Electrical Wire. *Proceedings of the Combustion Institute, 33*, 1145-1151. doi: 10.1016/j.proci.2010.06.155

19

Kochetov, R., Christen, T., & Gullo, F. (2017). FTIR analysis of LDPE and XLPE thin samples pressed between different protective anti-adhesive films. *1st International Conference on Electrical Materials and Power Equipment, Xi'an, 2017*, 49-52. doi: 10.1109/ICEMPE.2017.7982097

80

Konecna, Z. (2017). Cable Qualification for Nuclear Power Plants. *Poster*, 1-4. Retrieved from http://radio.feld.cvut.cz/conf/poster/proceedings/Poster_2017/Section_PE/PE_024_Konecna.pdf.

7

Laboratories, U. (1997). Test for Flammability of Plastic Materials for Parts in Devices and Appliances. *UL 94*. Retrieved from http://www.dxdlw.com/bbsupfile/2014/12/10/1501300105/UL94-2014.pdf.

45, 47, 48, 103

Laboratory, B. N. (2016). Fire-Induced Cable and Circuit Failure Modes. *Sandi National Laboratories and U.S. NRC*, SAND2016-0116PE. Retrieved from https://www.osti.gov/servlets/purl/1339068.

xiii, 17

Learner, T. (2002). The use of a diamond cell for the FTIR characterization of paints and varnishes available to twentieth century artists. *Infrared and Raman Users Group (IRUG)*. Retrieved from https://www.getty.edu/conservation/our_projects/science/modpaints/1Learner.pdf.

40

Lin, C., Chung, C., & Tang, S. (2007). Accurate Time Domain Reflectometry Measurement of Electrical Conductivity Accounting for Cable Resistance and Recording Time. *Soil Physics*, 1278-1287. doi: 10.2136/sssaj2006.0383

20, 24

Liu, S., Fifield, L. S., & Bowler, N. (2016). Towards aging mechanisms of cross-linked polyethylene (XLPE) cable insulation materials in nuclear power plants. *2016 IEEE Conference on Electrical Insulation and Dielectric Phenomena (CEIDP), Toronto, ON, 2016*, 935-938. doi: 10.1109/CEIDP.2016.7785636

79

Liu, S., Gong, W., & Zheng, B. (2013). The Effect of Peroxide Cross-Linking on the Properties of Low-Density Polyethylene. *Journal of Macromolecular Science, Part B, 53(1)*, 67-77. doi: 10.1080/00222348.2013.789360

88

Maier, P., & Stolarz, A. (1983). Long-Term Radiation Effects on Commercial Cable-Insulating Material Irradiation at CERN. *GENEVA*. Retrieved from https://inis.iaea.org/collection/NCLCollectionStore/_Public/15/004/15004876.pdf.

23, 143

Marmon. (2016). Firewall III Power Cable. *RSCC Nuclear Cable*. Retrieved from http://www.transitcableproducts.co.uk/pdfs/NU01%20-%20FWL%20III%20P%20NS.pdf.

31

Mecheri, Y., Bouazabia, S., Boubakeur, A., & Lallouani, M. (2013). Effect of Thermal Aging on the Properties of XLPE as Insulating Material for HV Cables. *International Electrical Insulation Conference. Birmingham, UK: International Electrical Insulation Conference*, 1-4. Retrieved from https://s3.amazonaws.com/academia.edu.documents/46413094/Paper_INSUCON_13_Mecheri_pg_191_Proceed.pdf?AWSAccessKeyId=AKIAIWOWYYGZ2Y53UL3A&Expires=1547530528&Signature=NQm4ucQ0UCiG28WCm1xE%2FJKzhUc%3D&response-content-disposition=inline%3B%20filename%3DEffect_of_thermal_Ageing_on_the_Properti.pdf.

22, 143

Melo, A., Martinez, M., & De Queiroz, A. (2013). Investigation and Analysis of Electrical Aging of XLPE Insulation for Medium Voltage Covered Conductors Manufactured in Brazil. *Dielectrics and Electrical Insulation, IEEE Transactions on. 20*, 628-640. doi: 10.1109/TDEI.2013.6508767

88

Method, N. (1992). NT Fire 045 Solid Materials: Spontaneous Ignition Temperature by Continous Heating. *Nordtest Method*. Retrieved from http://www.nordtest.info/index.php/methods/item/solid-materials-spontaneous-ignition-temperature-by-continuous-heating-nt-fire-045.html.

18

Milter, H., & Steckler, K. (1995). SPREAD - A model of Flame Spread on Vertical Surfaces. *Gaithersburg, MD: U.S. Department of Commerce*. Retrieved from http://citeseerx.ist.psu.edu/viewdoc/download?doi=10.1.1.455.8123&rep=rep1&type=pdf.

9

Mo, S., Zhang, J., Liang, D., & Chen, H. (2013). Study on Pyrolysis Characteristics of Cross-linked Polyethylene Material Cable. *Procedia Engineering, 52*, 588-592. doi: 10.1016/j.proeng.2013.02.190

88

Murphy, J. (2004). Determination of Failure Criteria for Electrical Cables Exposed to Fire for Use in a Nuclear Power Plant Risk Analysis. *Worcester Polytechnic Institute*. Retrieved from http://citeseerx.ist.psu.edu/viewdoc/download?doi=10.1.1.541.9526&rep=rep1&type=pdf.

10

Nowlen, S. (1991). An Investigation of the Effects of Thermal Aging on the Fire Damageability of Electric Cables. *Washington DC: Sandia National Laboratories Report*,

SAND90-0696. Retrieved from https://inis.iaea.org/search/searchsinglerecord.aspx?recordsFor=SingleRecord&RN=22085431.

21, 143

NRC, U. (2013). Expanded Materials Degradation Assessment. *United States Nuclear Regulatory Commission. Washington D.C.: United States Nuclear Regulatory Commission*. Retrieved from https://www.nrc.gov/docs/ML1427/ML14279A321.pdf.

xiii, 9, 17

of the Navy., D. (1969). Investigation of Forrestal Fire. U.S. Government, Navy. *Washington D.C.: Department of the Navy*. doi: 10.1016/j.proeps.2015.06.075

13, 14

Okonite. (2018). Engineering Handbook: Engineering Data for Copper and Aluminum Conductor Electrical Cables. *The Okonite Company*. Retrieved from https://www.okonite.com/media/catalog/product/files/EHB_2018.pdf.

48

Plastics, P. (2001). Specifications-UL Test Procedures. *Underwriters Laboratories*. Retrieved from https://media.digikey.com/pdf/Other%20Related%20Documents/GC%20Elect/UL_Test_Procedure.pdf.

3

Rabello, M. S., & White, J. R. (1997). The role of physical structure and morphology in the photodegradation behaviour of polypropylene. *Polymer Degradation and Stability*, 55-73. doi: 10.1016/s0141-3910(96)00202-9

94

RigExpert. (2014). AA-1400 User Manual. *Ukraine Ltd*. Retrieved from https://www.rigexpert.com/files/manuals/aa1000/aa-600-1000-1400-manual.pdf.

54

Rodica, S.-D. (2008). FTIR asbestos presence identification in the occupational environment. *Analele Universitatii Bucuresti : Chimie. 4*. Retrieved from https://pdfs.semanticscholar.org/1f34/c7b63710b95b52277e3e78229c219574113d.pdf.

80

Ross, R., & Smit, J. (1992). Composition and growth of water trees in XLPE. *Electrical Insulation, IEEE Transactions on, 27(3)*, 519-531. doi: 10.1109/14.142715

83, 89

Rosser, W., Wise, H., & Miller, J. (1958). Mechanism of Combustion Inhibition by Compounds Containing Halogen. *International Symposium on Combustion, 7*, 175-182. doi: 10.1016/S0082-0784(58)80039-9

69

Salley, M. (2000). An Examination of the Methods and Data Used to Determined Functionality of Electrical Cables When Exposed to Elevated Temperatures as a Result of a Fire in a Nuclear Power Plant. *University of Maryland, College Park*. Retrieved from https://www.nrc.gov/docs/ML0514/ML051450082.pdf.

9

Sawyer, R., & Elsner, J. (1976). Cable Fire at Browns Ferry Nuclear Power Plant. *Fire Journal*. Retrieved from http://www.tvsfpe.org/_images/sawyerelsner.pdf.

1, 12

Seguchi, T., Tamura, K., Ohshima, T., Shimada, A., & Kudoh, H. (2010). Degradation mechanisms of cable insulation materials during radiation-thermal aging in radiation environment. *Elsevier Ltd*. doi: 10.1016/j.radphyschem.2010.07.045

3

Short, T. (2004). Electrical Power Distribution Handbook. *CRC Press LLC*. Retrieved from https://goodboygunawan.files.wordpress.com/2010/03/electric-power-distribution-handbook.pdf.

xiii, 8, 9, 10

Simmons, K., Ramuhalli, P., Brenchley, D., Coble, J., Hashemian, H., Konnick, R., & Ray, S. (2012). Light Water Reactor Sustainability (LWRS) Program - Non-Destructive Evaluation (NDE) R&D Roadmap for Determining Remaining Useful Life of Aging Cables in Nuclear Power Plants. *Pacific Northwest National Laboratory*. Retrieved from https://www.osti.gov/servlets/purl/1133783.

4, 23

Sorin, I., & Radu, S. (2009). Polymeric Materials Review on Oxidation, Stabilization and Evaluation using CL and DSC Methods CERN. *Geneva. TE Department*, 62. Retrieved from https://cds.cern.ch/record/1201650/files/Ilie_TE_Technical_Notes.pdf.

93

Spilde, M. N., & Adcock, C. (2006). Scanning Electron Microscope Operator's Manual. *Department of Earth and Planetary Sciences and Institute of Meteoritics, University of New Mexico*. Retrieved from http://meteorite.unm.edu/site_media/pdf/SEM_Manual2006.pdf.

39

Taylor, G. (2012). Evaluation of Critical Nuclear Power Plant Electrical Cable Response to Severe Thermal Fire Conditions. *University of Maryland, College Park*. Retrieved from https://www.nrc.gov/docs/ML1212/ML121220175.pdf.

xiii, 15, 17

Tewarson, A. (1994). Flammability Parameters of Materials Ignition, Combustion and Fire Propagation. *Journal of Fire Sciences, 12*, 329-356. doi: 10.1177/073490419401200401

19

Tewarson, A., & Khan, M. (1989). Fire Propagation Behavior of Electrical Cables. *Proceedings of the Second International Symposium. New York: Fire Safety Science*, 791-800. Retrieved from http://www.iafss.org/publications/fss/2/791/view.

7

Thue, W. A. (2003). Electrical Power Cable Engineering Second: Edition. *Boca Raton*. doi: 10.1201/9781482287820

52

Turtola, A. (1999). Ignition of and Fire Spread on Cables and Electronic Components. *VTT Publications, 387*, 1-112. Retrieved from https://www.vtt.fi/inf/pdf/publications/

1999/P387.pdf.

18

U.S. Congress, O. O. T. A. (1993). Safety of Aging Nuclear Plants. In OTA-E-575 -Aging Nuclear Power Plants: Managing Plant Life and Decommissioning OTA. *Washington D.C.: U.S. Congress*, 37-79. Retrieved from http://large.stanford.edu/courses/2015/ph241/lee1/docs/9305.PDF.

9, 12

Xu, J., Liu, X., Yang, W., Lei, N. L., Zhao, J., Ma, B., & Kang, C. (2018). Influence of Montmorillonite on the Properties of Halogen-Antimony Flame Retardant Polypropylene Composites. *Polymer Composites*. doi: 10.1002/pc.24969

73

Yang, H. (2013). Investigation of the Flammability of Different Cables Using Pyrolysis Combustion Flow Calorimeter. *Procedia Engineering, 62*, 778-785. doi: 10.1016/j.proeng.2013.08.125

21

Vita

Justin Beeler received his B.S. degree in Aerospace Engineering from The University of Tennessee, USA, in May 2015. After that, he worked as a design engineer briefly before moving onto rocket engine design and testing. He has designed, researched, and/or tested rocket engines and control systems for both NASA Marshall Space Flight Center and TGV Rockets. In 2017, he joined the Department of Electrical Engineering and Computer Science at the University of Tennessee, Knoxville.